2015

Nanoparticle measurement, control and characterization: Procedure applied to machining processes and mechanical friction

Victor Songmene
ÉTS

Riad Khettabi
ÉTS

Martin Viens
ÉTS

Jules Kouam
ÉTS

Stéphane Hallé
ÉTS

See next page for additional authors

Auteurs

Victor Songmene, Riad Khettabi, Martin Viens, Jules Kouam, Stéphane Hallé, François Morency, Jacques Masounave, and Abdelhakim Djebara

Chemical and Biological Hazard Prevention

Studies and Research Projects

REPORT **R-864**

Nanoparticle measurement, control and characterization

Procedure applied to machining processes and mechanical friction

Victor Songmene
Riad Khettabi
Martin Viens
Jules Kouam
Stéphane Hallé
François Morency
Jacques Masounave
Abdelhakim Djebara

irsst
nano québec

The Institut de recherche Robert-Sauvé en santé et en sécurité du travail (IRSST), established in Québec since 1980, is a scientific research organization well-known for the quality of its work and the expertise of its personnel.

OUR RESEARCH is *working* for you !

Mission

To contribute, through research, to the prevention of industrial accidents and occupational diseases and to the rehabilitation of affected workers;

To disseminate knowledge and serve as a scientific reference centre and expert;

To provide the laboratory services and expertise required to support the public occupational health and safety network.

Funded by the Commission de la santé et de la sécurité du travail, the IRSST has a board of directors made up of an equal number of employer and worker representatives.

To find out more

Visit our Web site for complete up-to-date information about the IRSST. All our publications can be downloaded at no charge.
www.irsst.qc.ca

To obtain the latest information on the research carried out or funded by the IRSST, subscribe to *Prévention au travail,* the free magazine published jointly by the IRSST and the CSST.
Subscription: *www.csst.qc.ca/AbonnementPAT*

Legal Deposit
Bibliothèque et Archives nationales du Québec
2015
ISBN: 978-2-89631-788-2 (PDF)
ISSN: 0820-8395

IRSST – Communications and Knowledge Transfer Division
505 De Maisonneuve Blvd. West
Montréal, Québec
H3A 3C2
Phone: 514 288-1551
Fax: 514 288-7636
publications@irsst.qc.ca
www.irsst.qc.ca

Chemical and Biological Hazard Prevention

Studies and Research Projects

REPORT **R-864**

Nanoparticle measurement, control and characterization

Procedure applied to machining processes and mechanical friction

Victor Songmene, Riad Khettabi, Martin Viens, Jules Kouam, Stéphane Hallé, François Morency, Jacques Masounave, Abdelhakim Djebara

École de technologie supérieure

Clic Research
www.irsst.qc.ca

A PDF version of this publication is available on the IRSST Web site.

This study was funded by the IRSST. The conclusions and recommendations are solely those of the authors.
This publication is a translation of the French original; only the original version (R-814) is authoritative.

PEER REVIEW

In compliance with IRSST policy, the research results published in this document have been peer-reviewed.

ACKNOWLEDGMENTS

The authors wish to thank the following organizations:

• The *Institut de recherche Robert-Sauvé en santé et en sécurité du travail* (IRSST) for its financial support, technical support and the collaboration of the following researchers: Yves Cloutier (Metrology), and Chantal Dion (Characterization by Transmission Electron Microscopy);

• *Nano-Québec* for its financial support;

• The *École de technologie supérieure* (ÉTS) for equipment, and for the support provided to this project by the Office of the Dean for Research at the ÉTS;

• The Product, Process and Systems Engineering Laboratory (P_2SEL also known as *LIPPS* at ÉTS) for allowing us to use its infrastructure;

• The Aluminum Research Centre (REGAL) for providing additional scholarships to students participating in the project;

• The Research Team in Work Safety (ÉREST, at the ÉTS) for its collaboration.

ABSTRACT

While emerging nanotechnologies are opening promising paths in several economic sectors, some studies suggest the nanoparticles (NP) they generate could have negative effects, particularly on health and the environment. These NP can be generated during fabrication, shaping, handling and assembly of ordinary metallic and non-metallic workpieces and nanomaterial-based workpieces. Other everyday activities, such as automobile braking, can also produce NP. It is therefore urgent to find ways of controlling these risks. However, usual risk assessment techniques and methods are not directly applicable to NP. This project's objective is to establish an efficient NP measuring, control and characterization method applicable to industrial fabrication processes.

Laboratory machining and friction tests, performed on industrial-calibre machine tools, coupled with simulations of the behaviour of airborne particles and air flows within machine enclosures, were necessary to conduct this study. Several kinds of particle sampling equipment (SMPS, APS, MOUDI) and characterization equipment (scanning electron microscope – SEM, transmission electron microscope – TEM, and atomic force microscope – AFM) were used. This project made it possible, in particular, to:

- ✓ Establish a sampling, collection and measuring procedure: development of methods of collecting and preparing substrates adapted to NP and to the different microscopes used (*SEM, TEM* and *AFM);* then improve measurement by developing corrective factors to compensate for particle shapes and densities.
- ✓ Determine the conditions for NP generation during the friction and machining of aluminium alloy workpieces, as well as the concentrations and aerodynamic diameter distributions of these particles. We have thus developed strategies for NP emission reduction at source during machining and friction, based on the choice of operating conditions.
- ✓ Demonstrate that machining of common alloys, which are not considered nanomaterials, emits more NP than micrometre-sized particles, and that the majority of these NP are smaller than 20 nanometres.
- ✓ Classify common machining processes (milling, turning and drilling) and dry friction operation according to their NP emission capacity. For the aluminium alloys tested, milling was found to be the operation that emits the most NP.

This work showed the necessity of knowing the shape of particles and their trajectory during emission, in order to improve capture and measurement precision. It also revealed the presence of ultrafine particles during machine shaping of ordinary materials not containing NP. These particulate emissions depend on the processes and their parameters, the cutting materials and the cut materials, resulting in the possibility of being able to control these particulate emissions. The typical cases of nanomaterials and composites containing or not containing nanoparticles deserve to be examined.

In this report, the term nanoparticles (NP) refers to nanosized *ultrafine particles* emitted non intentionally during machining of metal workpieces (or other processes).

TABLE OF CONTENTS

LIST OF TABLES

LIST OF FIGURES

LIST OF ABBREVIATIONS AND ACRONYMS

AFM	Atomic force microscope
APS	Aerodynamic Particle Sizer or APS Spectrometer
C^P	Number concentration (#/cm^3)
C^S	Particle mean specific surface area concentration (nm^2/cm^3)
C^M	Mass concentration (µg/m^3)
CPC	Condensation Particle Counter
DMA	Differential Mobility Analyzer
EDX	Energy-dispersive X-ray spectroscopy
ELPI	Electrical Low Pressure Impactor
EPA	Environmental Protection Agency
ÉTS	École de technologie supérieure
EU-OSHA	European Agency for Safety and Health at Work
IRSST	Institut de recherche Robert-Sauvé en santé et en sécurité du travail
LDMA	Long Differential Mobility Analyzer, for ranges from 20 to 1000 nm
MOUDI	Micro-Orifice Uniform Deposit Impactor
SEM	Scanning electron microscope
NAS	Nanometer Aerosol Sampler
NDMA	Nano Differential Mobility Analyzer, for ranges from 5 to 500 nm
NP	Nanoparticles: Particles for which one of the three dimensions is nanosized (smaller than 100 nm)
NIOSH	National Institute for Occupational Safety and Health
OEL	Occupational exposure limit
OELV	Occupational exposure limit value
PC	Polycarbonates
$PM_{2.5}$	Particulate Matter for 2.5 µm or less, serving as an air quality index

SMPS	Scanning Mobility Particle Sizer
SUVA	Swiss National Accident Insurance Fund (*Schweizerische Unfallversicherungsanstalt)*
TEM	Transmission electron microscope
VARAN	Variance analysis
WHO	World Health Organization

1. INTRODUCTION

The emergence of nanomaterials has opened up new industrial, scientific and even social perspectives. Due to the risks associated with the growing use of nanomaterials, regulators are seeking to establish new standards for particles smaller than 100 nm. NP are present during fabrication (synthesis and shaping), handling and assembly of ordinary metal workpieces and nanomaterial-based workpieces. Other everyday activities, such as automobile braking, can also produce NP. It is therefore urgent to find means of protection or control.

Machining tests conducted at École de technologie supérieure (ÉTS), Product, Process and Systems Engineering Laboratory (P_2SEL *also known in French as LIPPS*), have shown that source reduction of the formation of micrometre-sized particles is possible. We estimate that a similar reduction should also be possible for NP. However, knowledge of NP is still at the embryonic stage, as are reproducible and reliable measuring methods. It is therefore essential to establish a reliable measuring procedure to validate NP source reduction efforts.

This report is divided into nine sections, including this introduction. Section 2 is devoted to the problem of measurement of NP, current scientific knowledge and research objectives. Section 3 presents the methodology used, while Section 4 relates the outcomes obtained. The discussion is presented in Section 5, which covers the NP aerodynamic behaviour, the effects of the process, the cut material, the tool and the cutting conditions. A conclusion (Section 6), the applicability of the outcomes (Section 7), recommendations (Section 8) and references (Section 9) complete the report.

2. PROBLEM, STATE OF KNOWLEDGE AND RESEARCH OBJECTIVES

2.1 Problem

2.1.1 NP in the work environment

NP are found in many industrial environments, including those engaged in fabricating composite materials. Several research studies address the interaction between NP and the matrix in composite materials to understand the phenomenon better. NP do not act as simple conventional additives, but also as a major reinforcement that significantly improves the mechanical properties of the materials (Bensadoun, 2011; Jancar et al, 2010; Pustkova et al, 2009; Laoutid et al, 2009).

According to Witschger et al, (2012), NP exposure can occur during synthesis, handling and shaping of nanomaterials (including machining, sanding and polishing), and during cleaning of equipment and waste collection, transportation and treatment.

In 2010, the number of workers in the nanotechnology sector was estimated at 20,000 worldwide (Boczkowski and Lanone, 2010), but the number of people who may be exposed to NP is surprisingly higher, due to additional processes that could occur. Indeed, some fabrication processes generate aerosols (dry or wet), which can be harmful to the health of machine tool operators and the environment. It was proved that metal machining processes produce broad spectra of particles (Tönshoff et al, 1997; Malshe et al, 1998) some of which are NP (Zaghbani et al, 2009; Khettabi et al, 2010). This is also the case for wood (Subra et al, 1999), which produces dust during machining. However, the outcomes of laboratory machining tests conducted on metals showed that metallic particle emissions (PM2.5) diminish as the cutting speed increases (Songmene et al, 2008a; Zaghbani et al, 2009). These outcomes are very interesting from the practical point of view, because it is possible to machine workpieces at very high cutting speeds, thus guaranteeing greater productivity, while reducing the production of harmful dusts.

Aitken et al (2004) estimate that in England, approximately one million employees would be exposed to NP via processes such as welding, working or processing of metallic materials. The work of Malshe et al (1998) indicates that most of the dusts generated during machining consist of very fine particles (diameter smaller than 1 µm). Their numeric concentration is around 10 to 35 times greater than that of the biggest particles (around 5 µm in diameter) and depends on the type of cutting tool used.

While countries such as Germany, the United States and England have set dust exposure limits (or indicative values) for fabrication sector workers, Canada still has no specific regulations in this regard. Work performed by Tönshoff et al (1997), in Germany, showed that, without a suction system, micrometer-sized dust emissions during part grinding represented a real danger for the operators' health, because these emissions exceeded 100% of the limit permitted in Germany, which was 6 mg/m^3. Note that the size of the particles studied by these authors ranged from 0.03 to 16 micrometres.

In the United States, the National Institute for Occupational Safety and Health (NIOSH) recommended exposure limits of 1.5 mg/m³ for fine TiO_2 and 0.1 mg/m³ for ultrafine TiO_2, in mean concentrations weighted over time, for a maximum of 10 h/day and 40 h/week.[1] Likewise, the European Agency for Safety and Health at Work (EU-OSHA, 2009) also indicates that benchmark levels (or exposure limit values) were proposed in the United Kingdom (UK) for four classes of nanomaterials:

- Insoluble nanomaterials: 0.066 × occupational exposure limit (OEL) of the corresponding microsized bulk material (expressed as mass concentration);
- Fibrous nanomaterials: 0.01 fibres/ml;
- Highly soluble nanomaterials: 0.5 x OEL;
- CMAR (carcinogenetic, mutagenic, asthmagenic or reproductive) nanomaterials: 0.1 x OEL of the corresponding microsized bulk material (expressed as mass concentration).

Boczkowski and Lanone (2010), after regretting the nonexistence of an NP-specific occupational exposure limit value, proposed the adoption of a prudent attitude to manufactured NP by limiting industrial exposures and instituting collective protection integrated into the fabrication process.

In 2012, the Swiss National Accident Insurance Fund (SUVA, 2012) published benchmark levels for some NP (6 mg/m³ for inert dusts; 2 mg/m³ for hardwood; 0.2 mg/m³ for mineral oil mists, 0.15 mg/m³ for crystalline silica and 0.1 mg/m³ for lead).

According to SUVA (2013), no international limit has been established or published yet for NP. However, SUVA (2013) mentions the following indicative limits:

Dusts in general:

- Alveolar dust: 3 mg/m^3
- Inhalable dust: 10 mg/m^3

[1] NIOSH Current Intelligence Bulletin: Evaluation of Health Hazard and Recommendations for Occupational Exposure to Titanium Dioxide. Draft, November 22, 2005.

Nanoparticles:

- Carbon nanotubes and nanofibres (length greater than 5 μm, diameter smaller than 3 μm, length-to-diameter ratio greater than 3:1): 0.01 fibre/ml
- Titanium dioxide nanoparticles: 0.3 mg/m^3 (alveolar fraction)

In this report, we focused on metal cutting processes and mechanical friction between two metallic materials. Undoubtedly, the development of an NP measuring method and the establishment of a database on emissions generated during workpiece fabrication and friction would help Canadian legislators propose regulations in this field. These outcomes could also raise manufacturers' awareness so that they implement corrective or preventive measures.

2.1.2 NP measurement, control and source reduction

Source reduction can be accomplished at three levels: production, substitution and work practices (WHO, 1999). The production or fabrication processes can be improved by applying methods that generate fewer particles. Regarding materials, or the nature of the dusts, materials can be changed so they generate less dust. Hoower et al (1990) showed that fragile materials produce more dust than ductile materials, and that metals produce more dust (around 500 times more) than alloys. If substitution is not possible, particle source reduction strategies must be researched or developed (WHO, 1999).

Machining tests conducted at the Fabrication Laboratory of the École de technologie supérieure (ÉTS), in Montréal, showed that source reduction of the formation of micrometre-sized particles is possible, sometimes by a factor of 10, by changing the parameters and the machining strategies (Songmene et al, 2008), or by local cooling of materials before machining (Balout et al, 2007). We therefore estimate that source reduction of NP generation is also possible. Preliminary work (Zaghbani et al, 2009; Khettabi et al, 2007, 2008, 2009a) confirms this hypothesis for some materials and under certain machining conditions. Songmene et al (2012) also showed that the mass concentrations of particles emitted during machining can be reduced, without harmful effects on productivity, by using the right tool geometry or judiciously combining the cutting parameters: speed and feed rate.

However, to achieve this, it is essential to establish a reliable NP measuring procedure, because NP behave differently than microparticles and are more difficult to measure. Also note that the ambient air, especially in fabrication shops, already contains many NP of varied sources and sizes. This is why it is necessary to conduct any study of NP control or source reduction in a controlled environment, as near as possible to the generating source (for example, the machine tool enclosure in the case of machining). This is necessary in order to identify the method that generates the fewest possible particles.

However, little is known about the interaction among the process, the material and NP formation. This deficiency is an even greater cause of concern for nanomaterials, which can generate many NP. Moreover, the methods usually employed in occupational hygiene to protect against aerosols are not adapted and do not allow adequate detection or characterization of ultrafine aerosols,

smaller than 0.1 µm (Mark, 2004). The potential for collection of this type of particle is low, because their airborne behaviour is not yet mastered (Witschger and Fabriès, 2005b).

Control of airborne NP by source ventilation or general ventilation poses a challenge due to their aerodynamic behaviour, generally associated with the behaviour of a passive scalar. At low concentrations, NP tend to behave like a gas in a forced air flow, which is why it is important to model the dispersion of a trace gas to predict and improve the efficiency of the means of capture. Moreover, according to Vincent (1989), the assessment of occupational exposure to aerosols has become more complex, because the nature of the processes implemented at the workstation and the type of aerosol released must be taken into account.

2.2 State of scientific and technical knowledge

2.2.1 Potentially harmful effect of NP relative to their size

The epidemiological studies show that metal dusts, including those produced in fabrication processes, represent an occupational safety risk (Tönshoff et al, 1997; Sutherland et al, 2000; WHO, 1999; Ostiguy et al, 2006). Their effects range from simple airway irritation to cancers, including bronchitis and asthma. The US Environmental Protection Agency (EPA) confirms that even low concentrations of certain metals can cause acute pulmonary effects (Sutherland et al, 2000). The people at greatest risk of developing stomach, pancreatic, prostate and rectal cancer are those who are frequently exposed to metal cutting particles (Hands et al, 1996; Mackerer, 1989).

Because of these problems, the occupational health and safety regulatory agencies increasingly urge manufacturers to reduce NP and metallic dust emissions. It is well known that the level of penetration of particles in the respiratory tract depends on the size of the particles (Ostiguy et al, 2006). In general, particles smaller than 2.5 µm will tend to be deposited in the alveolar region of the lung, while the largest particles will be deposited in the upper airway. Khettabi *et al.* (2007) have established correlations between the cutting tool geometry and the chip formation on generation of microparticles (PM2.5) during dry machining of steel and aluminium alloys. According to the work of Witschger and Fabriès (2005a), the size ranges that should be given special attention are those from 1 to 2.5 µm, as well as from 5 to 20 nm, because the particles with an aerodynamic diameter within the latter range are mostly deposited in the alveoli. It is therefore completely justified to work with NP with a diameter greater than 5 nm during *in vitro* studies of alveolar cells.

According to Zhang et al (2000), NP would be as harmful as microparticles, especially when they are absorbed by human body cells. Experimental studies conducted by Oberdörster et al (2005) showed that particles, even when inert, can become biologically active when they are nanosized. Due to this size, nanoparticles can enter the human body through the nose, mouth and skin, and then disperse to reach the pulmonary alveoli, the circulatory system, the liver and the brain; they can even pass through the intestinal walls and the placenta (Ostiguy et al, 2006). Gatti (2004) confirmed that some NP could migrate to the kidneys and the pancreas. Ahamed et al (2010) confirmed the risk of cutaneous penetration by NP and the risk of harmful effects on the vital organs.

It was also shown that it is possible to improve the penetration factor of therapeutic particles through diseased skin, particularly through the openings of hair follicles, by reducing the size of these particles to nanoscale (Tarl et al, 2011). This work gives reason to consider the risks of skin penetration by metal NP. However, other studies, including Sadrieh et al (2010), concluded that nanosized metal oxides, particularly TiO_2 and ZnO, are unable to penetrate healthy skin. Likewise, according to Lademann et al (2011), who analyzed the literature on the health and safety aspects of NP, there is no indication that particles of diameter ≥100 nm can pass through a healthy skin barrier. For NP of diameter ≤100 nm, the research is continuing, and it is expected that particles of diameter ≤40 nm cannot pass through the skin either. Similar studies also have to be conducted with NP that are not generated intentionally, particularly those produced when shaping materials.

Elder et al (2004) showed that the toxicity of NP is directly related to their number and specific surface area, and not only to their mass concentration, as is the case with microparticles. It is also admitted that the reactivity of particles increases when their size diminishes. In particular, the degree of oxidation increases with the decrease in particle size. Metal particles oxidize, and this reaction occurs very rapidly in air; most of the time, it is instantaneous.

Adequate measurement of NP eventually would allow examination of the correlations among the toxicity, nature, shape and size of NP, and then find means of predicting and limiting the production of hazardous particles. In the absence of standards for measuring metal particles, particularly those generated during fabrication of workpieces, it is impossible:

- to compare the outcomes of the different laboratories;
- to know the materials or the processes that emit fewer of these metal particles;
- to identify clean and economical fabrication techniques.

2.2.2 Measurement and characteristic parameters

The evaluation of metal particle emissions in relation to the fabrication processes, the materials or any other controllable variable must be performed with high-sensitivity methods. The measurements taken in the open air and far from the source are interesting to test air quality, but are inappropriate to study the emissivity of processes or materials; they also have the effect of increasing the measuring time (Songmene et al, 2007).

Air quality control or characterization of airborne suspended particles often uses their concentration as the principal parameter. With many instruments, this parameter is evaluated by counting the number of particles identified by the detector of the measuring instrument, which sucks in air at a known flow rate, and by calculating the mass concentration (mg/m^3) based on the density of the particles, according to the assumption that they are spherical. The mass of the particles is also deduced by calculation. These parameters (mass, concentration) are adequate for large or fine particles, but not necessarily for NP (Witschger and Fabriès, 2005a).

Many researchers (Ostiguy et al, 2006, Witschger and Fabriès, 2005a) have suggested considering the specific surface area as an essential parameter for NP; there would be a better correlation between their specific surface area and their toxicity, while this is not the case with measurements relative to the mass of NP. As illustrated in Figure 1, the particle distribution varies depending on whether one is interested in their number, mean diameter, specific surface area or mass.

Palmqvist and Gustafsson (1999) proposed a parameter, the *Dust Unit*, which indicates the quantity of dusts generated per unit of volume removed according the equation:

$$\text{Dust Unit} = A * K \qquad (1)$$

where:

A = measured value of the dust concentration;

K = 100*(5.0/s)*(1.6/d), a parameter varying according to the cutting speed (s) and cutting depth (d). Factor K would compensate for the values of the cutting parameters in relation to the benchmark levels, i.e. s=5.0 m/min and d=1.6 mm. The authors did not specify how these benchmark levels were selected.

(a)

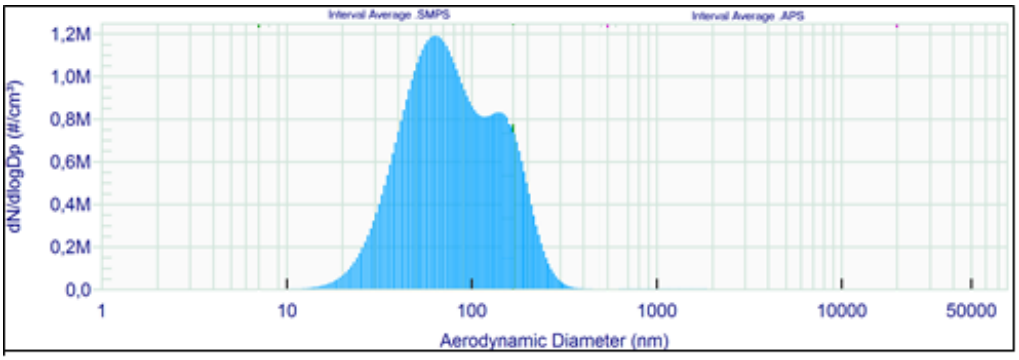

(b)

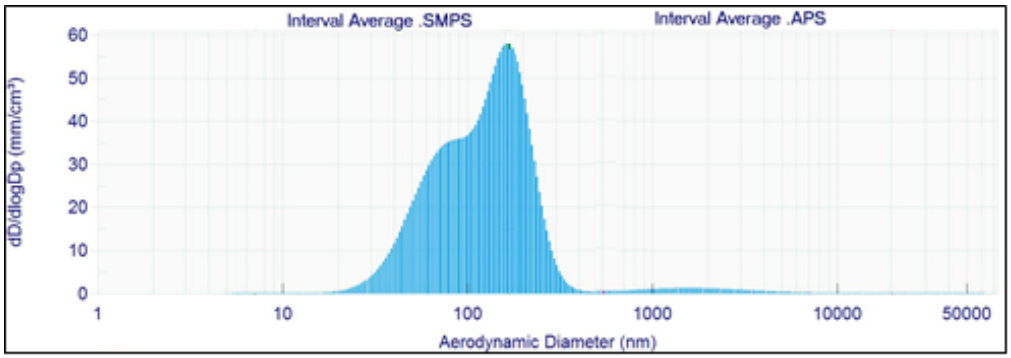

(c)

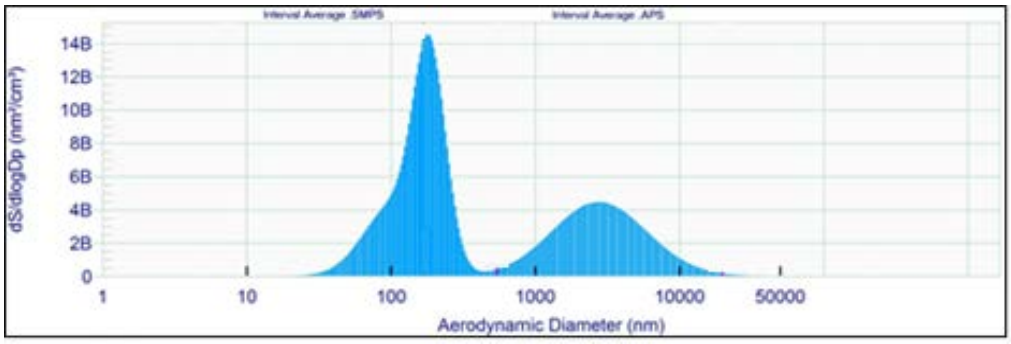

(d)

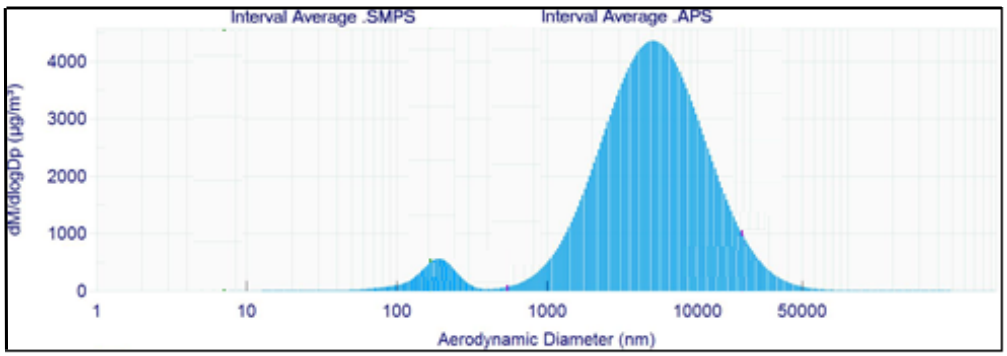

Figure 1 – Mean size distributions of metal particles during an aluminium (6061-T6) machining operation, according to the four distribution modes: (a) by number ($M = 10^6$), (b) by mean diameter (mm/cm^3), (c) by specific surface area ($B = 10^{-9}$ nm^2/cm^3) and (d) by mass ($\mu g/m^3$).

Arumugan et al (2006) introduced a new parameter, the *Green Factor*, as the ratio between the metal removal rate (m^3/min) and the aerosol mass concentration (mg/m^3). The greater this factor, the lower the airborne particle concentration and the more environmentally friendly the process. This factor has a dimension that causes confusion (m^3 of metal x m^3 of air x min^{-1} x mg^{-1} of particles) and has no physical interpretation. This is why the ÉTS researchers (Khettabi et al, 2007), and then Rautio et al (2007), preferred to use an adimensional parameter (Dust Unit, or D_u), defined as the ratio between the mass of the particles and the mass of the chips generated, knowing that the goal of machining is to give a new shape to a workpiece by removing the metal. The new parameter (which we intend to use in the project, in addition to the concentration, the mass and the specific surface area) is defined by Equation 2:

$$Du = \frac{m_{Dust}}{m_{Chip}} \qquad (2)$$

where:

m_{Dust} (g) = total mass of dusts measured (under the negligible loss assumption),

m_{Chip} (g) = mass of chips removed.

2.2.3 Progress in the study of metal particles generated during machining

All machining processes generate aerosols (dry or wet), which can be harmful to the health of machine tool operators or which deteriorate the work environment (Sutherland, 2000; Aitken et al, 2006; Yue et al, 2000). Occupational exposure to NP is possible for all NP fabrication and handling processes. In general, NP are more toxic than larger particles of the same nature (Honnert, 2007). The NP emissions related to certain industrial processes (machining, sanding, fine polishing) are as hazardous to workers' health as manufactured NP emissions (Hervé-Bazin, 2007; Witschger and Fabriès, 2005a). The nature, degree and probability of exposure to these particles depend on the process and the phase of the work considered (Derk, 2010).

Songmene et al (2008b) showed that a tool worn 50% (flank wear of 0.15 mm) generates more metal particles during machining than a new tool and that this emission varies according to the type of material, as can be seen in Figure 2. The materials tested in the case of Figure 2 are aluminium alloys (6061-T6 and A356), brass 70/30 and magnesium alloy (AZ91E).

Similarly, Djebara et al (2013) showed that machining conditions (tool coating, cutting speed, feed rate and the interactions among these conditions) affect the specific surface area of fine particles (PM2.5). It is therefore interesting to see whether this applies to NP, especially since it is recommended to use this metric, or failing this, the number concentration, to study NP and ultrafine particles, because it is known that there is a better correlation between the specific surface area of these particles and their toxicity (Witschger and Fabriès, 2005a).

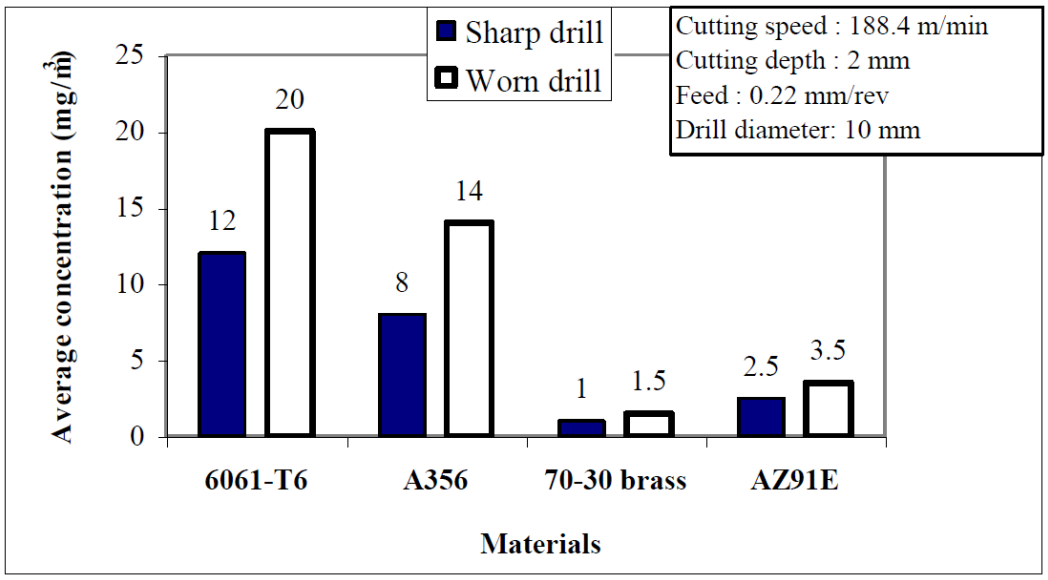

Figure 2 – Influence of the condition of the tool and the materials of the workpiece on microparticle ($PM_{2.5}$) emissions during drilling (Songmene et al, 2008b).

Balout et al (2007) and Songmene et al (2008a) explained dust generation by shearing, deformation and friction phenomena. The dust-generating zones are described in Figure 3 and represent the particle emission zones in the case of a groove milling operation: shear zone, deformation and chip fall zone, tool-chip friction zone and tool-workpiece friction zone.

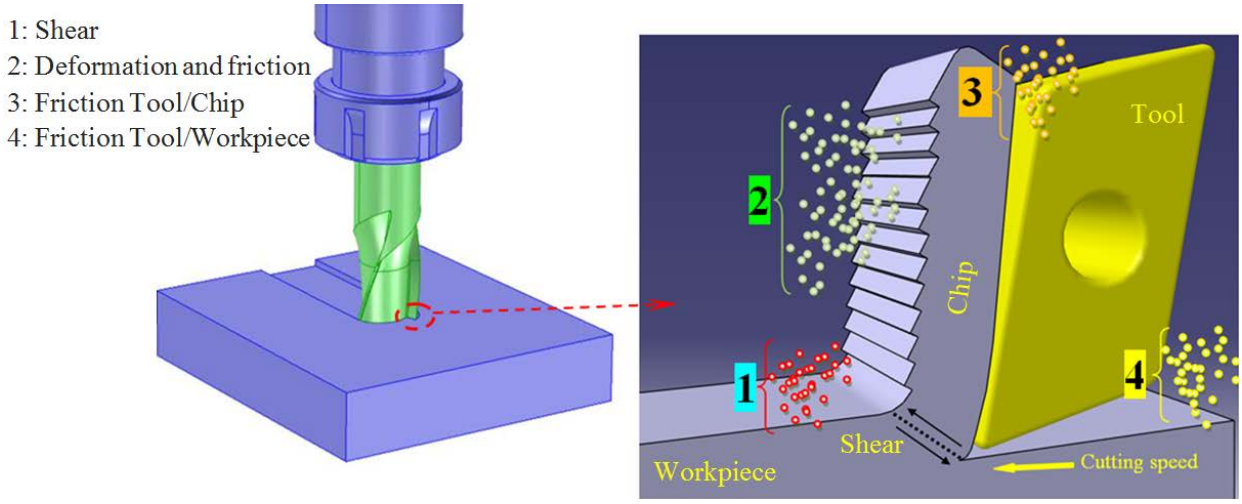

Figure 3 – Dust production zones in the case of milling. Adapted from Balout et al (2007) and Songmene et al (2008a), by Djebara (2012).

It was shown that a correlation exists between chip shape and particulate emissions during cutting of metal matrix composites (Kremer, 2009; Kremer and El Mansori, 2009). If chip formation is controlled, particulate emissions can also be controlled (Balout et al, 2007). Kremer (2009) observed that composites containing 25% SiC and which have not been heat treated produce between 3 and 23 times fewer dusts than those subjected to structural hardening (T4 treatment). Note that Kremer (2009) did not study nanoparticle emissions, which has yet to be done.

Since 2002, ÉTS researchers have studied dust generation during dry machining processes (less costly and offering chip recycling possibilities) with a view to source reduction of the production of these effluents. These studies, most of which deal with drilling and focus on microparticles, have made it possible to:

- Develop new cutting strategies that reduce generation of metal particles (PM2.5) by a factor of 10, while maintaining competitive productivity (Songmene et al, 2008b; Balout et al, 2007).
- Establish that dust is produced by micro-friction of the deformation planes against each other (Balout et al, 2003, 2007; Khettabi et al, 2008). Any mechanism that suppresses this micro-friction will significantly reduce particle production.
- Show that dust production diminishes under specific cutting conditions (Songmene et al, 2007, 2008b; Khettabi et al, 2007).
- Show that ductile materials produce more micrometric dusts than fragile materials. They have also designed a new cutting strategy that favours generation of fragile chips and reduces dust generation by at least 70% (Balout et al, 2007).

2.2.4 Progress in the study of airborne NP behaviour

The determination of NP exposure levels depends on the refinement of experimental techniques, particularly by the use of appropriate exposure metrics. Parallel to the experimental aspect, digital simulation can be used advantageously as an exposure level forecasting tool. However, a precise characterization of the aerodynamic behaviour of NP requires that several parameters be taken into account. Currently, no model exists that allows simultaneous consideration of all the phenomena governing the aerodynamic behaviour of nano-aerosols. In the current state of knowledge, the work addresses the parameters considered most important. One of them is Brownian diffusion, which results in the statistically random motion of particles subject to the effect of collisions with neighbouring molecules. This Brownian motion can be characterized by a diffusion coefficient (Hervé-Bazin, 2007). Hinds (1999) calls on the Stokes-Einstein equation to express the diffusion coefficient as a function of particulate mobility. The resulting expression indicates that the diffusion coefficient is proportional to the ambient temperature and inversely proportional to the square of the diameter of the particle. Rudyak et al (2001) presented the outcomes of an analysis based on molecular dynamics to determine NP diffusion in a dense medium. The authors compared their model to the diffusion coefficients obtained from Einstein's theory.

All this work provides very useful information on the order of magnitude of the diffusion coefficient as a function of the aerodynamic diameter of NP. However, the coefficients obtained vary according to the approach used. It is clear that other research will be necessary to determine the NP diffusion coefficient with greater accuracy. Moreover, although diffusion is responsible for the transport of NP over distances ranging from tens to hundreds of μm, transport on the macroscopic scale is mainly governed by "turbulent diffusion". Given the flow rates usually observed in industrial ventilation, Vincent (1989) estimated that this "turbulent" diffusion coefficient is significantly higher than the Brownian diffusion coefficient. This finding indicates that, in practice, the process of transport of NP by diffusion is primarily governed by turbulent effects.

The coagulation mechanism is another factor to consider in predicting NP behaviour. Contrary to gas molecules, aerosol particles that collide will tend to adhere to each other to form aggregates, which will change the particle size distribution over time. However, few studies exist on the subject. We can cite the work of Park et al (2002), who present a temporal evolution model of the particle size distribution of an aerosol due to Brownian and turbulent coagulation. Hinds (1999) insisted that it is necessary to differentiate two types of coagulation: a) monodisperse coagulation, which involves NP of identical diameter, and b) polydisperse coagulation, for which the NP diameters exhibit a certain distribution. In the case of a monodisperse aerosol, Hinds' data (1999) suggests the agglomeration phenomenon is negligible if the particle concentration is lower than 10^5 particles/cm^3. Polydisperse coagulation involves highly complex relationships.

This analysis shows remarkable progress in the understanding, forecasting and source reduction of micrometre-sized particles, but much still has to be done regarding NP, particularly:

- Refinement of the nanoparticle measuring method;
- Characterization of the behaviour of these airborne particles (at rest or drawn into a fluid in motion) and the influence of this behaviour on measurement;
- Development of a measuring standard, including correction factors relative to the shape, size, density, degree of agglomeration and chemical composition;
- Design of emission maps of common fabrication processes, and development of NP reduction or prevention strategies;
- Creation of rapid, efficient, portable detection instruments accessible to small and medium enterprises.

2.3 Research objectives

The main objective of this project was to develop an NP measuring, control and characterization procedure. This procedure then was applied to the fabrication processes and to friction, in order to define these processes in terms of NP production. The specific objectives were to:

i) Develop a procedure for measurement and characterization of NP produced in a controlled environment (machine tool enclosure);

ii) Study the behaviour of airborne NP to refine measurement and limit particle losses in the different measuring systems;

iii) Apply the procedure to the evaluation of a metal workpiece fabrication process and the study of friction between two workpieces, thus simulating certain braking methods;

iv) Design source reduction strategies for NP produced by the two above-mentioned processes.

The study of metal cutting processes allowed us to show the influences of the cutting tool (geometry and coating), the cut materials and the cutting conditions and parameters on NP emissions. Similarly, the friction study allowed us to quantify the contribution of friction to NP emissions during machining, as well as informing us about the influence of the parameters, such as rubbing speed.

This project was not about the toxicity of NP, but rather the development of an efficient measuring and characterization method, and the search for factors that could limit the generation of NP considered hazardous by toxicologists. In the longer term, we plan to develop NP source reduction strategies, applying the effects of the tools and cutting conditions studied.

3. RESEARCH METHOD

3.1 Procedure for studying NP emissions during machining and friction

We conducted machining and friction tests at the ÉTS Fabrication Laboratory on industrial-calibre machine-tools and measuring instruments (Fig. 4): high-speed machine-tool (maximum rotation speed: 30,000 revolutions per minute; maximum torque the machine can withstand: 50 Nm). This machine tool was connected to a particle suction, filtration and treatment system with a capacity of 1.5 m^3/h. During the machining tests, the tool cut the metal and a sampling device brought particle-loaded air to measuring instruments. Table 1 summarizes the machining parameters and conditions used.

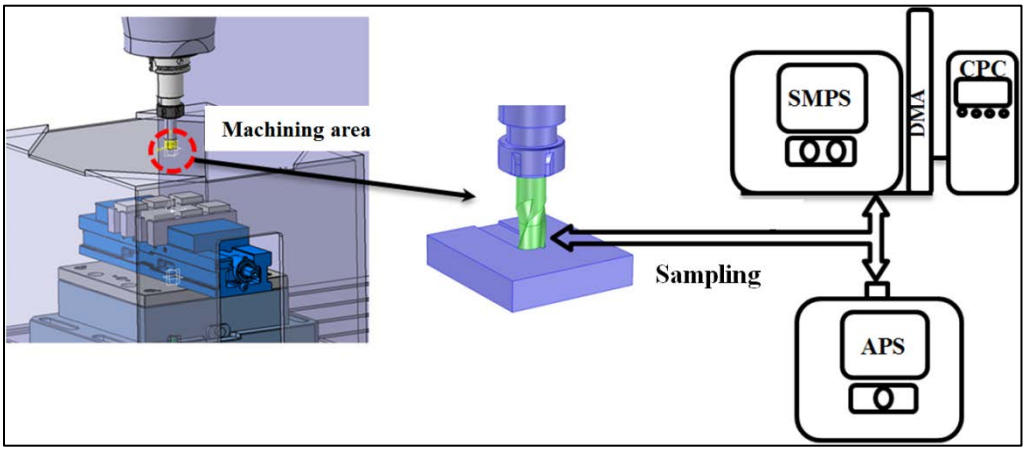

Figure 4 – Experimental device: Machine tool and particle measuring system: SMPS + DMA+ APS + CPC.

Table 1: Machining parameters used in the experimental study.

Factors		Factor level		
		1	**2**	**3**
A: Cutting speed (m/min)		300	750	1200
B: Cutting feed rate per tooth (mm)		0.01	0.055	0.1
C: Cutting depth (mm)		1	2	
D: Workpiece material		Al 6061-T6	Al 2024-T351	Al 7075-T6
E: Cutting tool (Iscar Ref: E90A-D.75-W.75-M); 3 teeth	Ref.	IC 328	IC 908	IC 4050
	Coatings and hardness	TiCN 2400 HV	TiAlN 3000 HV	TiCN+Al2O3+TiN 2400 HV
	Corner radius (mm)	0.5	0.83	0.5
F: Cutting fluid		None		

During the friction study, the workpiece was mounted on the same machine-tool table, and a rubbing tool, *also called a pin*, was mounted on the machine-tool spindle instead of the cutting tool (Fig. 5). Two setups were studied: a first case, called "Setup 1", in which the pin was rotating around the same centre spot, and a second case, called "Setup 2", in which the pin was driven by two motions: a rotational movement and a translatory movement. The first setup was similar to the braking mechanism of cars and trains, while the second simulated the friction that occurs between a tool and a workpiece during machining (zone 4 of Fig. 3). The workpieces were aluminium alloy (6061-T6 and 7075-T6), while the pin consisted of an uncoated carbide cylinder, with a diameter of 19.05 mm. In the case of Setup 2, the pin rotated at predetermined speeds and moved along the workpiece at a constant feed rate of 50 m/min.

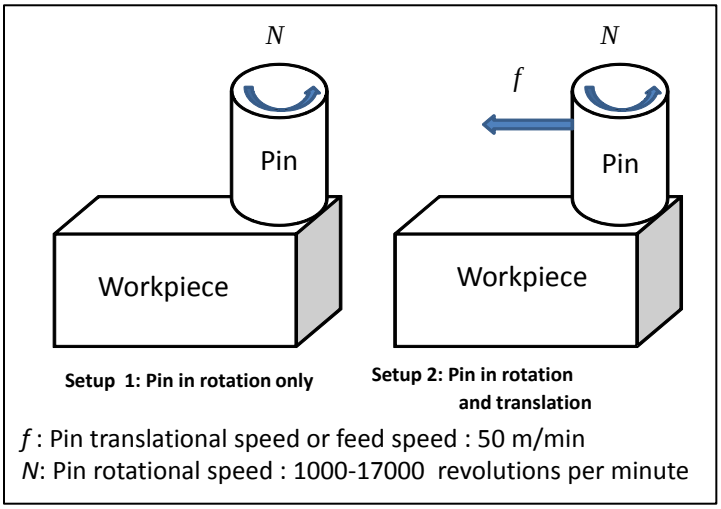

Figure 5 - Setup of workpieces used for the friction study (adapted from Kouam et al, 2010).

During the tests described above, the cutting forces were also measured to estimate the energy required for cutting and for friction. The information obtained on these forces allowed refinement of the particle emission prediction models during machining and friction. The chips were also collected to correlate chip formation and deformations with particulate emissions.

3.2 Study of the motion of particles in an air flow and integration with the measuring system

During a machining procedure, an additional difficulty in the study of particle generation arises from the fact that the processes generate air turbulence caused by the relative motion of the tool and the workpiece, which can alters the behaviour of the particles and can affect the precision of the measurement. Since the measurements were taken during machining (possibility of particle turbulence) and after machining, until the concentration reaches the same level as before the cutting operation, we note there was little chance that the total concentration would be largely affected by the tool's rotating motion. Nonetheless, a procedure for visualizing the displacement

of particles and the motion of the air during machining was designed and applied (Fig. 6). It consisted of using dry ice blocks and filming the motion of the dust released.

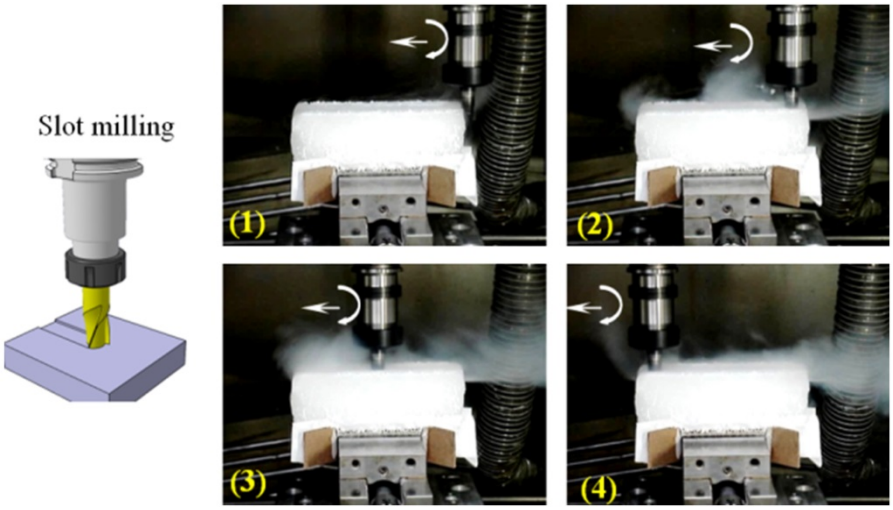

Figure 6 - Simulation of the direction taken by particles emitted during slot milling (750 m/min, 0.165 mm/revolution, tool diameter 19 mm).

Using this dry ice block machining approach, Djebara et al (2012) developed a procedure to show the behaviour of microparticles and NP in the vicinity of the cutting zone. This procedure, applied to drilling, grooving and face milling, revealed that NP trajectories are governed by the type of machining operation and the velocity field created by the motion of the tool; they also depend on the geometry of the cutting tool and the machining conditions. For example, in the case of slot milling (Fig. 6), most of the dusts produced are projected according to the machined slot in the opposite direction of the cutting feed rate. It should be noted that, in this figure, the tool is moving from the right of the block to its left and is filmed in positions 1, 2, 3 and 4. Knowledge of these trajectories allowed better positioning of the metal particle capture and/or measuring system during machine grooving tests. However, it was shown that the trajectory and the dispersion mode of the particle change with the processes (face milling, drilling, etc.).[2]

Likewise, digital simulation models were developed to improve the reliability of digital predictions by putting the emphasis on NP Browning and turbulent diffusion phenomena (Morency and Hallé, 2013; also see Section 5.1 of this report). This work allowed assessment and limitation of losses in the sampling and measuring systems, by limiting the length of the tubes.

[2] Djebara, Ph.D. thesis (2012), available on the ÉTS website (http://espace.etsmtl.ca/1014/) [Last consultation: February 10, 2014].

3.3 Particle sample capture and sample preparation procedures for microscopy

Sampling was assured by pumping or suction of the air from or near the cutting zone. An enclosure was used to confine the volume of air containing the particles emitted by the machining process. Measuring instruments were used to classify the particles according to their aerodynamic diameter or their electrical mobility.

A particle capture procedure was developed in the laboratory with a view to recovering particles on substrates so that they can be analyzed by microscopy (AFM and SEM) or by energy-dispersive X-ray diffraction, classic EDX. Two substrate types were used for sampling and characterization: metal (aluminium) substrates and polycarbonate (PC) substrates. The experimental sampling setup varied according to the type of substrate necessary for microscopic analysis. For the aluminium substrate, the particles were directed directly to the sampler (NAS), while for the polycarbonate substrate, a cassette was used upstream of the NAS as a pumping source, to suction the particles (Fig. 7).

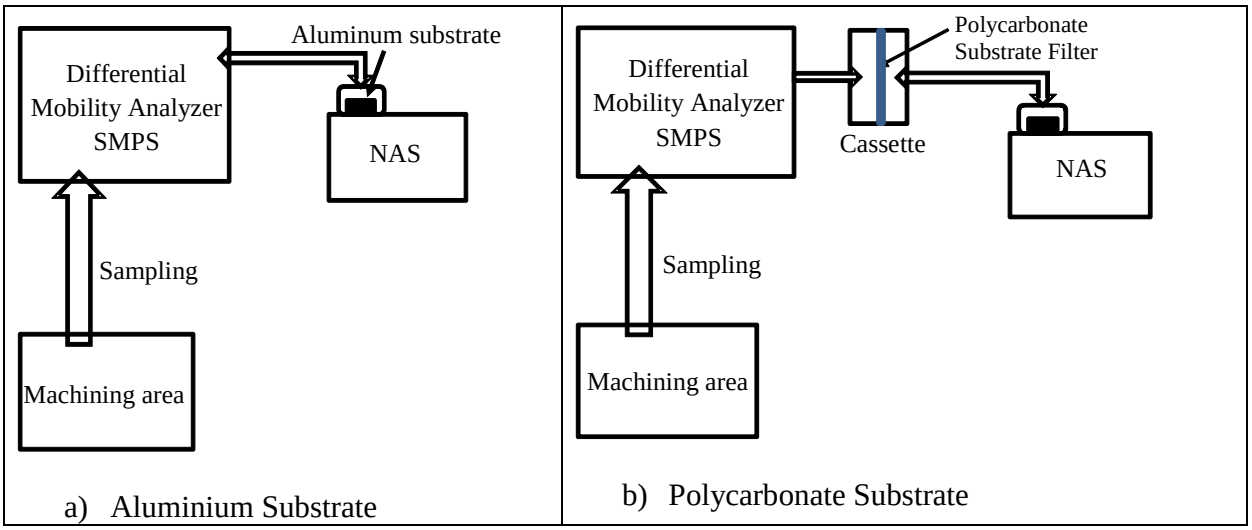

Figure 7 – Experimental setups for NP sampling by the SMPS and the NAS.

3.3.1 Setup of NP capture devices

Scanning Mobility Particle Sizer (SMPS): The Scanning Mobility Particle Sizer measures particle size distribution according to electrical mobility related to diameter, between 2.5 and 1000 nm. It uses a bipolar charger to establish a balance of known charges for the sampled aerosol. The particles are classified under the effect of an electrical field. The system using electrical mobility adopts the assumption that the shape of the particles is spherical. It is possible to select particle size according to the difference in potential imposed by the operator. In this way, it is possible to target a range of sizes and use a cassette with a substrate so that only particles of the desired size are collected. They then will be analyzed by microscopy. The SMPS

couples a particle selection technique based on mobility with a Differential Mobility Analyzer (DMA) and a Condensation Particle Counter (CPC). Measurement is precise, but the device has low mobility and is very expensive, over $100,000. Despite this high cost, the SMPS is one of the most commonly used instruments to measure the aerosol spectra in the size range from 2.5 to 1000 nm.

The instrument is composed of three main parts: the particle charger, the classification column and the particle detection system. Sampling is performed through an impactor (MOUDI). The particles with high inertia end their path on an impaction plate. The smallest particles with low inertia avoid any contact with the plate and exit the impactor via the 90° flow path. The aerosol then penetrates the Differential Mobility Analyzer (DMA), which classifies the particles according to the electrical mobility (proportional to the particle diameter). The DMA exists in two types of classification columns: a Long Differential Mobility Analyzer (LDMA) or a Nano Differential Mobility Analyzer (NDMA). After the monodisperse sample exits the DMA classifier, the monodisperse aerosol flows to a particle counter, which measures the number concentration. Once the unit is activated, the monodisperse sample enters the saturator, where it is exposed to distilled water vapour. The particle and the vapour then flow through the condenser, where the distilled water vapour condenses on all the particles. This phenomenon increases the initial size of the particles. These larger droplets then pass through a laser beam, and each droplet diffuses light. The diffused light intensity peaks are counted continuously and expressed as particles/cm^3 per second. For more information on the SMPS, refer to Witschger and Fabriès (2005b), Görner and Fabriès (1990) or the website of the manufacturer TSI.[3]

MOUDI: This device uses cascade impactors to classify particles according to their aerodynamic diameter (Fig. 8). The MOUDI can sample particles ranging in diameter between 56 nm and 10 µm (Table 2). For sizes smaller than 10 nm, the NANO-MOUDI is used. This device operates according to the same principle, except that low pressure is used for the lower stages. A suction pump with a flow rate of 30 l/min is connected to the impactors to ensure collection of the particles. To obtain better MOUDI efficiency, a coat of grease or oil is applied delicately to the substrates to avoid the rebound and resuspension phenomena. The MOUDI used for the ÉTS laboratory machining tests is the model 110 rotary with 10 impaction stages.

[3] http://www.tsi.com/scanning-mobility-particle-sizer-spectrometer-3936 [Last consultation: February 10, 2014].

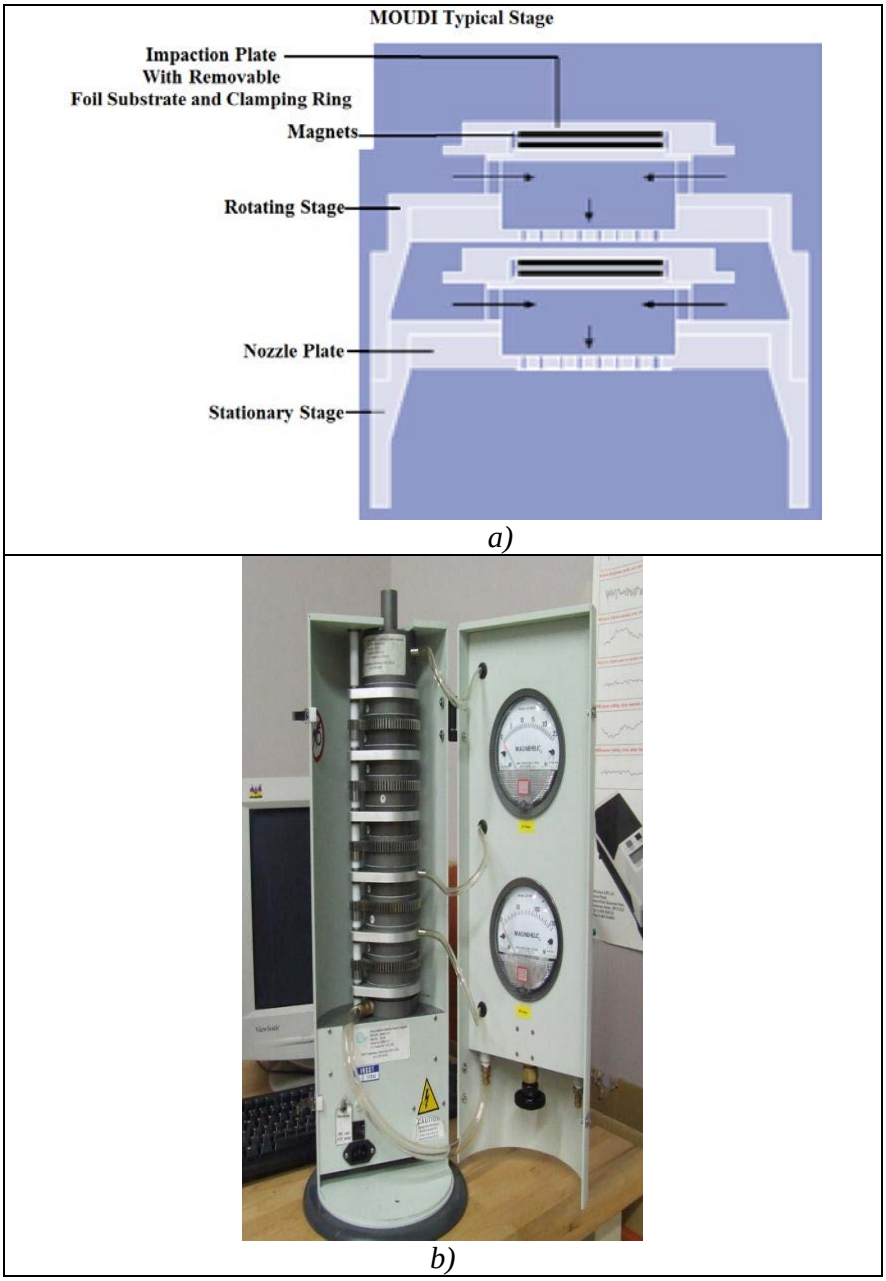

Figure 8 - Presentation of the MOUDI: a) Description of an individual stage, b) Structural overview of the stages.

The MOUDI setup is the same for the two substrate types. The substrates are placed on the MOUDI's different stages to recover the deposited particles, (Fig. 9). The substrates must be treated to prepare them for microscopic characterization.

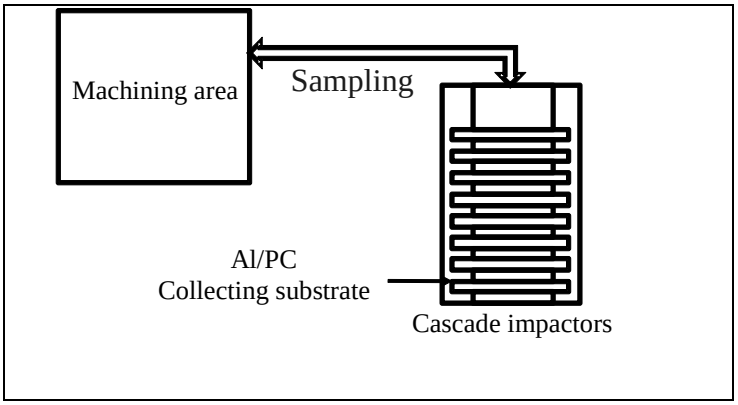

Figure 9 – Experimental setup for NP sampling by the MOUDI.

Table 2: The ten impaction stages of the MOUDI and the diameters of the particles corresponding to each stage.

MOUDI stage	Aerodynamic diameters of the particles at the cutting points (μm)
1	18
2	10
3	5.6
4	3.2
5	1.8
6	1.0
7	0.56
8	0.32
9	0.18
10	0.1
Filter	0.056

For sampling, a substrate is deposited on each stage of the impactors. The substrate must be flat and thin enough to be nested on the impactor plate by a clamping ring. Generally, aluminium substrates of 35 mm or 47 mm in diameter are used. One day before their use, the substrates must be dipped in methanol, washed in deionized distilled water and dried in the oven at 100°C for three hours, then stored in a clean place.

Nanometer Aerosol Sampler (NAS): With the NAS sampler, only one substrate is used to collect NP. An impactor serves to preselect the sucked-up particles. This instrument can sample only charged particles. The three possibilities are:

- Use the SAN substrate directly;
- Use another flat metal substrate, placed before collection on the NAS substrate: this will allow certain manipulations, such as the application of a metallization layer or transparization to use the substrate on the TEM;
- Use the NAS combined with the SMPS or the APS, as shown in Figure 7.

3.3.2 Substrate preparation procedure

To characterize NP, it was necessary to recover them on a substrate, which could be used in microscopy. As already mentioned, two substrate types were used for sampling: polycarbonate and metal. The polycarbonate substrates were prepared for use on the TEM. However, the SEM requires conductive substrates, which is why thin aluminium substrates were used.

For polycarbonate (PC) substrates, a protocol was developed at the IRSST. It consisted of the following steps:

- First metallization by carbon layer on the blank PC substrate to obtain a premetallized filter;
- Sampling on the premetallized filter;
- Second metallization after sampling;
- Transparization by transfer of a portion of the filter to a copper grid. This supported the sample sandwiched between two carbon metallization layers.

For aluminium metal substrates, several tests were conducted to determine an optimum preparation method for better characterization using the SEM or the AFM. Figure 10 shows a blank substrate before sampling.

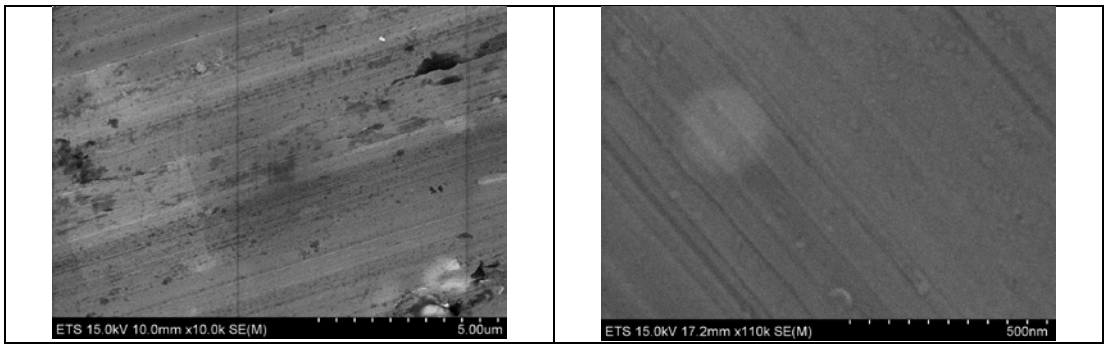

Figure 10 - Aluminium substrate without metallization.

For the SEM, the substrate had to be electrically conductive, flat and covered with a metallized layer after sampling, in order to ensure fixation of the particles (the application of the vacuum in the SEM could tear away the particles) (Fig. 11). This metallized layer consisted of a gold coating applied by a plasma deposit (EMITECH K550x Sputter Coater). This coating's thickness varies according to the size of the deposited particles. To ensure better NP analysis, it was therefore necessary to establish the optimum thickness of the metallization layer. For NP, different substrate metallization layer thicknesses were applied, namely 7 nm, 14 nm and 21 nm, with a blank substrate (uncoated). The outcomes shows that a 14 or 21 nm coating completely hides the nanometric particles and that the coating observed by the SEM is only the metallization layer (Fig. 12a and b). The 7 nm coating leaves a contrast between the sampled particles and the metallization layer (Fig. 12c).

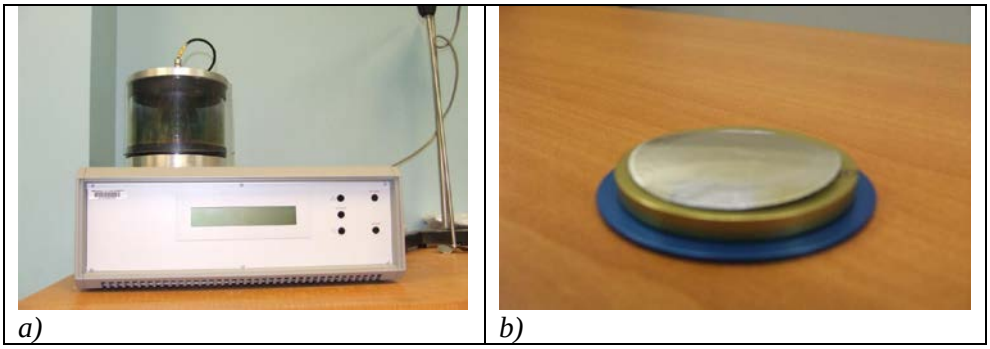

a) *b)*

Figure 11 - Metallization: a) EMITECH K550x Sputter Coater metallizer, b) substrate with deposit of a gold coating of around 7 nm.

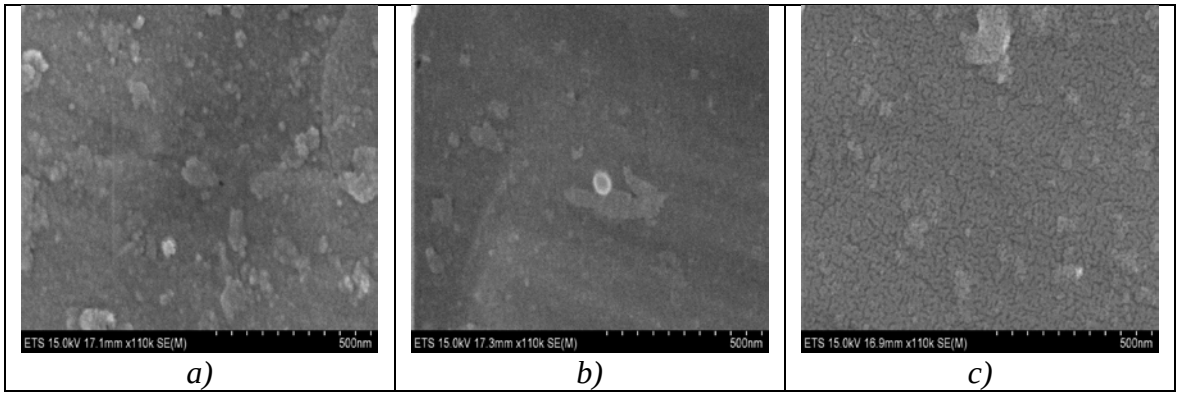

a) *b)* *c)*

Figure 12 – Different metallization layer thicknesses: a) 21 nm, b) 14 nm and c) 7 nm.

3.4 SMPS Characterization of NP concentrations

The NP emitted during the machining study or the friction study were characterized using instruments illustrated in Figure 4 and described in the following section. The system combined two equipment units to cover the ranges from 2.5 nm to 20 µm. Software made it possible to extract all the information coming from these two instruments and merge the outcomes. This system was composed of a Scanning Mobility Particle Sizer (SMPS) and an APS spectrometer. The SMPS provided, directly, the particle size distribution and the particle count for particle aerodynamic diameters ranging between 10 nm and 1 µm, while the APS allowed measurement of the distribution of particles with aerodynamic diameters between 0.5 and 20 µm.

The particles then were collected, either on a substrate placed on the sampler medium (TSI NAS 3089) by electrostatic precipitation, or directly on a separator stage by impaction (MOUDI). Next, the substrates were analyzed by microscopy (scanning, transmission, atomic force) to identify their composition and degree of agglomeration and to confirm their size and shape. For this purpose, the substrate preparation and microscopic analysis methods were adapted to the NP.

The first NP analyses performed during machining and friction operations, using the SMPS spectrometer, provided the number concentration, the mass concentration and the specific surface area concentration according to the sizes measured (aerodynamic diameter). These

concentrations were measured before, during and after the cutting process, until the return to the ambient concentration.

In the first place, the SMPS is based on classification of particles according to their electrical mobility to determine their diameter. These particles then are quantified by a counter, the CPC (Fig. 4), and the system gives the number concentration per cubic centimetre or air (#/cm^3) for each size (C^P). The other metrics, such as the mass concentration or total mass of the particles (C^M) and the mean specific surface area concentration, or surface concentration (C^S), were calculated by using formulas presented in Tableau 3.

Table 3: **Formulas and metrics used for SMPS characterization of NP**.

Number concentration	**Specific surface area concentration**	**Mass concentration**
C^P (#/cm^3)	C^S (nm^2/cm^3)	C^M (μg/m^3)
$\sum_l^u \frac{c}{tQ}\frac{\phi}{\eta}$	$\sum_l^u \pi D_p^2 \frac{c}{tQ}\frac{\phi}{\eta}$	$\sum_l^u \rho \frac{\pi D_p^3}{6}\frac{c}{tQ}\frac{\phi}{\eta}$

Where:

c: Number concentration by size (#/cm^3)

η: Efficiency factor

ϕ: Dilution factor

D_p: Particle mobility diameter (nm)

Q: Sampling flows (cm^3/s)

t: Sampling time (s)

ρ: Particle density (g/cm^3)

3.5 Other sampling instructions for SMPS or MOUDI instruments

3.5.1 Conditions of connection and operating conditions of the instruments

According to the studies performed by the different members of our team, it was necessary to take certain rules into account to increase measuring efficiency. Table 4 summarizes all these rules to ensure a standard approach that guarantees the conformity of the measurements.

Table 4: Experimental rules suggested for use of SMPS and MOUDI instruments.

	General rules to observe	**Purposes and comments**
1	Shorten the length of the suction tube	To avoid losses.
2	Choose the collection method	Recover the particles on a substrate or measure their concentration.
3	Define the suction flow rate	From 1.7 to 30 l/min to increase measuring efficiency.
4	Connect only one measuring system	The use of two or more systems will result in sharing of the quantity generated. The measuring systems are limited by the size ranges.
5	Calibrate the measuring instruments	Ensure that the instruments are working correctly.
6	Ensure the concentration level is the same and the lowest between tests	Be able to separate the operations and to determine the quantity generated by a single operation.
7	Ensure the repeatability of the outcomes	Verify the fluctuations of measuring outcomes.

A study conducted by François Morency and Stéphane Hallé of the ÉTS (Morency et al, 2008, Morency and Hallé, 2010) has already shown that the losses in the sampling tube can be considerable if the length, size and nature of this tube are neglected. To improve measuring efficiency, it was therefore necessary to increase the flow rate, render the tube conductive and shorten it as much as possible. However, the increase in the sampling flow rate can reduce the time the sampled air stays in the measuring device. For some devices, this can cause measuring errors. Indeed, these devices are equipped with a neutralizer of aerosol-borne electrical charges and use a radioactive bipolar charger, thus allowing neutralization of the incoming particles. These particles are charged under the influence of an ion field generated by a radioactive source of ^{85}Kr to satisfy the Boltzmann distribution. The neutralizer's precision and efficiency require a balanced charge distribution, which requires the particles to stay in the measuring device for a sufficient length of time.

3.5.2 Setting the charge, density and shape of the particles

The NP measuring devices present some limitations due to their method of use, as well as the charge, density and shape of the particles. The SMPS is considered to be one of the devices most often used in the measurement of NP with ELPI and NANO-MOUDI impactors. In this type of instrument, the sampled particle is charged and then it passes through an electrical field. The capacity to pass through this field thus depends on the charge of the particle, and the charge, in turn, varies according to the particle's size. The larger the particle, the more it can be charged. Before operating the instruments, it was necessary to configure the control software of these devices. Each instrument requires a specific procedure to set the charge, density and shape of the particles.

The ***particle charge*** problem is difficult to resolve. If the charge is multiple and is too high, the measurement may be wrong. When using the SMPS, the correction can be made directly by adequate configuration of the device, on condition that the polarity is known in advance. Other processes are used to solve the problem of the high electrical charge, such as unipolar diffusion charging (Covert et al, 1997; Kruis and Fissan, 2001) or photo-charging (Burtscher, 1992). The relationship between the electrical field applied and particle size can be obtained by the following equation, for the SMPS system (valid for long and nano DMA: LDMA and NDMA):

$$\frac{D_m}{C_C} = \frac{2Ne\overline{V}L}{3\mu q_{sh} \ln\left(\frac{r_2}{r_1}\right)} \qquad (3)$$

Where: D_m = Electrical mobility diameter;

$\overline{V}$ = Mean potential of the inner cylinder (V);

L = Classifier length (m);

q_{sh} = Flow rate in the classifier ($m^3.s^{-1}$);

r_1 = Inner radius (m);

r_2 = Outer radius (m);

N = Number of elementary charges borne by the particle;

e = Elementary charge (1.6×10^{-19} C);

C_C = Cunningham correction factor;

μ = Dynamic viscosity of the fluid ($\mu = 1.832 \times 10^{-5}$ Not for air, under standard temperature and pressure conditions).

The influence of activation or non-activation of multiple charges on measurement was verified in the laboratory. For milling of aluminium alloy 2024-T351, no significant difference was observed between the corrected data and the uncorrected data (Fig. 13) for the sizes studied (electrical mobility diameters smaller than 350 nm). A slight difference was observed for particles with diameters between 50 and 200 nm. For particles larger than 200 nm, the correction given by the SMPS analysis system is largely sufficient. The larger the particle, the less

necessary it seems to correct multiple charges. This outcome still has to be conformed for other alloys used in industry.

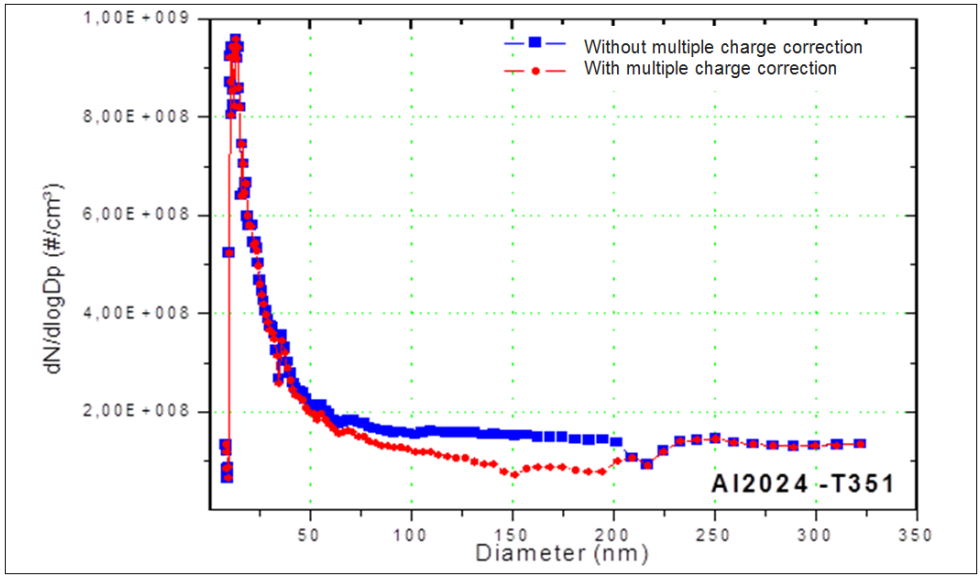

Figure 13 – Influence of correction of multiple charges on particle size distribution.

The efficiency of the aerosol charge neutralizer in the case of the SMPS can be limited by the highly charged particles. However, when the flow rate is high, the performance of the aerosol charge neutralizer drops. To obtain a balanced charge distribution, it is necessary to have a long enough particle residence time in the system. The ion concentration and the residence time must be high enough to obtain good outcomes. The correction of particle diffusion is also necessary and must be accomplished for particles smaller than 100 nm.

The other factor that must be corrected, also related to the shape and nature of the particle, is ***density.*** It is important to know the density of the particles in advance in order to introduce this data into the configuration of the device. Density can be estimated only after characterization of the sampled particle. The shape and reactivity of the particles considerably affect the density. If the sampled air contains particles of different densities, the resolution becomes complicated, and even impossible. Most measurements give concentrations according to the aerodynamic diameter or the electrical mobility of the particles (based on the assumption that the particles are spherical, which is not always the case). Based on the particle shape analysis outcomes, correction factors accounting for the shape and density of the particles can be developed.

The correction procedure and equations accounting for the shape and density of the particles are presented in detail in Chapter 3 of Djebara's Ph.D. thesis (2012).[4]

[4] Thesis available on the ÉTS website (http://espace.etsmtl.ca/1014/) [Last consultation: February 10, 2014].

4. OUTCOMES AND ANALYSES

4.1 Microscopic characterization of particle shapes and composition

4.1.1 Characterization by scanning electron microscopy (SEM)

The scanning electron microscope used has a microanalyzer (EDX) that allows collection of the photons produced by the primary electron beam. The X-ray detector is able to determine the energy of the photons it receives. By analyzing these rays, information is obtained on the chemical nature of the atom. Figures 14 and 15 show particles collected during milling of a workpiece and analyzed by SEM. This analysis allows the following findings:

- The particles emitted are oxidized (Fig. 14). The chemical analysis performed shows the particle is made of aluminium and oxygen (quantitative outcomes, Fig. 14), and thus aluminium oxide. Consequently, the density introduced in the measuring instruments must be adjusted to account for the fact that aluminium oxide is involved, and not only aluminium.
- The shape, distribution and degree of agglomeration of the particles obtained during milling vary according to the cutting speed (Fig. 15). The particle size is generally smaller than 100 nm (Fig. 15a, c and d), but depending on the degree of agglomeration, it is possible to find agglomerates that appear to be larger.

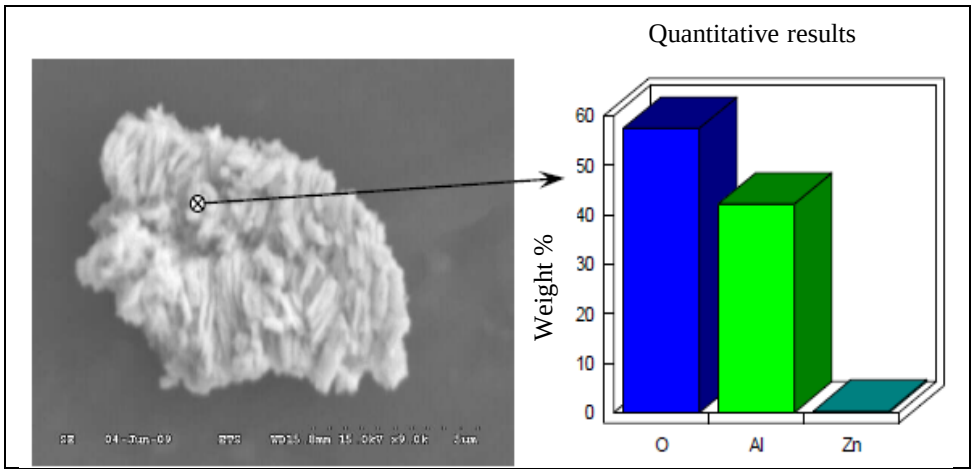

Figure 14 – Example of particle emitted during milling of Al7075-T6, analyzed by SEM (Al: aluminium, O: oxygen).

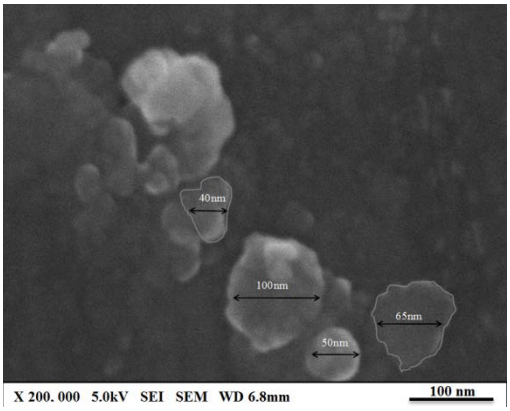

a) Speed: 100 m/min

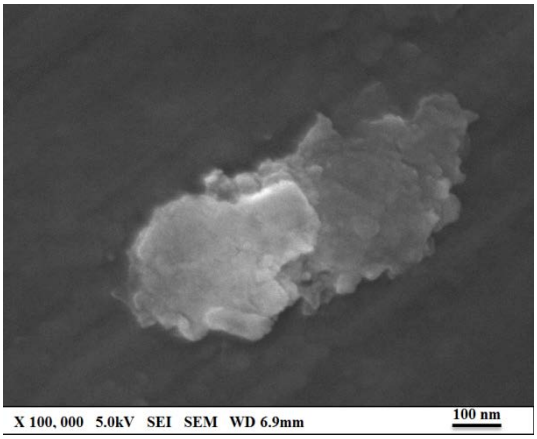

b) Speed: 150 m/min

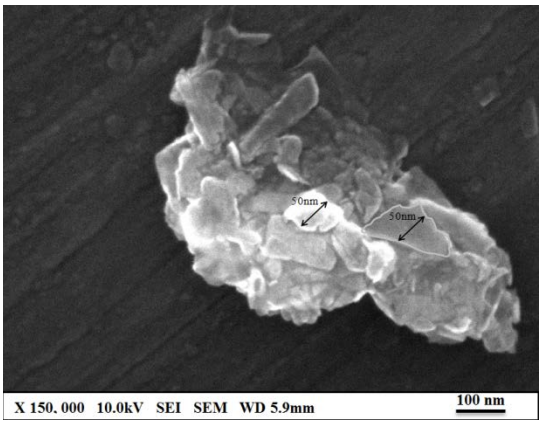

c) Speed: 300 m/min

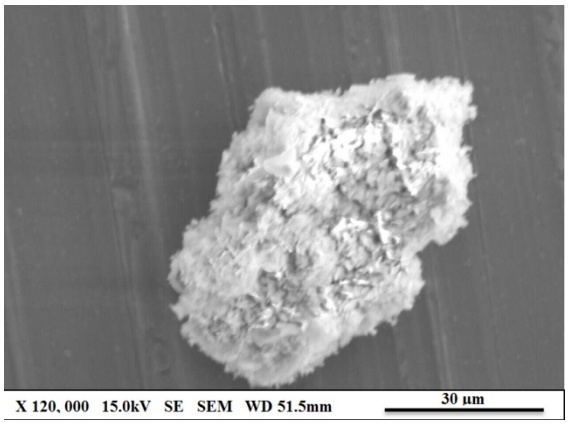

d) Speed: 750 m/min (agglomerate)

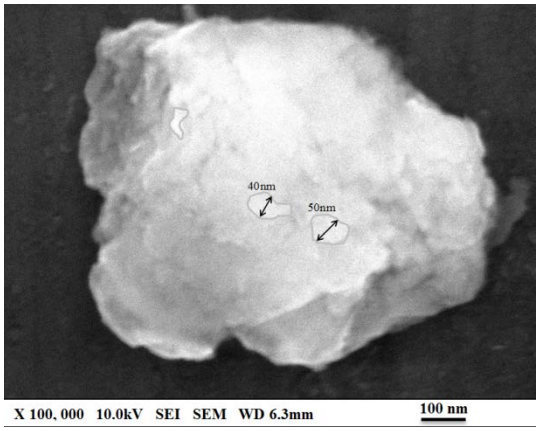

e) Speed: 1200 m/min (agglomerate)

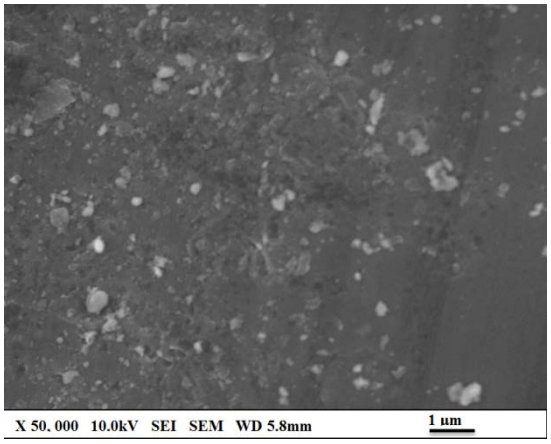

f) Speed: 750 m/min, distribution

Figure 15 –SEM images of particles obtained during milling, depending on cutting speed.

The microscopic analysis also showed different shapes of heterogeneous NP, in addition to agglomerates (Fig. 16). This morphology depends both on the nature of the material constituting the particles and the generation mechanism. Likewise, NP agglomeration also does not lead to the production of spherical particles. In general, two main morphological families could be distinguished:

- nano-isometric particles, which have essentially the same dimensions in all three dimensions (Fig. 16 a and b);
- agglomerates (flat particles): these are particles which have two dimensions larger than the third (Fig. 16c).

This information on shape will be very useful during correction of the measurement (Section 4.2 of this report), because the default data of several devices is based on the assumption that the particle is spherical.

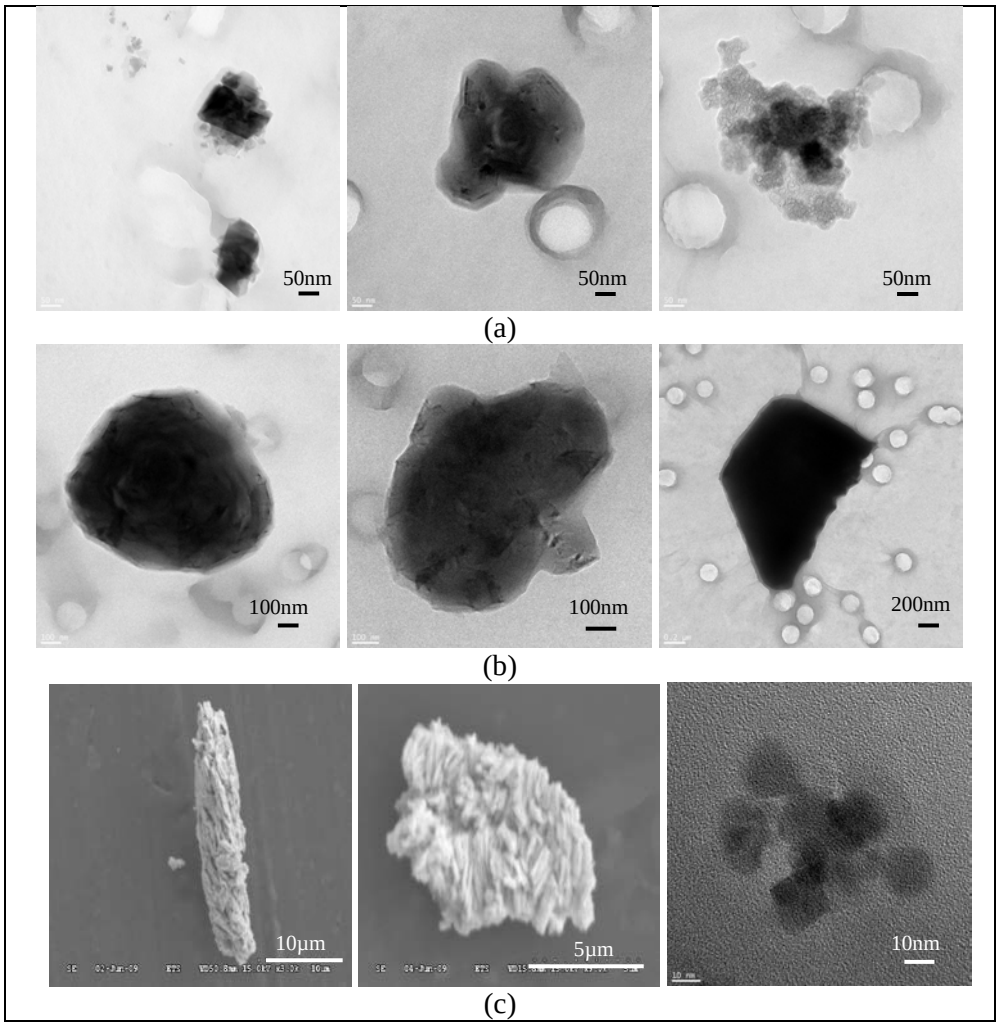

Figure 16 – Morphological families of particles produced during machining: (a, b) nanoparticles and (c) agglomerates.

4.1.2 Characterization by transmission electronic microscopy (TEM)

The polycarbonate substrates did not produce satisfactory outcomes neither with the transmission electron microscope nor with the scanning electron microscope. The TEM was unable to detect particles. The origin of the problem may be the preparation of the grids. This point must be resolved to be able to use TEM to characterize metal NP generated by machining or by friction.

4.1.3 Characterization by atomic force microscopy (AFM)

The same substrates analyzed by SEM were used in atomic force microscopy (AFM). AFM is used only for better viewing of the shape of the particles and for confirmation of the existence of agglomerates. Similar outcomes therefore were obtained by AFM, but in three dimensions (Fig. 17). The shape, the distribution and the degree of agglomeration depend on cutting speed, among other factors. Analyzing the shape of three-dimensional particles increases measurement precision and the efficiency of the devices used, allowing NP size to be obtained in the third dimension, which serves to calculate the correction factor with a more precise spatial resolution and a minimal error ratio.

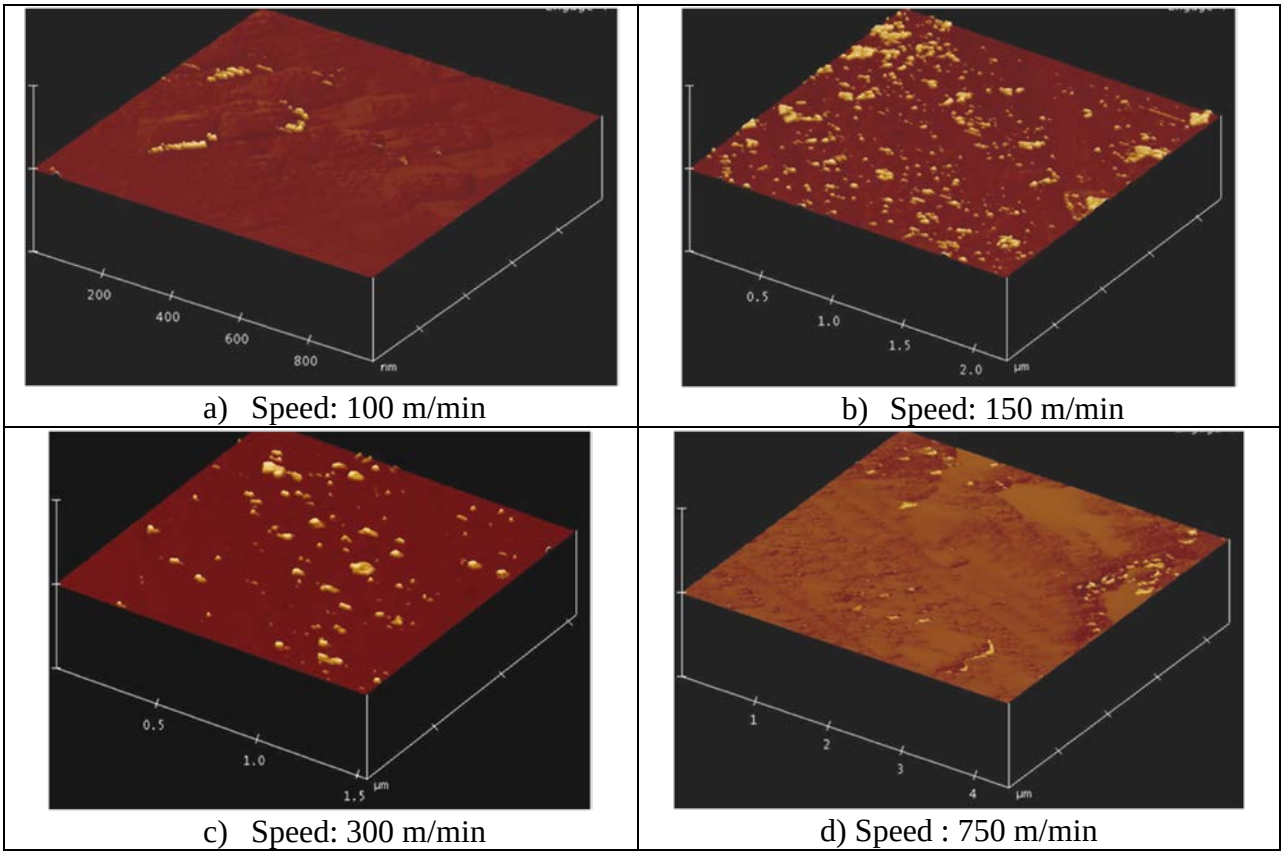

a) Speed: 100 m/min

b) Speed: 150 m/min

c) Speed: 300 m/min

d) Speed : 750 m/min

Figure 17 – Images obtained by AFM of particles generated during machining, depending on cutting speed.

In our study, the bidimensional analysis showed the irregularity of the shape of the particles. The development of correction based on these outcomes was a major success, but the future use of

AFM will certainly increase measurement precision. The analysis of the outer face of a chip produced during milling shows it is very likely that the emission of a large quantity of dusts occurred during chip shearing and segmentation (see the particles identified on the face of the chip, Fig. 18).

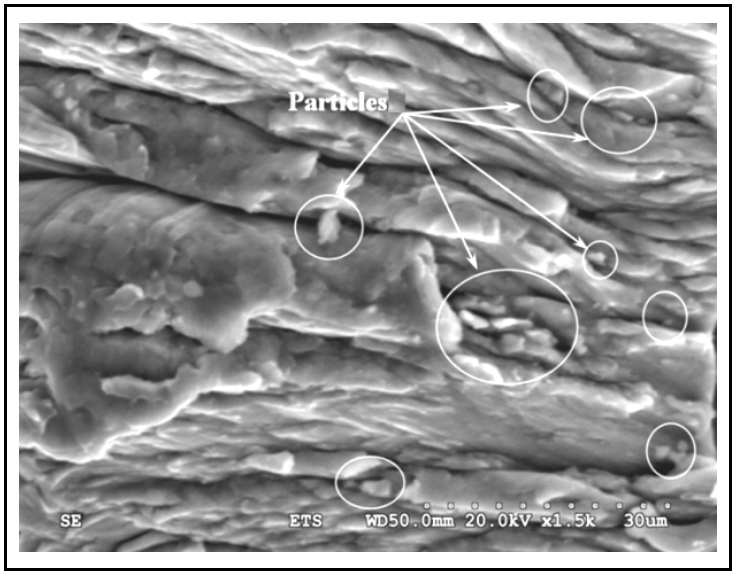

Figure 18 - Image obtained by SEM of a chip, showing particles emitted in the segmented zone of this chip (Djebara, 2012).

4.2 Correction of data depending on the shape, morphology and nature of particles

Before presenting the correction outcomes, it is necessary to recall the theory and the assumptions used by most measuring instruments. Generally, solid NP come in highly variable shapes, contrary to liquid NP, which can be likened to spheres. The determination of the parameters characterizing solid NP therefore call for different techniques to ensure a correction in relation to the morphology. A particle in motion within a measuring instrument is subjected to forces distributed on the surface, depending on the neighbouring gas, its physical state, its relative speed and, of course, the corpuscular shape and its surface roughness. The resultant of these forces that influence measurement can be divided into a component directed in the opposite direction of the velocity, called resistance or drag, and a perpendicular component called lift, in aerodynamics (Fig. 19).

Non-spherical particles generate more drag than their equivalent volume or spherical mass, because they present a larger interaction surface with the neighbouring air. If the drag force is expressed as a function of the diameter of an equivalent volume, a second correction factor must be used to offset the increase in drag due to the non-spherical shape. This correction is linked to a factor called the "dynamic shape factor χ" (Fuchs, 1964). It is defined as the ratio between the resistance force F^{P}_{drag} (drag force) on the non-spherical particle considered and the resistance

force F^{ev}_{drag} exercised by the spherical particle of equivalent volume, when the two particles move at the same speed relative to the gas (Hinds, 1999):

$$\chi = \frac{F^{p}_{trainée}}{F^{ev}_{trainée}} \qquad (4)$$

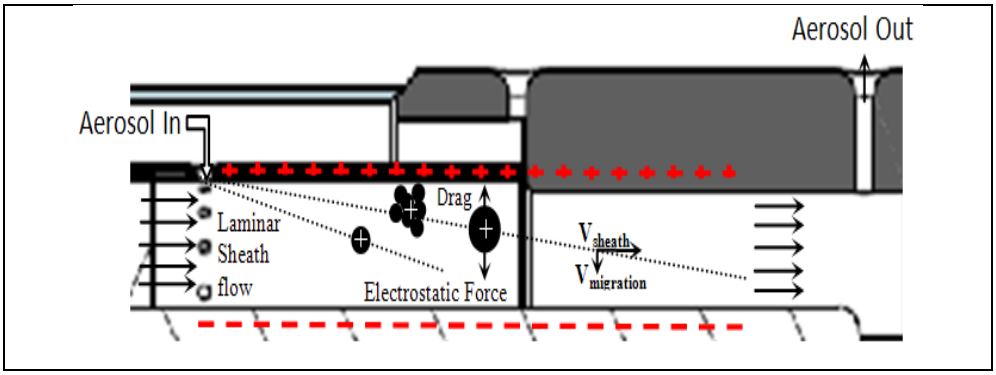

Figure 19 – Representation of a particle in motion in a measuring instrument.

The physical behaviour of aerosols most often is established for spherical particles, while in reality, they are rarely spherical (see Figs. 16 to 18 of the previous section). For the SMPS, measuring this distribution depends on the principle of selection of particles according to electrical mobility, making assumptions on the particles' spherical shape and density. The outcomes have been corrected for the following two shapes:

- For a size smaller than 100 nm, the particle belongs to the nano-isometric morphological family (elongated spherical shape);
- For a size greater than 100 nm, the particle belongs to the nanoplate morphological family (thin parallelepipedic shape or thin disk).

Table 5 and Figure 20 present examples of corrected data. The SMPS raw data varies by size class. It is important to remember that in the case of particles generated during machining, the measured diameter is one of equivalent mobility (D_m), meaning the diameter of a sphere that would behave identically to the measured particle, if this sphere were in the same electrical field. The number concentration is then calculated from the measurement of the electrical charge carried by the particles (see Eq. 3 and Table 3). Microscopic analysis of the particles is used to assess the parameter of the size called "volume-equivalent diameter" (D_{ev}). It corresponds to the diameter a sphere of the same volume as the particle would have and it allows estimating of particle density.

In the case of particles generated during machining, the D_{ev} can be expressed as a function of the shape of these particles and is calculated from the correction factor introduced for non-spherical shapes. The shapes and populations are then adapted manually (using the Excel spreadsheet) to

describe the distribution by the SMPS as well as possible. The correction of the raw data is thus applied to each response before any analysis.

Table 5: Examples of corrections of concentrations given by the SMPS for distribution of machining metal particles.

Raw data				Corrected data			
Diameter D_m (nm)	**C^P (#/cm³)**	**C^S (nm²/cm³)**	**C^M (µg/m³)**	**Diameter D_{ev} (nm)**	**C^P (#/cm³)**	**C^S (nm²/cm³)**	**C^M (µg/m³)**
14.1	1.62E+03	1.01E+06	0.0185	9.6	1.62E+03	4.65E+05	0.0018
14.6	1.46E+03	9.78E+05	0.0185	9.9	1.46E+03	4.50E+05	0.0058
15.1	4.76E+04	3.41E+07	0.6720	10.2	4.76E+04	1.57E+07	0.2096
49.6	2.29E+05	1.77E+09	113.8216	33.6	2.29E+05	8.14E+08	35.4992
51.4	2.27E+05	1.88E+09	126.2952	34.9	2.27E+05	8.66E+08	39.3895
53.3	2.29E+05	2.04E+09	141.8872	36.1	2.29E+05	9.40E+08	44.2524
94.7	2.54E+05	7.16E+09	880.9480	64.2	2.54E+05	3.29E+09	274.7540
98.2	2.68E+05	8.12E+09	1036.8680	66.6	2.68E+05	3.73E+09	323.3831
101.8	2.81E+05	9.15E+09	1208.3800	69.0	2.81E+05	4.21E+09	376.8750
105.5	2.88E+05	1.01E+10	1379.8920	71.5	2.88E+05	4.63E+09	430.3669

D_m: mobility equivalent diameter; D_{ev}: volume-equivalent diameter
C^P: number concentration; C^S: specific surface area concentration; C^M: mass concentration

Table 5 compares the raw outcomes and the corrected outcomes, using the equations from Table 3. The manual correction of the concentrations must be based on a volume-equivalent diameter, regardless of the distribution level. As could be expected, the correction affects the specific surface area and the mass concentration, but not the number concentration.

Figure 20 represents the correction of our raw outcomes. Based on this correction, one can remark that the morphology and density of the particles have significant effects on the measurement of the particle concentrations (overestimation by a factor of 2) and on the distribution of these particles by diameter.

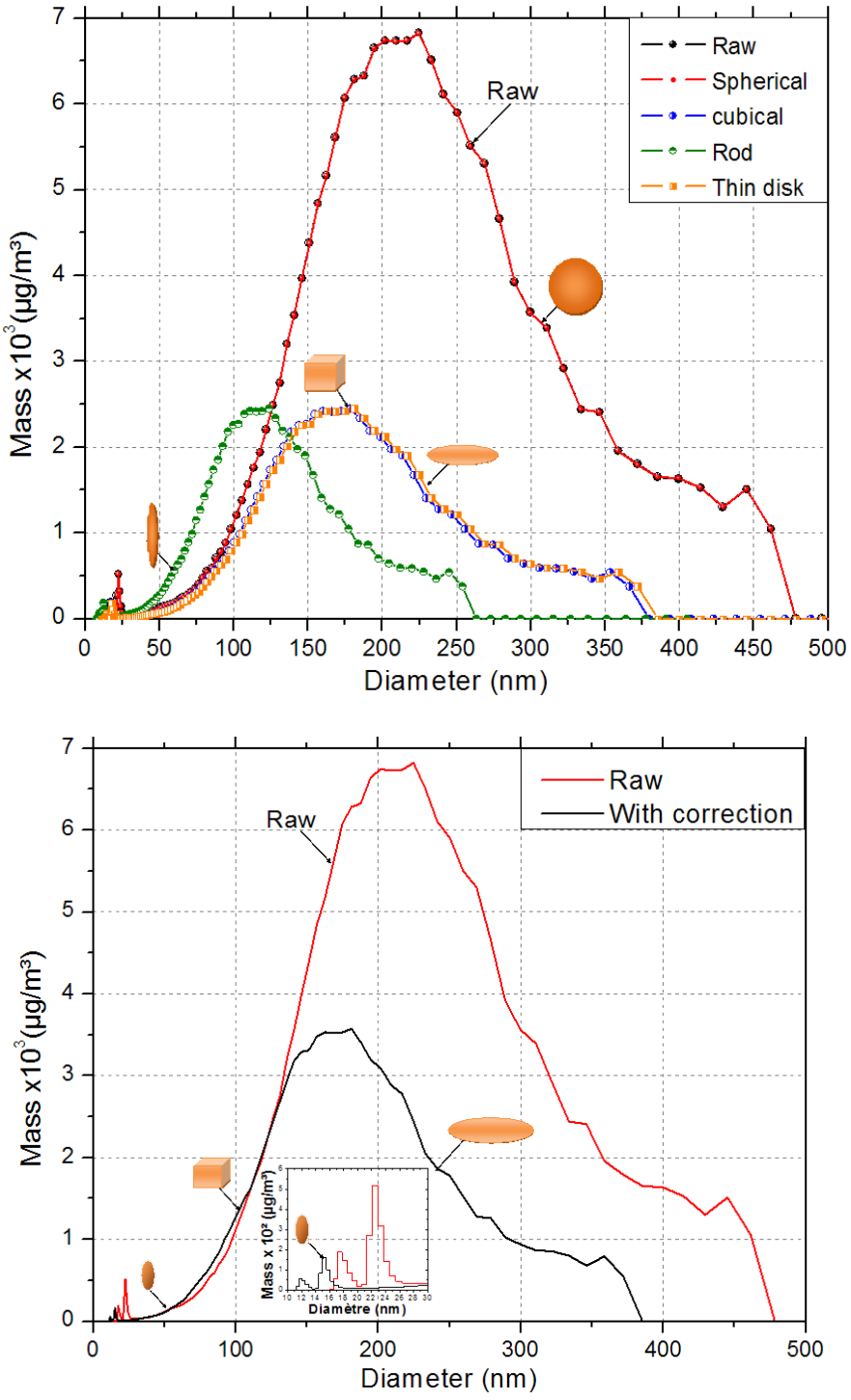

Figure 20 – Effects of shape correction on the mass distribution of ultrafine particles as a function of their diameter (taken from Djebara, 2012).

4.3 Study of NP emissions during friction

Many mechanisms involve friction (braking of cars and trains, for example). During friction, two materials come into contact and the interfacial interactions play an important role. The friction tests were conducted by using the procedure and the setup described in Section 3.1. Remember that two setups were used: a mechanism similar to the one allowing braking of cars and trains (Fig. 5, Setup 1) and another mechanism simulating friction between a tool and a workpiece during machining (Fig. 5, Setup 2). In the case of Setup 2, the tool (pin) turned at predetermined rotation speeds and moved along the workpiece at a constant feed rate of 50 m/min.

Figures 21 and 22 present the total concentrations in number of NP emitted during friction of aluminium alloys 6061-T6 and 7075-T6, respectively. Figure 23 illustrates the number concentrations of NP emitted during milling, compared to those obtained during friction in the case of aluminium alloy 6061-T6.

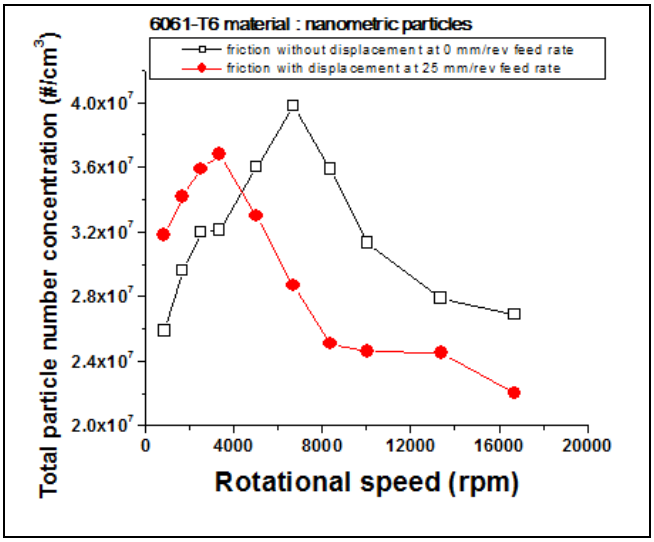

Figure 21 – Number concentration of NP (7-500 nm) generated during friction with the tool in rotation only or combined with one translation, for aluminium alloy 6061-T6.

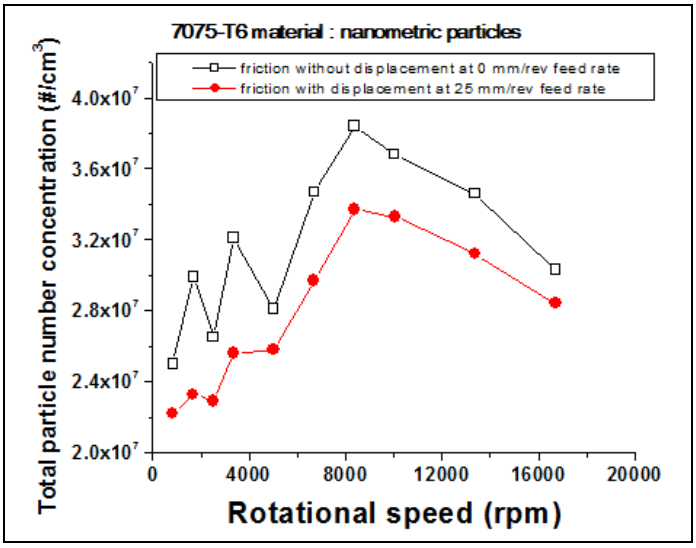

Figure 22 - Number concentration of NP (7-500 nm) generated during friction with the tool in rotation only or combined with one translation, for aluminium alloy 7075-T6.

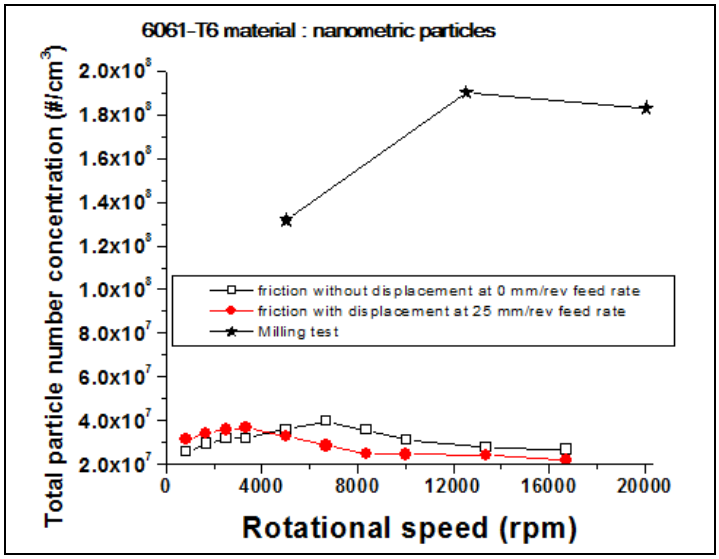

Figure 23 - Number concentration of NP (7-500 nm) generated during friction (with or without translation) and milling for aluminium alloy 6061-T6.

These outcomes made it possible to demonstrate the following:

- In general, more NP are emitted when the tool turns in place than when the rotating tool moves in translation (Figs. 21 and 22). It therefore follows that friction during which the surface contact is constantly renewed (case of friction between the tool and the workpiece during machining), produces fewer NP than when the tool or the slug turns in place (Kouam *et al.* 2011).

- The existence of critical rotation speeds at which NP emissions are maximum was confirmed for friction (Figs. 21 and 22). In the case of friction, depending on the angular speed, NP are emitted at a maximum corresponding to a critical speed. The intermediate speed range between the low and high speeds must therefore be avoided to reduce source NP production (Kouam et al, 2011).
- However, friction produces much fewer NP than the milling process, as shown in Figure 23. For the tested aluminium alloys 6061-T6 and 7075-T6, the number concentration obtained from friction was 2 to 10 times lower than the one obtained during milling (Kouam et al, 2011).

4.4 Study of NP emissions during machining

In Section 4.1, we presented the characterization of the different shapes and the composition of the particles obtained during milling. The effects of the materials of the workpiece and the tool, and the effects of the cutting conditions, were also studied for other machining processes during this project. The drilling tests performed revealed that the presence of a pre-drilling hole results in the emission of a greater quantity of particles smaller than 10 µm, but the critical cutting speed for which the emissions are maximum remain unchanged (Figs. 24 and 25).

However, cast aluminium alloys (Fig. 25), which are considered to be fragile materials, emitted fewer particles than wrought alloys (Fig. 24), which are considered ductile materials. This confirms the outcomes of Balout et al (2007), according to which ductile materials produce more microparticles than fragile materials. This finding confirms the assumptions adopted during modelling and the outcomes of the different cutting and friction processes (Section 4.5). Nonetheless, these assumptions still have to be confirmed for NP.

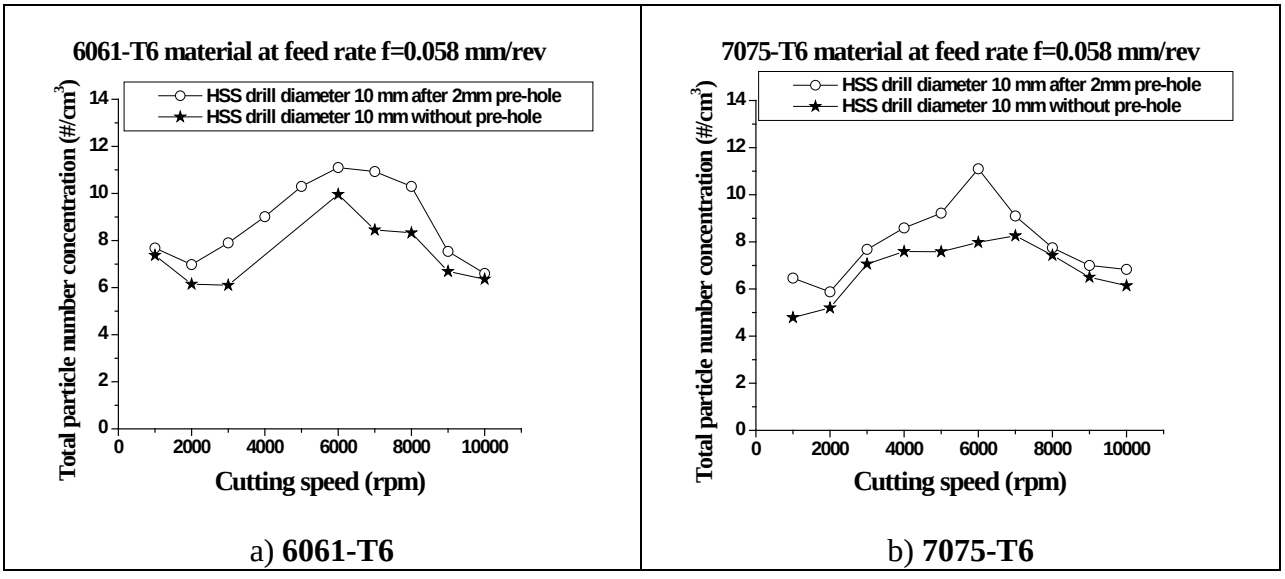

a) **6061-T6** b) **7075-T6**

Figure 24 - Number concentration for sizes between 0.5 µm and 10 µm, emitted during drilling of two wrought aluminium alloys: 6061-T6 and 7075-T6 (Kouam et al, 2010b).

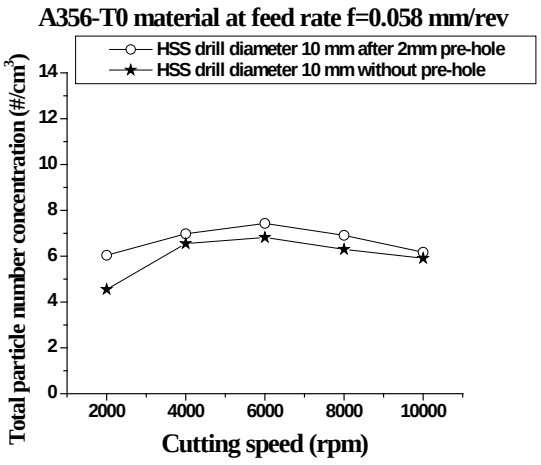

a) A356-T0

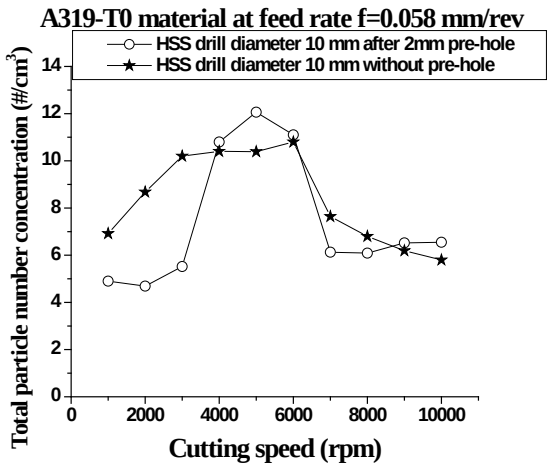

b) A319-T0

Figure 25 - Number concentration for sizes between 0.5 µm and 10 µm during drilling of two cast aluminium alloys: A356-T0 and A319-T0 (Kouam et al, 2010b).

For milling, tests were conducted under the conditions described in Table 1 (Chapter 3). The goal was to determine the conditions and the factors influencing NP generation. In all, 162 tests were performed. The graphs of the effects of each parameter on the number concentration (Fig. 26) and on the mass concentration (Fig. 27) of the particles generated immediately show the factors with the greatest influence on NP emissions: the material and the type of tool. In fact, it was found that:

- A change of material, by replacing 2024-T351 with 7075-T6, for example, can reduce NP emissions (from 4 x 10^8 to 0.2 x 10^8 particles per cc, Fig. 26; a decrease of nearly 95%);
- Likewise changing a tool with small corner radius (IC328 or IC4050, for which the radius is 0.5 mm) to a tool with a larger corner radius (IC908, for which the radius is 0.83 mm), increases NP emissions.

However, the graphs of the effects of milling conditions on the surface concentration of the particles emitted (Fig. 28) immediately show the “cutting speed”, “cutting depth”, “feed rate” and “tool” factors as parameters that greatly influence NP emissions during milling. However, the specific surface area concentration does not seem to depend on the milled material.

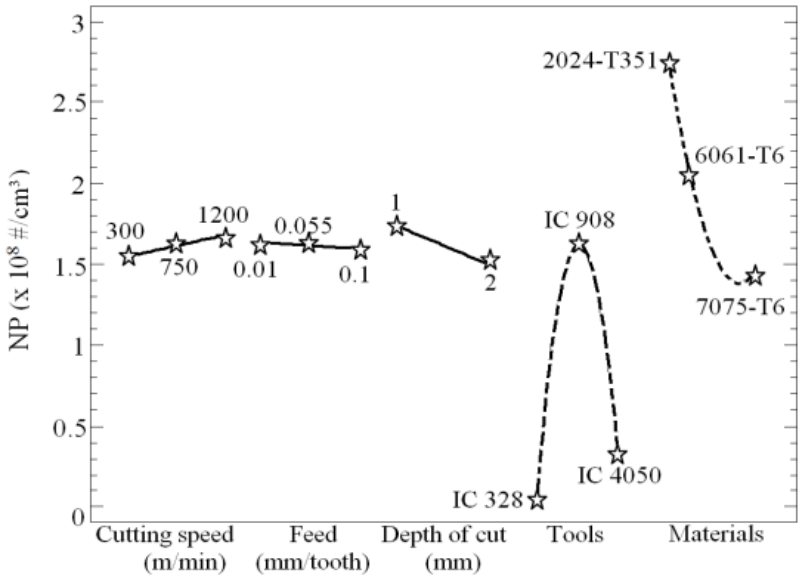

Figure 26 – Effects of milling conditions on the number concentration (C^P) of NP.

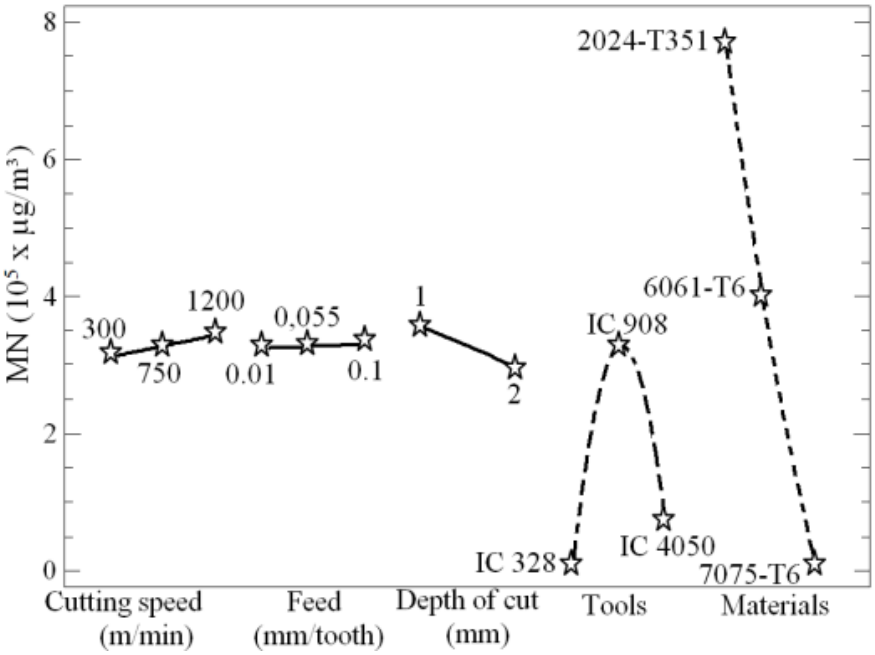

Figure 27 - Effects of milling conditions on the mass concentration (C^M) of NP.

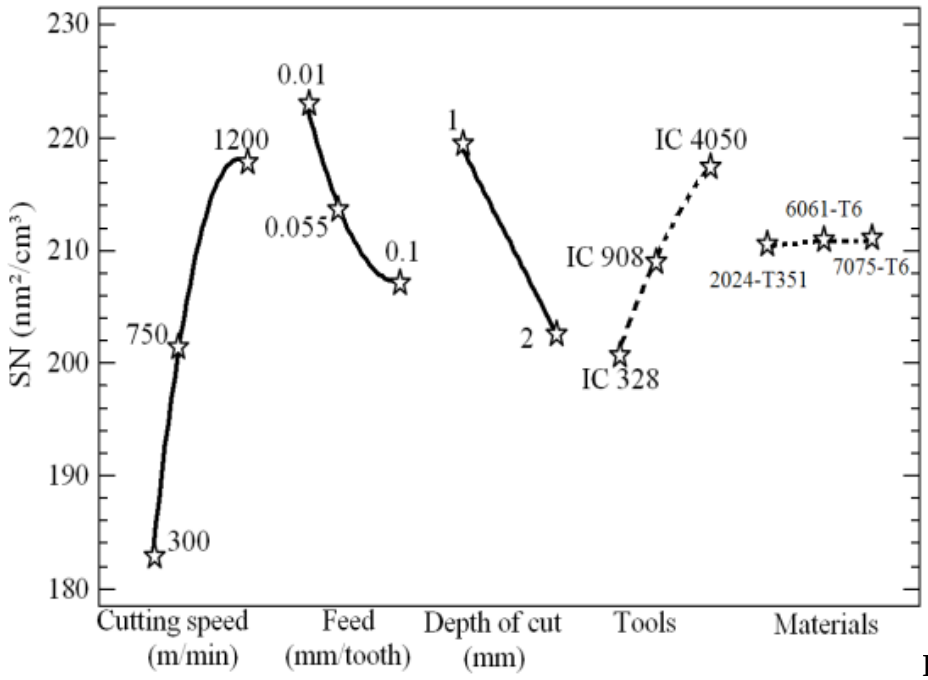

Figure 28 - Effects of milling conditions on the surface concentration (C^S) of NP.

In examining all the 162 data samples obtained, we find that nearly 65% of the NP produced have aerodynamic diameters smaller than 20 nm (Table 6).

Table 6: **Distribution of the number of NP produced during milling, according to their diameter (Djebara et al, 2012).**

Diameter range	Percentage of the total number of particles generated
100 nm < Φ < 300 nm	15
20 nm < Φ < 100 nm	20
Φ < 20 nm	65

An analysis of variance (ANOVA) allowed a study of the main effects of the independent parameters and their interactions, in order to know their combined effects on the dependent response. The ANOVA determines which of these effects in the regression model is statistically significant by using the probabilities (P) and the F ratios of Table 7. The higher the F ratio, the more strongly the effect considered the response studied. The variance analysis outcomes presented in Table 7 show, for the aluminium alloy 2024-T351 analyzed, the preponderant importance of cutting speed for the particle number and mass concentrations among the main

milling parameters: speed, feed rate and depth. For the specific surface area concentration, the effects of the cutting depth and the interactions with the feed rate are the most significant. The other significant effects of the interactions, including the feed rate, concerning the specific surface area concentration, are: AAB (speed× speed× feed rate), ABB (speed × feed rate × feed rate), BBC (feed rate × feed rate × depth), and AB (speed × feed rate). The feed rate must therefore be chosen with care if one wishes to control the specific surface area concentration of the NP produced during milling of aluminium alloy 2024-T351.

Table 7: Outcomes of the analysis of variance performed on the factors influencing the concentrations of NP emitted during milling of aluminium alloy 2024-T351.

Variance analysis of the number concentration, C^P (R^2 = 0.7)				
Factors	Sum of the squares ($x10^{17}$)	DOF	F	P
A:Speed	1.999	1	17.71	0.0012
B:Feed rate	0.104	1	0.92	0.3565
C:Depth	0.015	1	0.14	0.7175
BB	0.967	1	8.56	0.0127
ABB	1.371	1	12.14	0.0045
Total error	1.355	12		
Variance analysis of the mass concentration, C^M (R^2 = 0.88)				
Factors	Sum of the squares ($x10^{17}$)	DOF	F	P
A:Speed	1.0307	1	51.89	0.0000
B: Feed rate	0.0862	1	4.34	0.0614
C:Depth	0.0014	1	0.07	0.7954
AA	0.1366	1	6.88	0.0237
BB	0.2977	1	14.99	0.0026
ABB	0.8550	1	43.05	0.0000
Total error	0.2185	11		
Variance analysis of the specific surface area concentration, C^S (R^2 = 0.78)				
Factors	Sum of the squares ($x10^{17}$)	DOF	F	P
A:Speed	9.92	1	9.92	0.0016
B:Feed rate	3.24	1	3.24	0.0719
C:Depth	10.14	1	10.14	0.0015
AA	4.27	1	4.27	0.0388
AB	37.41	1	37.41	0.0000
BB	13.56	1	13.57	0.0002
BC	11.80	1	11.80	0.0006
AAB	33.37	1	33.37	0.0000
ABB	7.59	1	7.59	0.0059
ABC	10.81	1	10.81	0.0010
BBC	48.30	1	48.30	0.0000
Total error	86.25	6		

DOF: degrees of freedom

The Pareto diagrams presented in Figures 29 to 31 classify the factors tested and the interactions between them in order of importance. The vertical reference line appearing in each of these diagrams indicates the statistically significant effects, with a 95% degree of confidence. The Pareto diagram, where the coefficients are classified in diminishing order of absolute value, helps to determine the value below which a factor does not have a significant effect on the response studied, in which case said factor can be removed from the prediction model.

The process parameters and the conditions governing the specific surface area concentration of the particles emitted are different from those governing the particle number or mass concentrations (Figs. 29, 30 and 31). These two concentrations are governed by the machined material and the type of tool used (factors E and D, and interactions DDE, DD and EE, Figs. 29 and 30), whereas the specific surface area concentration is governed by the tool (factor D) and the interactions between the tool and the feed rate (factor BBD), on the one hand, and the tool and the depth (factor CDD), on the other hand. It therefore becomes difficult to identify the prescription for the best operating conditions if the metric that will be used by the toxicologists is unknown. This difficulty is reflected, for example, in Figure 32, which shows the influence of the interaction between the machining feed rate and the material on the mass concentration and the specific surface area concentration of the NP. Thus, for a feed rate of 0.1 mm per milling cutter tooth, cutting aluminium alloys 2024-T351 and 7075-T6 generate NP with the same specific surface area concentration (Fig. 32b), but very different mass concentrations (Fig. 32a).

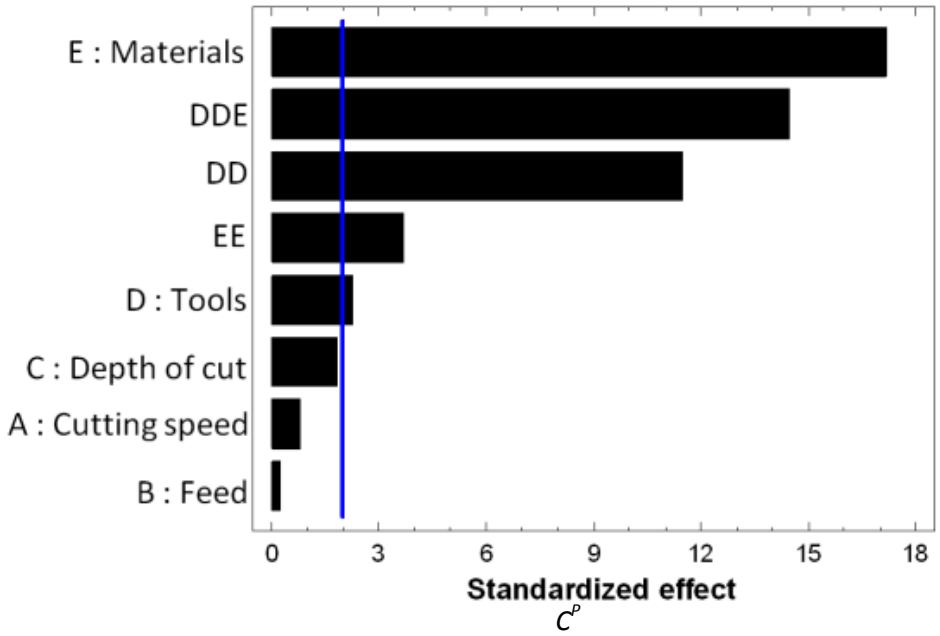

Figure 29 - Pareto diagram of the effects of milling factors on the number concentration of the particles emitted (Djebara, 2012).

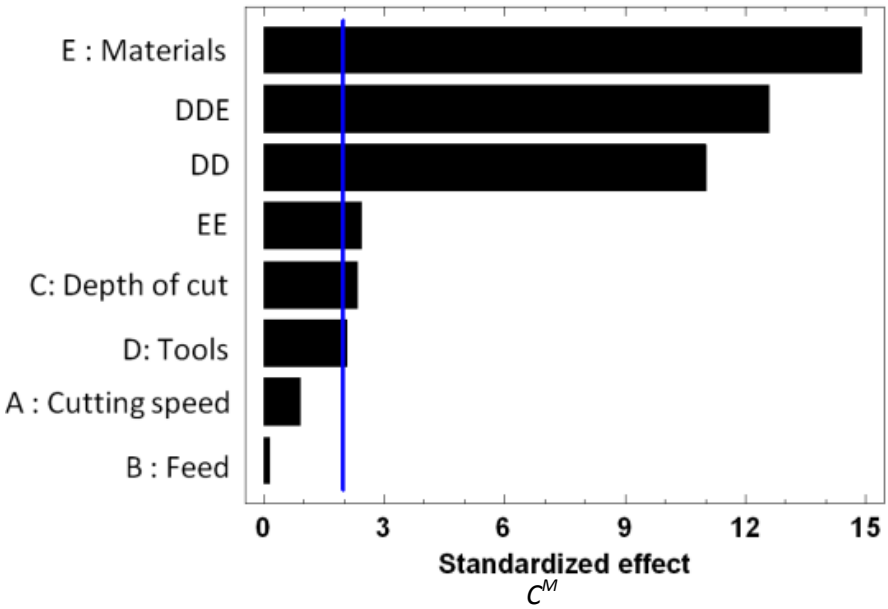

Figure 30 - Pareto diagram of the effects of milling factors on the mass concentration of the particles emitted (Djebara, 2012).

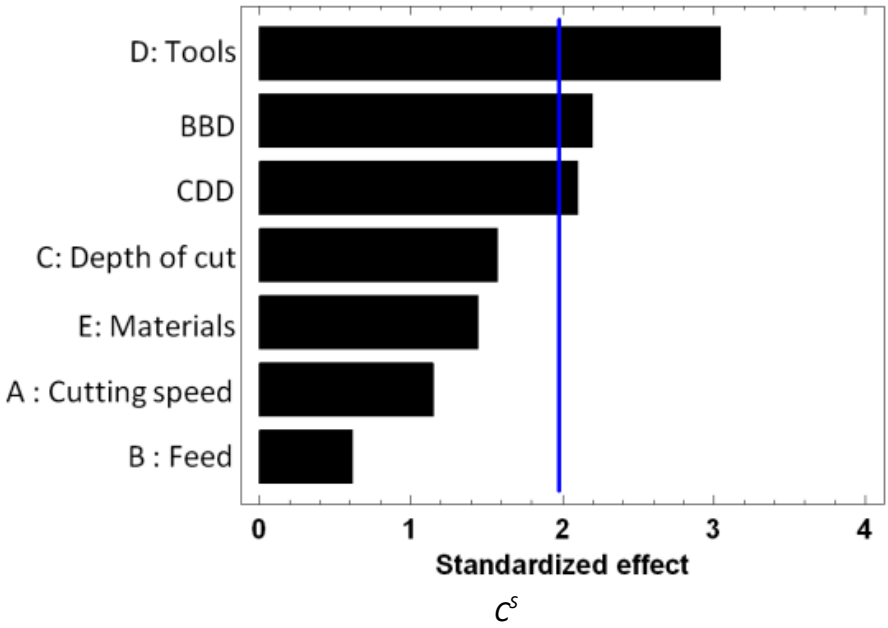

Figure 31 - Pareto diagram of the effects of milling factors on the specific surface area concentration of the particles emitted (Djebara, 2012).

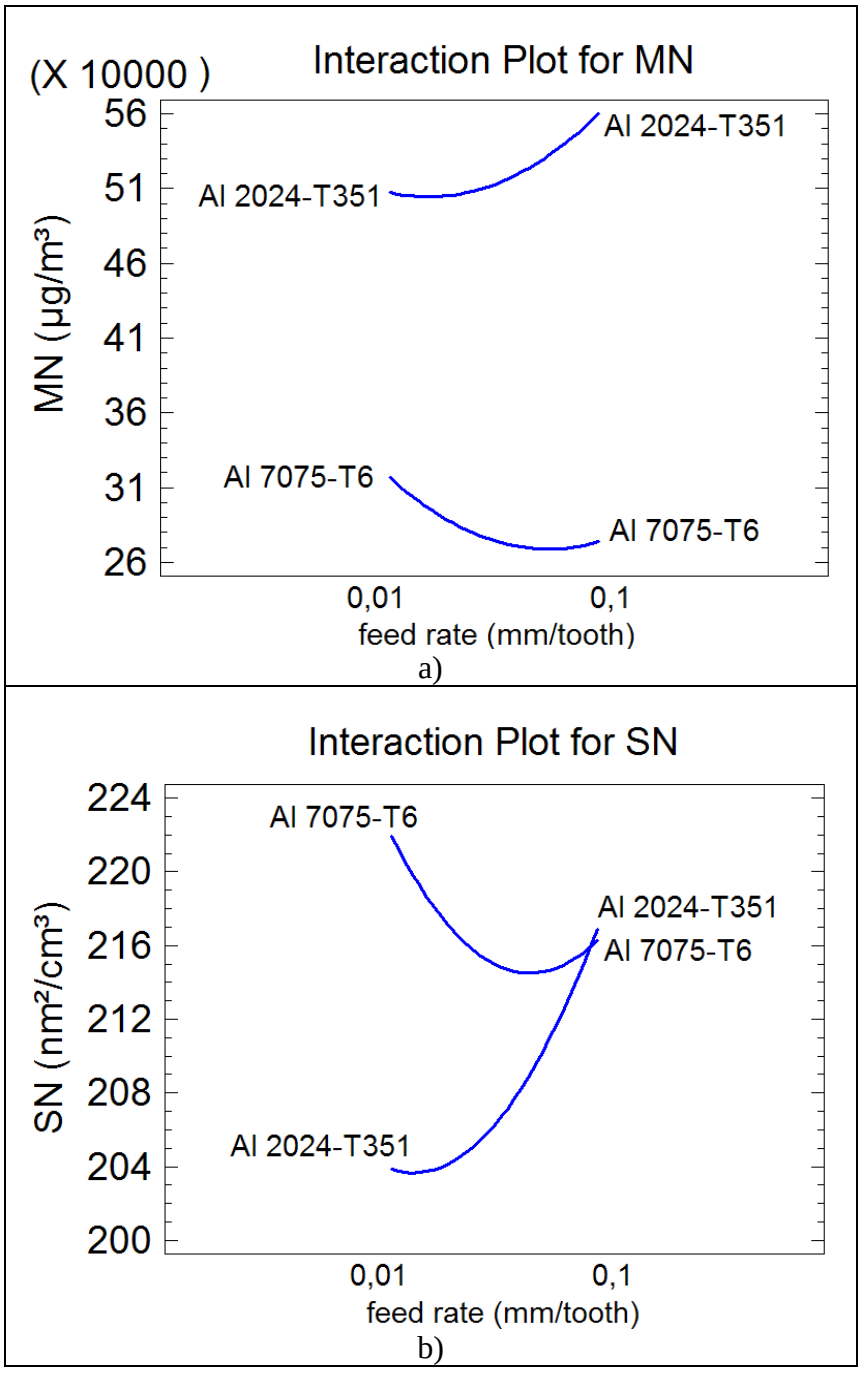

Figure 32 - Effects of the interaction between feed rate and materials on the mass concentrations (a) and the specific surface area concentrations (b) of NP emitted during milling (Djebara et al, 2012).

Following a complete statistical analysis, regression models predicting the emissions according to the tool, the cut material and the machining conditions were developed (for the methodological details of this approach, see Djebara's Ph.D. thesis, 2012). These models served to develop surface graphs, such as those presented in Figures 33, 34 and 35.

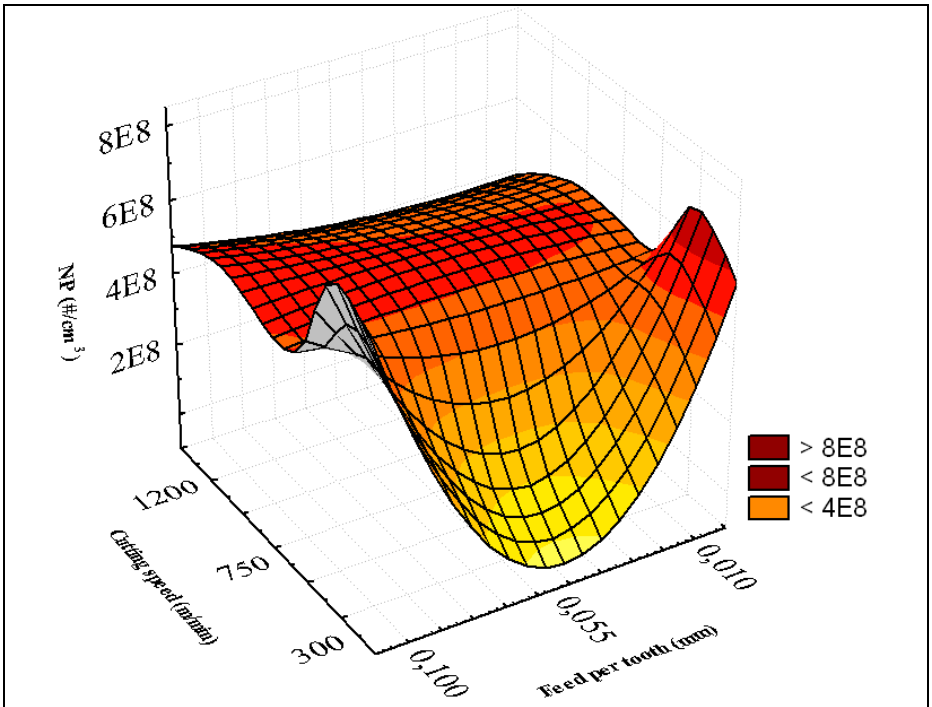

a) Number concentration (NP) for alloy **2024-T351**

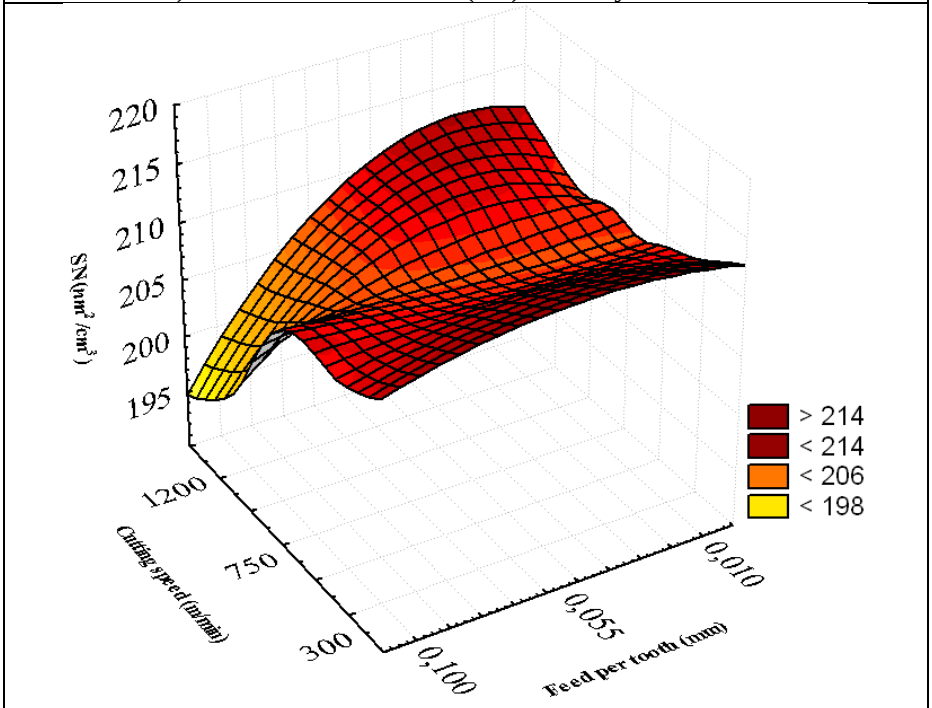

b) Specific surface area concentration (SN) for alloy **2024-T351**

Figure 33 – Prediction of the particle number and specific surface area concentrations of NP emissions during milling (tool IC908) on an aluminium alloy 2024-T351 workpiece: Effects of cutting speed and feed rate (Djebara et al, 2010a).

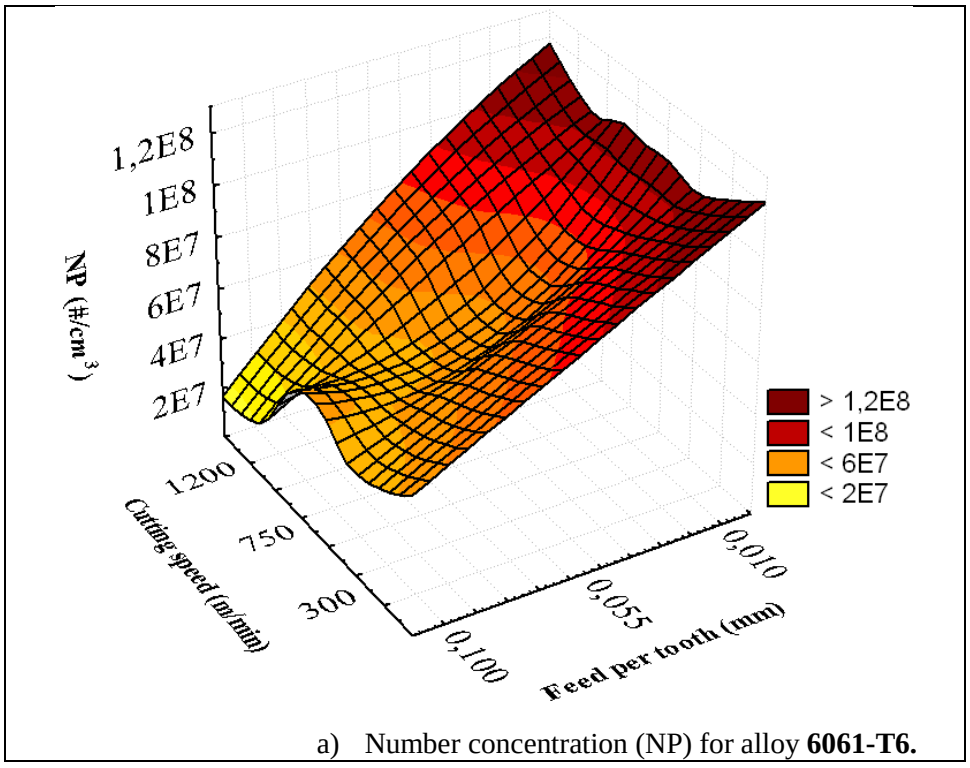

a) Number concentration (NP) for alloy **6061-T6.**

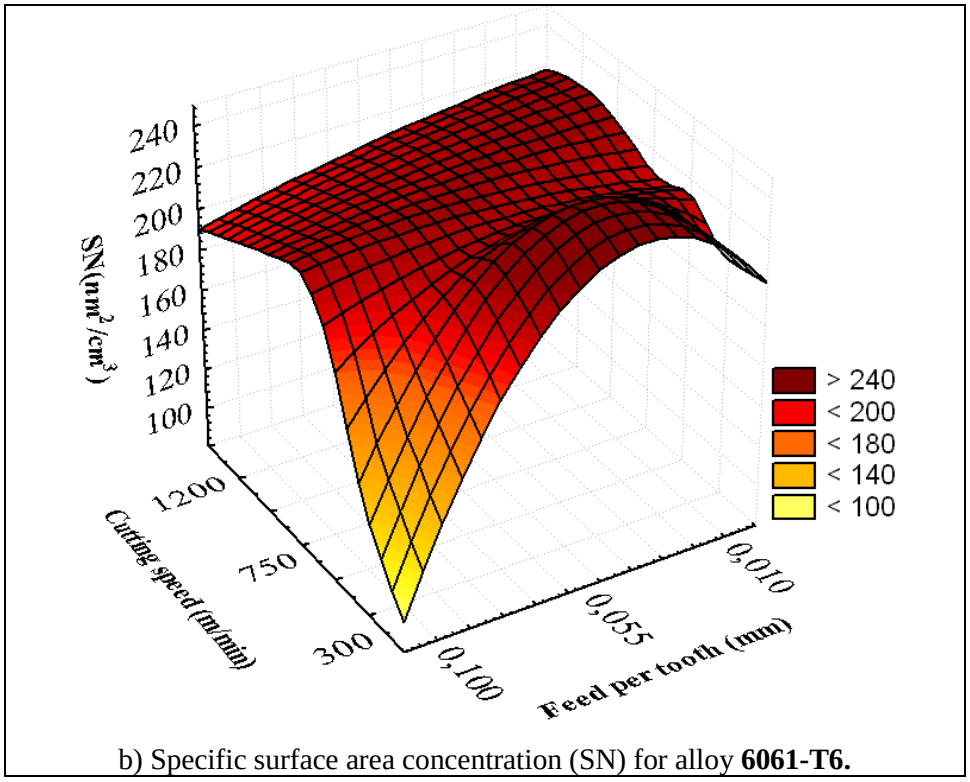

b) Specific surface area concentration (SN) for alloy **6061-T6.**

Figure 34 – Prediction of the particle number and specific surface area concentrations of NP emissions during milling (tool IC908) on an aluminium alloy 6061-T6 workpiece: Effects of cutting speed and feed rate (Djebara et al, 2010a).

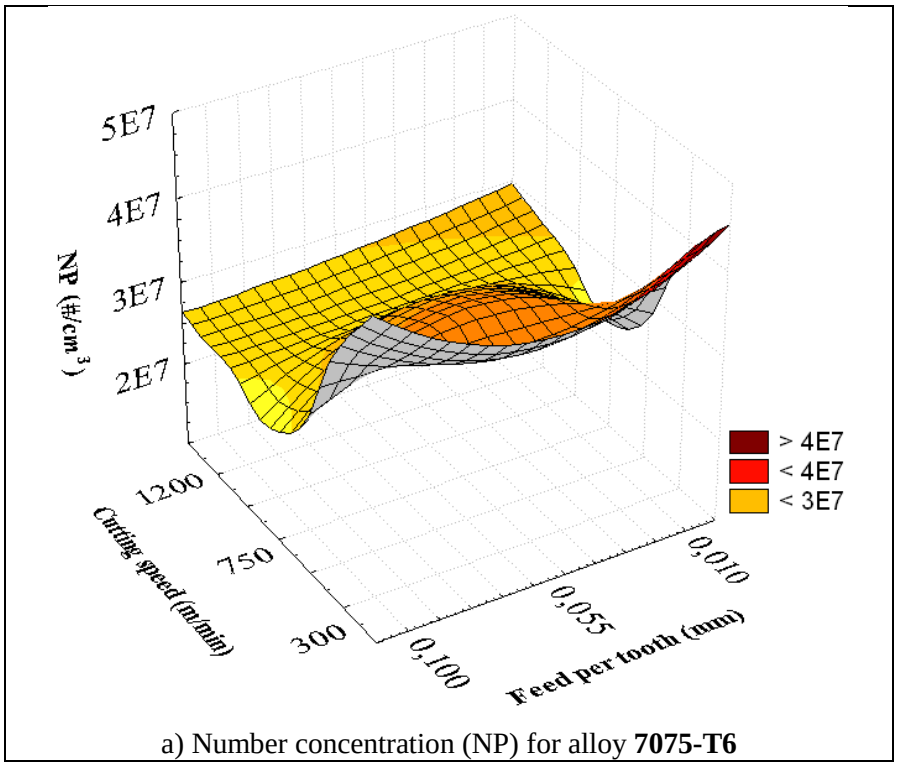

a) Number concentration (NP) for alloy **7075-T6**

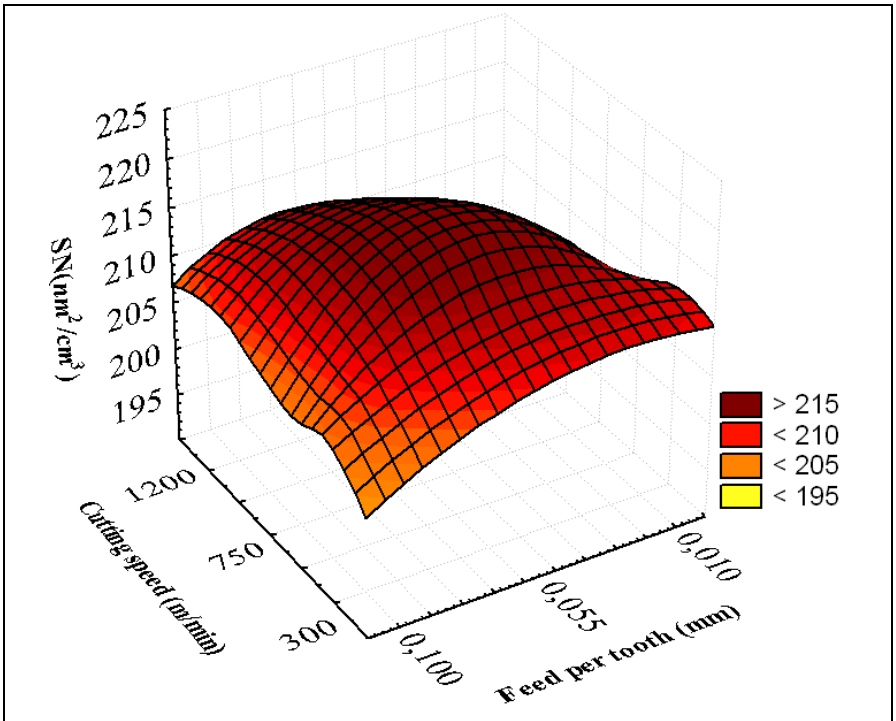

b) Specific surface area concentration (SN) for alloy **7075-T6**

Figure 35 – Prediction of the particle number and specific surface area concentrations of NP emissions during milling (tool IC908) on an aluminium alloy 7075-T6 workpiece: Effects of cutting speed and feed rate (Djebara et al, 2010a).

These response surfaces illustrate the variation of NP concentrations, according to the cutting speed and the feed rate. They show a variation that identifies the zones of the experimental field for which NP emissions are maximum or minimum, depending on the material used. The main conclusions resulting from these graphs are:

- Cutting speed and feed rate combinations exist for which NP emissions are low.
- In the experimental field considered, the surface graphs emphasize the importance of the "material" and "tool" factors for the cutting speed reached by the NP emissions.
- The "cutting depth" factor also plays a non-negligible role in obtaining high NP emissions, but to a lesser degree than the feed rate. This can also be explained by the relatively small cutting depth range tested. We can conclude that the "cutting speed" factor is important in management of emissions and that the existence of a critical speed at which these emissions are maximum is currently well known (Khettabi, 2009).

4.5 Modelling and prediction of particulate emissions

The prediction of particulate emissions was based on an index designed by Khettabi et al (2007), which consists of calculating the mass of the particles emitted relative to the chip mass throughput. This index, called *Du* (Dust Unit), was defined in Equation 1 in Section 2.2.2. The

study of microparticle and NP emissions during this project allowed the development of a predictive model serving as an emission reduction source. This modelling adopted a hybrid approach by integrating the energy aspect and micro-friction and macro-friction (Khettabi et al, 2010a).

The energy aspect is based on the fact that the energy provided by the cutting tool must be sufficient to break the chemical bonds and form corpuscles of different sizes. The quantity of particles produced during machining therefore follows Arrhenian type of exponential law ($D_U \propto e^{-\frac{E_A}{E}}$). This quantity of particles depends on the energy applied (cutting energy E) relative to the energy state of the particle before separation (E_A). In this situation, it must be admitted that the particles of the same size that separate from the same zone are in the same energy state (same activation energy). In other words, E_A depends on the size of the particle, the emission zone (E_A on the surface is the lowest) and the material.

The influence of multiple mechanisms occurring during the cutting process makes quantification difficult. The energy aspect is also linked to other phenomena responsible for NP emissions. This aspect therefore must be coupled with the effect of macro-friction and micro-friction. The chip formation mode that favours the creation of alternating chip fall zones between soft and hard layers also triggers micro-friction between these zones. The degree of segmentation can give this phenomenon a quantifiable character. A segmentation coefficient β, which identifies the appearance of segmentation according to the cutting conditions and the material developed by Xie et al (1996), was used in modelling. The effect of friction at the tool-chip interface on microparticle emissions is governed by two parameters: the segmentation density of η_S and the roughness of the cutting face of tool R_a. The correlation between the different aspects leads to their combination by adopting their multiplicative character to design a general model.

$$D_u = A \times \frac{\beta_{max} - \beta}{\beta_c} \times R_a \times \eta_S \cdot \left(\frac{V_0}{V}\right)^{\delta} \exp\left(\frac{-E_A}{\tan\varphi(1 - C_h \sin\alpha) V \frac{F_{sh}}{bf}}\right) \quad (5)$$

where A: proportionality factor;

β: segmentation coefficient that identifies the appearance of segmentation according to the cutting conditions and the workpiece material;

β_c (resp. β_{max}): critical value (resp. maximum value) for which the chip becomes segmented;

Ra: arithmetic mean roughness of the surface finish;

$\eta_{s:}$ segmentation density;

*V (*resp. V_0*):* Cutting speed (resp. critical speed at which the particulate are maximum;

E_A*:* activation energy of the material;

ϕ: shear angle during machining;

C_h : chip compression rate

α : tool rake angle;

$F_{sh:}$ shear force;

b: cutting width;
f: feed rate;
δ: parameter of the material characterizing its ability to produce metal particles.

Parameter δ is determined experimentally and its value allows materials to be classified as follows:

$$\delta \equiv \begin{cases} \delta \geq 1.0 \rightarrow \quad Matériau : Ductile \\ 0.5 < \delta < 1 \rightarrow Matériau : semi - ductile \\ 0 < \delta \leq 0.5 \rightarrow \quad Matériau : Fragile \end{cases} \tag{6}$$

For cast aluminium alloys, which are considered fragile, this parameter is $0 \leq \delta \leq 0.5$, while for wrought aluminium alloys, which are considered ductile, it is $\delta \geq 1.5$ (example, for 6061-T6: δ=1.5).

The parameters such as rake angle α, shear angle φ, cutting speed *V*, feed rate *f*, roughness R_a and β_{max} and β_c, can be determined easily. The shear force and the temperature can be measured directly or estimated theoretically. Nonetheless, measuring is very difficult in some processes. The Needelman-Lemonds constitutive equations can be used to estimate stresses and temperature. The development of an algorithm represents the behaviour of certain properties (Khettabi et al, 2011). Zaghbani et al (2009) proposed a force-temperature predictive model for high-speed dry milling with ductile materials. This oblique cutting model is transferred to a calculation model to determine the shear stresses and the temperature for an orthogonal cut. The outcomes of the simulations (Fig. 36) were validated experimentally (Fig. 37). For more information, we recommend the readers consult Khettabi et al (2010a).

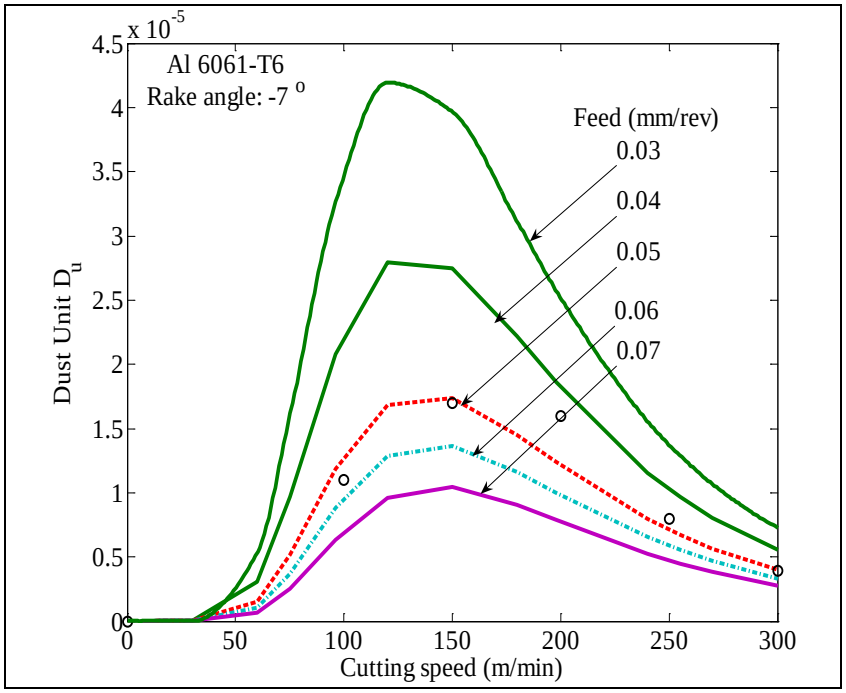

Figure 36 – Outcomes of the simulations (Eq. 5) of the influence of cutting speed and feed rate on NP emissions for alloy Al6061-T6 (Khettabi et al, 2010a).

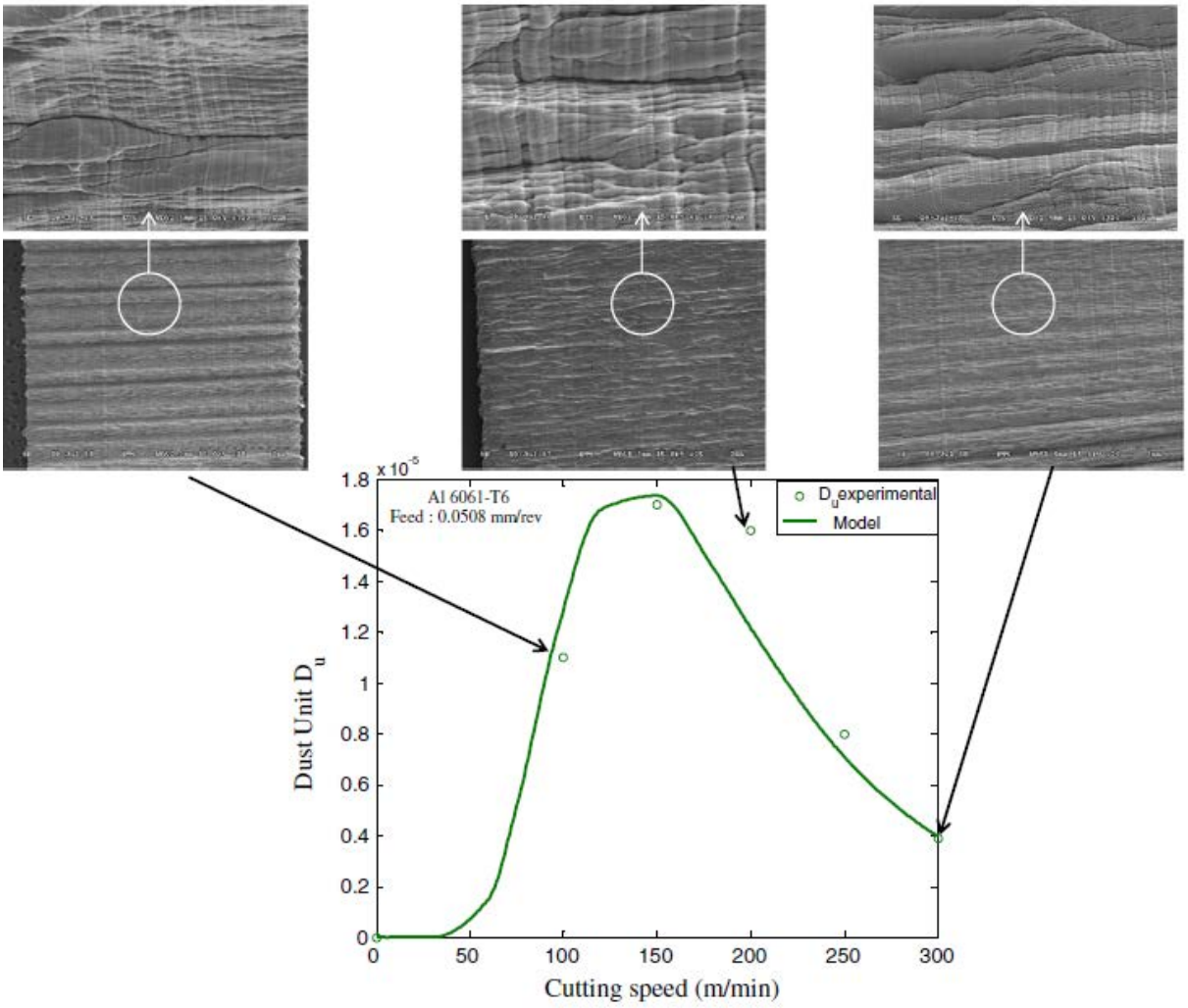

Figure 37 – Experimental outcomes and simulation of particulate emissions during dry machining (Khettabi et al, 2010a).

5. DISCUSSION

For the purposes of this study, the sampling technique was reviewed and improved to correspond to the theoretical principles and experimental requirements. A procedure was also developed and applied to allow viewing of the displacement of particles and the movement of the air during machining. It consists of machining dry ice blocks and filming the motion of the particles this releases. This study allowed better positioning of the measuring system. Similarly, models were developed to improve the reliability of numerical predictions by focusing on the phenomena of Brownian and turbulent diffusion of NP. This work also allowed assessment and imitation of losses in the sampling and measuring systems, by limiting the length of the tubes.

A procedure for capturing particles and preparing them for observation under the microscopes was designed and used. The study of the shapes of particles and the simulation of the flows around them showed the necessity of designing correction algorithms, better adapted sampling techniques and even higher-performance measuring instruments. However, for polycarbonate substrates, the protocol and/or the preparation method must be reviewed to improve characterization, particularly for the transmission electron microscope (TEM).

The outcomes of this study showed that the conditions of friction and machining (tool geometry, workpiece material and thermal state of the workpiece) considerably affect NP emissions. Mastering these effects will help control NP better, reduce emissions at the source or target emissions of a particular size, for example, a less harmful size. The predictive model developed by Khettabi et al (2010a-d) shows the correlation between these different parameters and NP emissions. New machining and friction strategies were developed under this study and will allow source reduction of NP generation (Khettabi, 2009; Khettabi and Songmene 2009, Khettabi et al, 2010a-d; Songmene et al, 2008a,b; Kouam et al, 2010a,b; Djebara et al, 2010a,b).

5.1 Aerodynamic behaviour of particles

During fabrication, an additional difficulty in the study of particle generation stems from the fact that the processes generate air turbulence, caused by tool-workpiece relative motion. This changes the behaviour of the particles and can affect measurement precision. To reduce this adverse effect, the concentration measurements were taken a few seconds before the beginning of the cutting process and sampling continued a few minutes after the process (when no machine component was still rotating), until the concentration was equivalent to the one measured before the cutting operation.

As mentioned in the experimental procedure, a technique allowing viewing of displacement of the particles and movement of the air during machining was developed and applied in order to determine how to position the measuring system optimally. Likewise, modelling and trace gas simulation were performed. The small particles tend to behave like a passive scalar in a forced air flow. Therefore, dispersion modelling of a trace gas is likely to provide very useful information to predict NP dispersion according to the operating conditions around the machine tool. Parallel to characterization of the behaviour of these airborne particles and the influence of

this behaviour on measurement, experimental tests were conducted with a trace gas. The NP transport/diffusion models were compared with the local concentrations of a trace gas in order to 1) verify whether the trace gas technique can actually be used in the work environment to assess workers' NP exposure, and 2) determine the limits of application of this technique.

It was shown that dispersion modelling of a trace gas can provide very useful information to predict the NP transport and diffusion, depending on ventilation conditions (Hallé et al, 2009, Morency et al, 2010). Flow modelling inside a machining enclosure is very complex due to *i)* the absence of symmetry in the volume to be discretized and *ii)* the difficulty associated with the imposition of borderline conditions, whether during drilling, milling or turning operations. Therefore, the publications cited above focused on modelling the flow and transport of airborne NP in an inhalation chamber, which represents a "simpler" geometry to model. The numerical resolution of the Navier-Stokes equations in a turbulent regime, coupled with the NP mass transport equation, allowed prediction of transport and diffusion of a TiO_2 aerosol 30 nm in diameter (aerodynamic diameter), accounting for the phenomenon of NP capture by the walls. The numerical outcomes were compared with experimental outcomes obtained by means of a Dekati cascade impactor. The outcomes indicated an excellent match between the mass fractions predicted numerically and the experimental outcomes, namely 6.02×10^{-8} kg of TiO_2/kg of air (numerical) vs. 5.59×10^{-8} of TiO_2/kg of air (experimental).

Morency et al (2008) also assessed four Browning NP diffusion models. The friction (*f*) and diffusion (*D*) coefficients of three different models were compared with the predictions of the kinetic theory of gases. Apart from the outcomes obtained from the kinetic theory of gases, it was shown that the *f* and *D* coefficients of the different models are highly comparable. The most significant differences were observed for the Stokes model, which slightly underestimates the diffusion coefficient compared to the Friedlander and Gussman models; the variances are more significant for aerodynamic diameters greater than 60 nm. Figure 38 compares the *D* coefficients for TiO_2 NP, as a function of the aerodynamic diameter. It was also shown that the Brownian diffusion coefficient increases with temperature (Morency and Hallé, 2013). However, this dependence should not significantly affect NP aerodynamic behaviour in the context of high-speed machining processes.

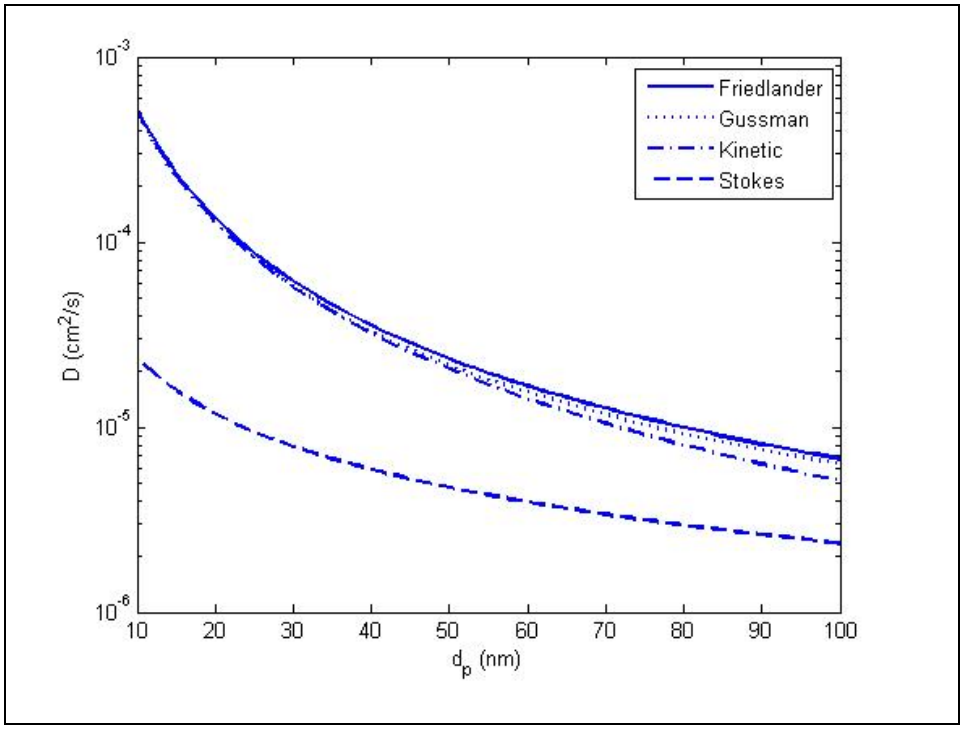

Figure 38 –Brownian diffusion coefficient as a function of the aerodynamic diameter obtained for four models (Morency and Hallé, 2013).

Another aspect of this study was the application of the trace gas technique for prediction of the NP deposition coefficient in measuring systems using a suction tube for aerosol collection, such as the SMPS. The study of these losses by laminar and turbulent diffusion in a circular tube 1 cm in diameter was published, in part, by Morency and Hallé (2010). Figure 39 compares the numerical outcomes obtained with the Friedlander correlations for the mass fraction of the NP, as a function of the length of the suction tube. According to these outcomes, the larger the diameter of the suction tube, the smaller the losses. Longer tubes thus could be used. However, for small-diameter tubes (e.g. in the order of 10 mm or less), there is an interest in not exceeding a length of one metre.

Morency and Hallé (2013) also studied NP deposition by the trace gas approach in enclosures ventilated according to the dilution principle. Such a study allows better viewing of particle dispersion and could help choose the positioning of the air inlet and outlet. However, its application to machine tools must be refined to account for moving parts during a machine tool cutting process.

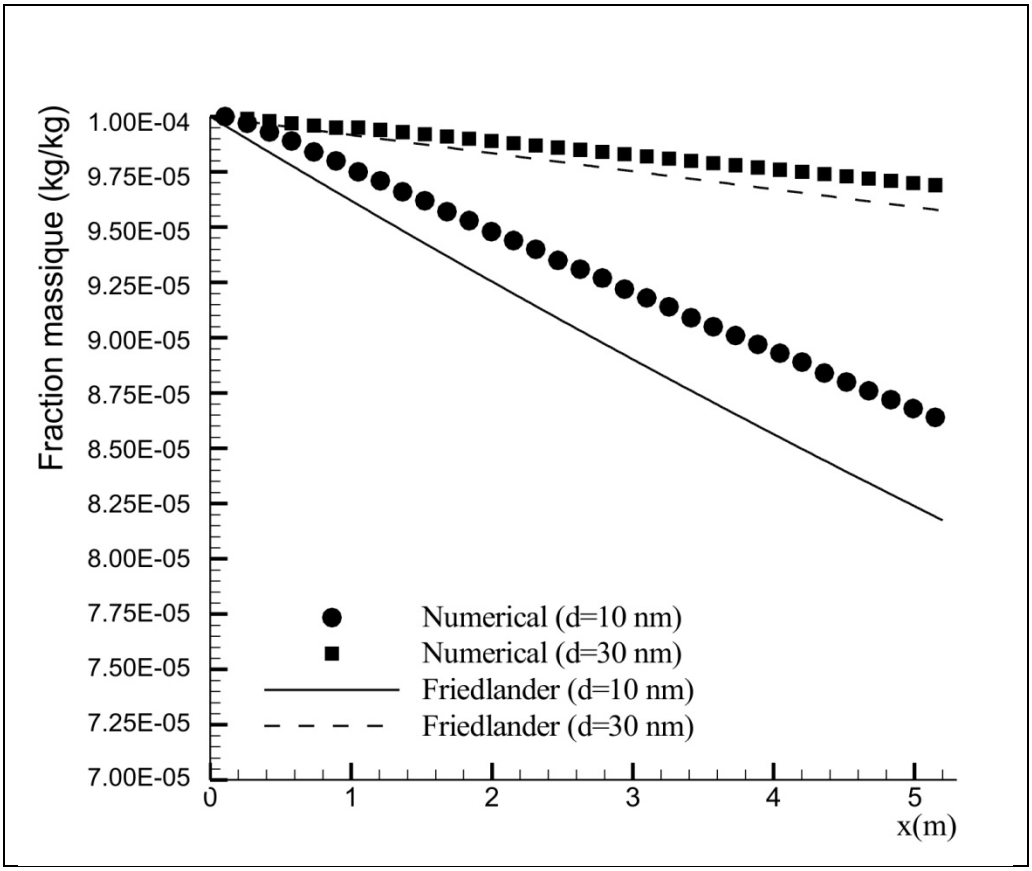

Figure 39 – Mass fraction of airborne NP in a circular tube (1 cm) as a function of length (adapted from Morency and Hallé, 2010).

5.2 Effect of the process and cutting strategies

The behaviour of the workpiece material during deformation and the chip formation mode attest to the difficulty of comparing different machining processes. From the standpoint of particulate emissions, comparison is possible but interpretation remains complex. It is important to remember that the friction processes produce much fewer NP than the machining processes (Kouam et al, 2011). However, it would be preferable to be able to classify the machining processes according to their particulate emission power.

Following this project, Khettabi et al (2011) designed an assessment model for the sustainability during machining of aluminium alloys. This model includes particulate emissions, machining costs and the energy required for cutting. With this model, it is now possible to classify materials and processes according to their sustainability and their particulate emissions (Fig. 40). Following this classification, milling appears to be the process that generates the most particles, followed by turning. Drilling, a very common operation in industry, emits few particles compared to the other processes.

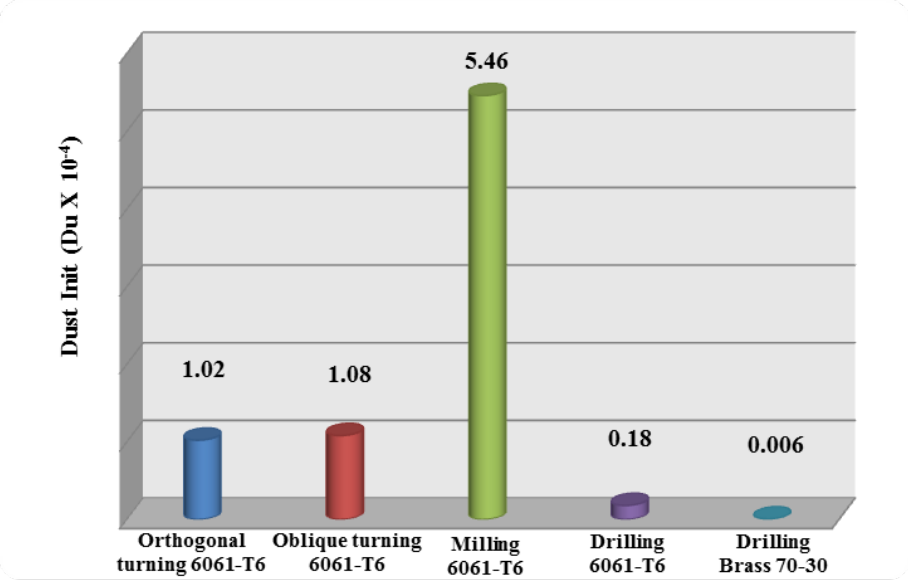

Figure 40 – Comparison of emissions of different processes, using the Dust Unit (Eq. 2) (Khettabi et al, 2011).

Lubrication also plays a role in particulate emissions (Fig. 41) (Kouam et al, 2012). In the presence of lubricant, the quantity of aerosol increases due to the droplets produced during the impact of the fluid on the workpiece or during the motion of the components of the tool-workpiece system. This increase in aerosols formed by metal particles and cutting fluid droplets is greater in semi-dry cutting (Fig. 41), because the fluid is projected onto the tool in the form of mist. It would be necessary to conduct an additional study to determine the exact proportion of metal particles in all the aerosols measured, with a view to establishing the effects of the cutting fluid and its conditions of application to NP generation (Kouam et al, 2012).

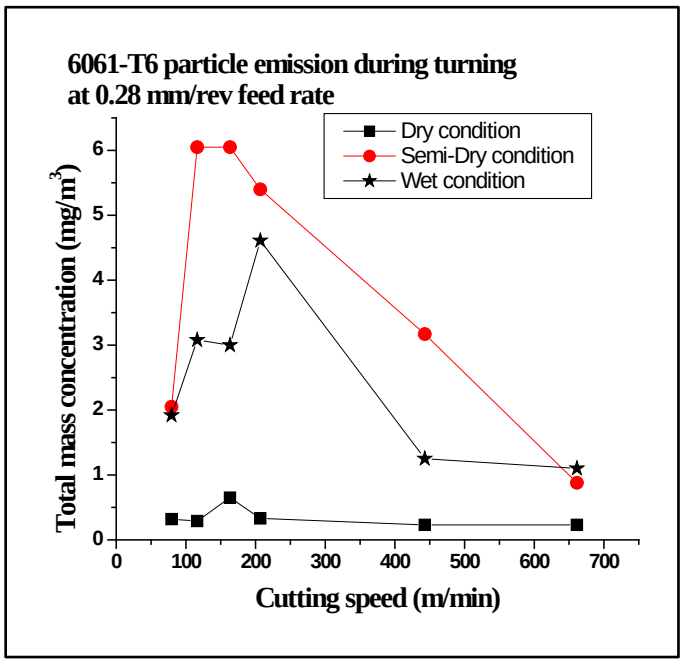

Figure 41 – Comparison of aerosol emissions ($PM_{2.5}$) during turning of aluminium 6061-T6, as a function of lubrication conditions (Kouam et al, 2012).

5.3 Tool effect: Geometry and coating

The tool parameters likely to influence chip formation, shear, deformations, cutting stresses and heat generated during machining, and therefore the emitted particles, include their geometry (rake angle, clearance angle, helix angle, corner radius and edge preparation) and the exterior coating of the tool. Figure 42 presents a simplified geometry of the cutting tool. The chip flows onto the cutting face of the tool. This face (which can be coated or uncoated) forms a rake angle or clearance angle (γ) with the normal of the freshly machined surface. This rake angle can be positive or negative (as indicated in Figure 42), which will influence chip formation and chip flow, shearing of the material, deformation of the material and the energy necessary for cutting.

Regarding the tool coating, Djebara et al (2013) tested two milling tools with the same corner radius (0.5 mm), but made with a different coating (TiCN for grade IC328, compared to TiCN/Al_2O_3/TiN multilayers for grade IC4050) on aluminium alloys. The outcomes showed that the coating first influences the specific surface area of fine particles (PM2.5), before the machining process parameters (speed, feed rate, depth) and the type of machined material (aluminium alloys: 6061-T6, 7075-T6 and 2024-T351) (Fig. 43). The multilayer coated tool (IC4050) generated particles with a total specific surface area greater than that of the particles generated with the tool coated with TiCN (IC328). This is explained by the difference between the surface finishes of these two coatings, which alters the real contact surface.

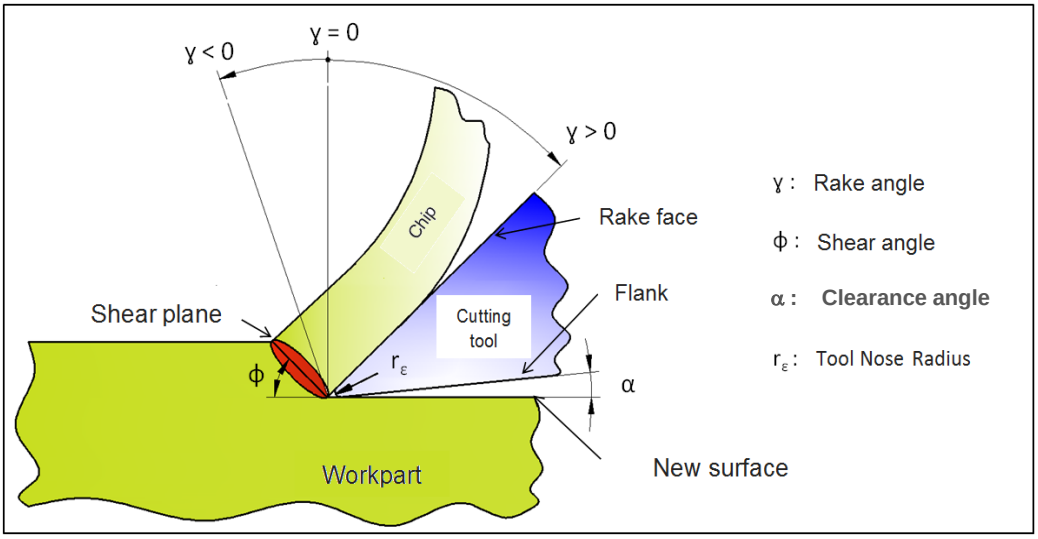

Figure 42 – Simplified schematic representation of tool geometry: rake angle, shear angle, clearance angle and corner angle.

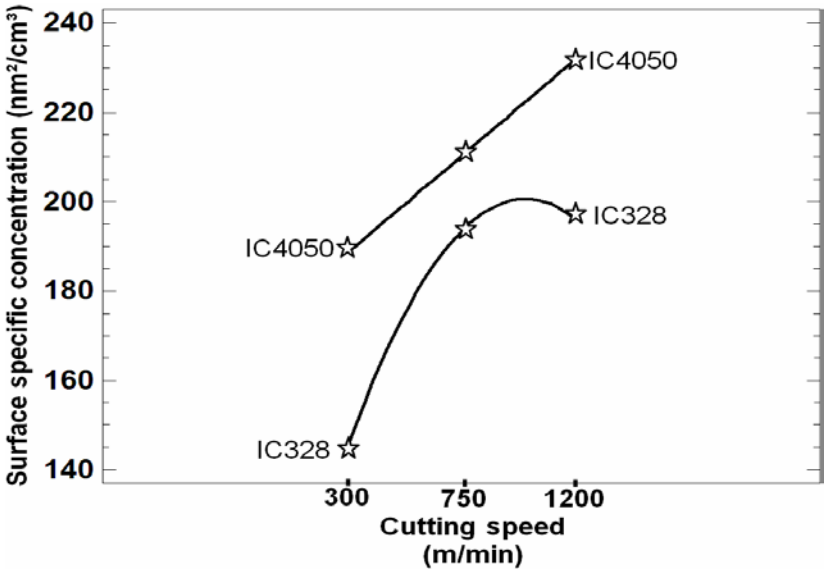

Figure 43 – Effects of interactions between the cutting speed and the grade (tool coating) on the specific surface area of fine particles (PM2.5) (Djebara et al, 2013). The coatings are TiCN for grade IC328 and TiCN/Al_2O_3/TiN for grade IC4050.

Regarding the tool corner radius (r_ε, Fig. 42), it has been shown, in the Outcomes section (Section 4) of this report, that changing from milling tool with a small corner radius (IC328 or IC4050, which has a 0.5 mm radius) to a tool with a larger corner radius (IC908, which has a radius of 0.83 mm), increases NP emissions (number concentration, Fig. 26, and mass concentration, Fig. 27). In fact, the larger the corner radius, the greater the deformations in the main cutting zone and along the shear plane, and the more particles may be generated during the

process. However, having more particles is not synonymous with a greater total specific surface area of these particles (Fig. 28).

For drill bits, it can be expected that the corner radius, the helix angle or the web size influence particulate emissions. For example, when drilling wrought and cast aluminium alloys, Kouam et al (2010b) showed that the pre-drilling hole has a considerable influence, in addition to the cutting conditions, on particulate emissions ranging between 0.5 and 20 micrometres. It is known that a pre-drilling hole is often made in industry to improve the stability of the process and the quality of the workpieces, but little is known about the resulting particulate emissions. In general, for each material, the maximum particle concentration is always emitted at the same cutting speed and has the same order of magnitude (Figs. 24 and 25). Particulate emissions during drilling are independent of the drill web, because the pre-drilling hole eliminates the web effect. These outcomes, which are very interesting in practical terms, will have to be verified later to determine whether they apply to NP.

The effects of rake angles on particulate emissions were assessed. Figures 44-46 present the effects of a negative rake angle (-7 degrees) or a positive rake angle (+7 degrees) on number concentration, specific surface area concentrations, mass concentrations, and particle size distribution (aerodynamic diameter) of NP. It clearly emerges that the use of a tool with a positive rake angle (+7 degrees) generates more NP (number concentrations, Fig. 45, specific surface area concentrations, Fig. 46) than cutting with a tool with a negative rake angle (-7 degrees). This can be explained by the change in the chip formation and on the chip flow process. The existence of two peaks in the aerodynamic diameter range from 15 nm to 25 nm for machining with a positive rake angle reveals the existence of two particle formation processes in this case, compared to machining with a negative rake angle. This finding is worth further investigation.

However, changing the tool's rake angle, at least for this turning operation and for the tested conditions, does not seem to influence the size distribution of the particles emitted, but instead influences their concentrations. This is valid for the three metrics used (number concentration, Fig. 44; specific surface area concentration, Fig. 45 and mass concentration, Fig. 46).

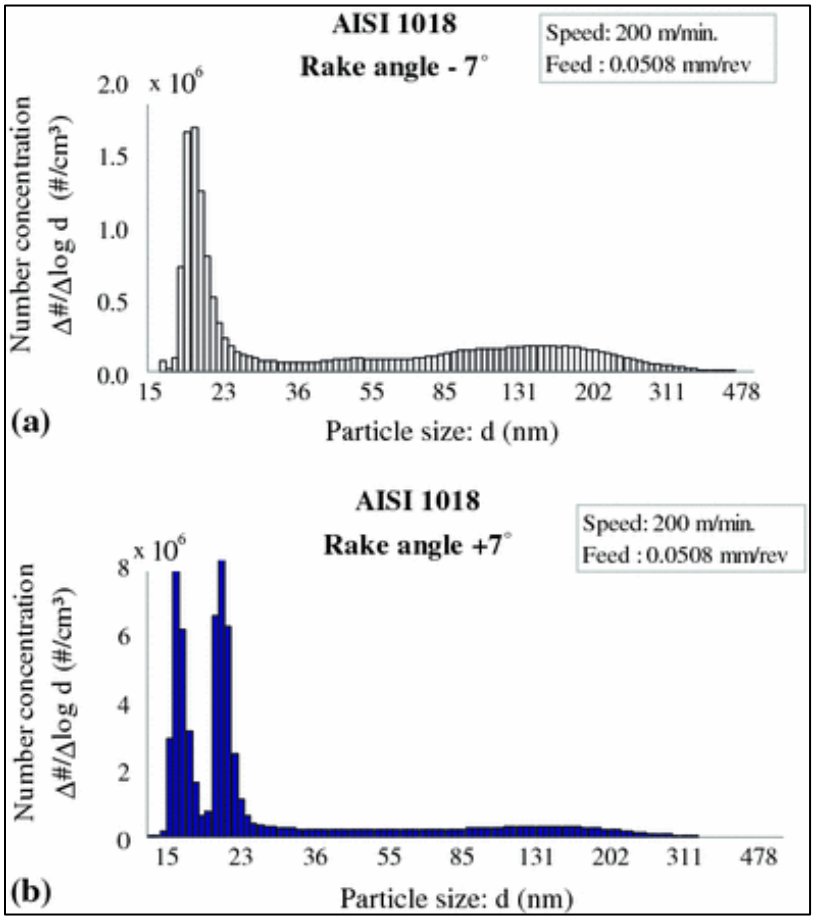

Figure 44 – Effect of the tool's rake angle on number concentration and particle size distribution of NP during orthogonal turning of steel AISI 1018: a) negative angle; b) positive angle (Khettabi et al, 2010b).

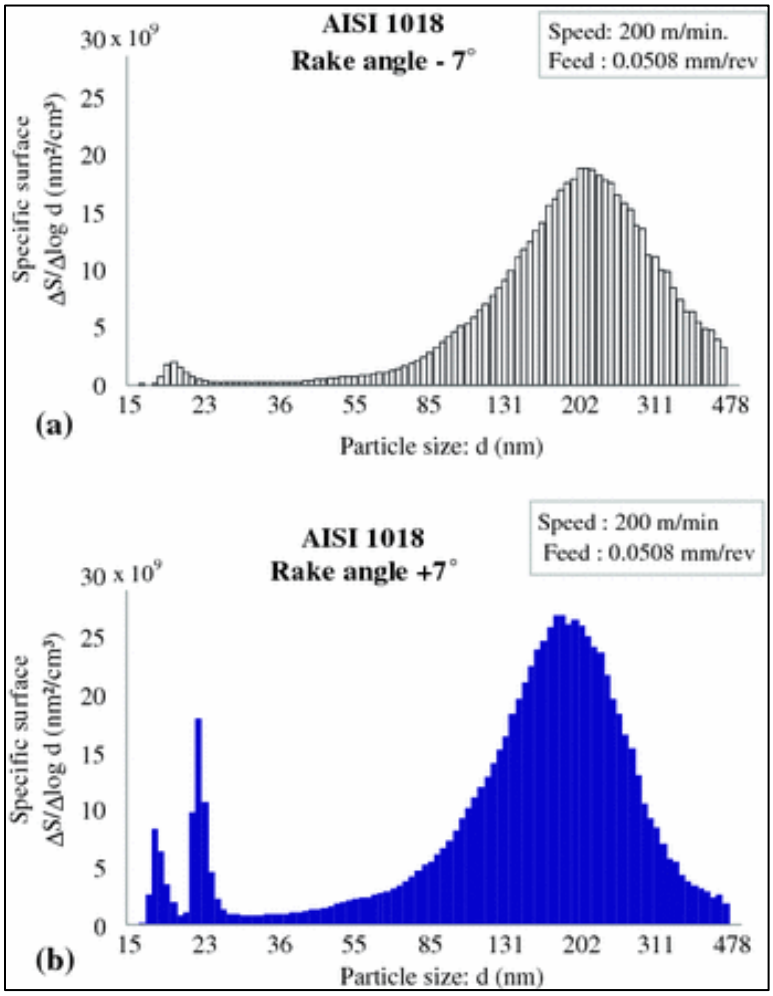

Figure 45 – Effect of the tool's rake angle on specific surface area concentration and particle size distribution of NP during orthogonal turning of steel AISI 1018: a) negative angle; b) positive angle (Khettabi et al, 2010b).

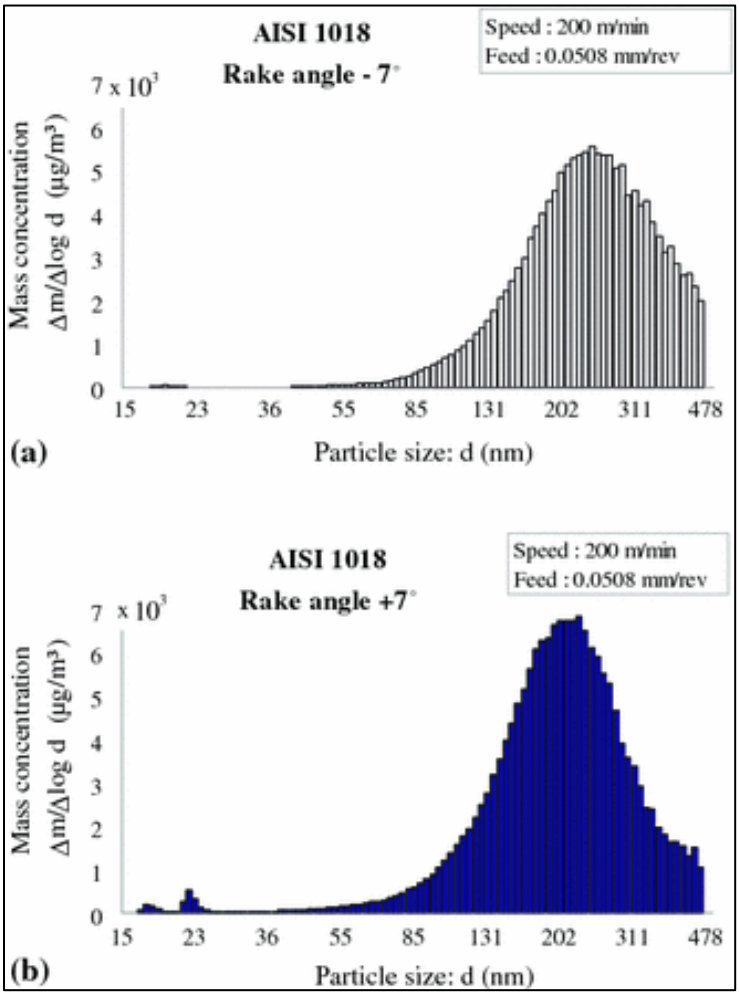

Figure 46 – Effect of the tool's rake angle on mass concentration and particle size distribution of NP during orthogonal turning of steel AISI 1018: a) negative angle; b) positive angle (Khettabi et al, 2010b).

5.4 Effect of the material

The workpiece material and its thermal state considerably affect NP emissions during machining and friction. A fragile material generates much fewer NP than a ductile material. In the same family of materials, the tenacity seems to be the sign that determines the alloy's emissivity. Thus, in wrought aluminium alloys, 2024-T351 produces more particles than 6061-T6, which in turn produces more than 7075-T6 (see Fig. 26, 27, 33-35 and 47). Figure 47 summarizes such a comparison in the case of aluminium alloys. However, there is little difference in specific surface area concentrations from one alloy to another. Let us not forget that the feed rate used can affect these outcomes (see Fig. 32). It was also shown that the material influences the critical value of the speed associated with maximum emission (Khettabi and Songmene, 2009).

Particle generation during fabrication processes is at the origin of friction in two places, one at the tool-chip interface and the other between the different chip fall zones. Particle formation therefore involves two main stages that depend specifically on the material (Khettabi et al, 2008). First, the contact roughnesses are deformed locally. Then, if the material is ductile, the deformed parts will be further modified and strain hardened, which will weaken them locally so that they end up separating. However, if the material is fragile, the part that tends to deform will break off, producing large fragments. Thus, in the case of a fragile material where chip fall zones do not exist and where tool-chip friction is limited, the processes can only produce large particles, and therefore almost no nanometric particles. This explains why ductile materials produce so many NP.

Because of their size, NP emitted during friction or machining are highly reactive. They oxidize instantaneously when they separate from the workpiece. The material of the particle is therefore different from the material of the workpiece (see Fig. 14).

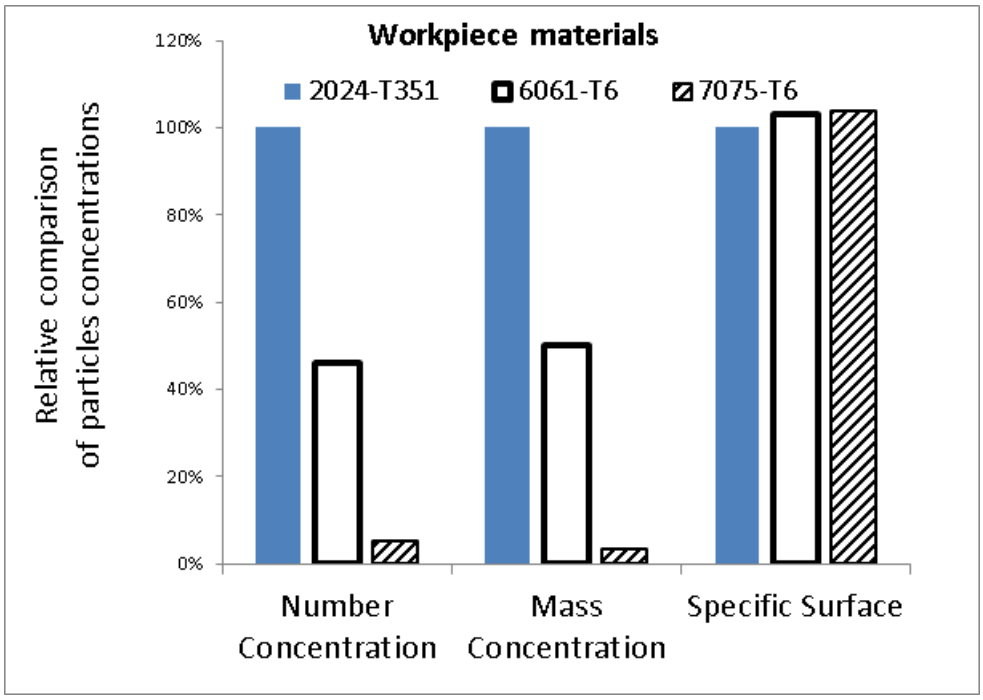

Figure 47 – Comparison of the influence of the workpiece materials on NP emissions during milling of 2 aluminium alloys (7075-T6 and 6061-T6) relative to aluminium alloy 2024-T351.

5.5 Critical speed and experimental conditions

During machining and during friction, the cutting speed is the most conclusive parameter. It influences productivity, surface finish, workpiece quality, the chip formation mode, the life cycle of the tool and ultrafine aerosol emissions. Cutting speed and cutting conditions influence the size, shape and distribution of NP emitted (Khettabi et al, 2010d; Djebara et al, 2012). The quantity of particles emitted by friction or by machining depends on a maximum that

corresponds to a critical speed. This speed is found in an intermediate range between the low and high speeds. However, the critical speed at which the maximum quantity of particles is emitted depends much more on the workpiece material than on the process (Khettabi and Songmene 2009). This quantity of particles emitted also varies according to the metric considered (specific surface area concentration, number concentration or mass concentration).

The speeds adopted to generate the simulations appearing in Figures 33 and 34 are medium and high speeds. If particulate emissions are examined for lower speeds (<300 m/min), there is first an increase in emissions, and then a decrease beginning at a certain speed qualified as critical (also see Figs. 36 and 37). The model developed (Eq. 5) and the simulation outcomes (see Fig. 36) show the critical speed is identical for the same material. The variation of cutting conditions for the same material in Equation 5 essentially affects the quantity of NP emitted and not the critical speed. These outcomes were also confirmed when drilling wrought aluminium alloys (see Fig. 24) and cast aluminium alloys (see Fig. 25), and during friction (see Fig. 22). The exact determination of this critical speed for common shaping applications will allow better prescription of the conditions that emit few undesirable particles and thus will open a door to source reduction of NP emissions.

6. CONCLUSION

The research conducted during this project allowed the development of a sampling method accounting for the behaviour of particles (during generation and capture) and the development of a characterization procedure adapted to NP. An NP collection, transfer and processing procedure for microscopic analysis (TEM, SEM, AFM) was also implemented. The application of the trace gas technique for prediction of the NP deposition coefficient in the measuring systems allowed assessment of losses in the tube.

These methods, tested during machining of certain aluminium alloys and during friction tests of aluminium alloys with carbide slugs allowed the following conclusions:

- NP sampling and capture depend on the measuring instrument used and are necessary for microscopic analysis and characterization. However, provision must be made for some particularities, such as the application of nanolayered metallization to ensure fixation of deposited NP.
- Machining and friction processes generate NP. Numerically, these processes produce more NP than microparticles. Friction emits more NP (around $3x10^8$ particles/cm^3 for aerodynamic diameter particles between 10 nm and 100 nm) than microparticles (about ten particles per cm^3 for particles between 0.5 μm and 3 μm). However, friction produces far fewer NP than machining processes.
- The degree of agglomeration is greatly affected by cutting conditions (cutting speed). We should note this agglomeration can occur during particle generation, after particle generation (interactions according to their airborne behaviour), during the sampling process (suction) or during deposition on the substrate. In the context of this work, it was not possible to identify the level at which agglomeration occurs. It would be desirable for later studies to address this point.
- The metal particles emitted during machining are of varied shapes (isolated particles, aggregates or agglomerated particles). In general, for a size smaller than 100 nm, the particle belongs to the nano-isometric morphological family (elongated sphere), while for a size greater than 100 nm, the particle belongs to the nanoplate morphological family (cubic shape or thin disk). This variation imposes the need for data correction to improve measuring efficiency. It was demonstrated that overestimating by a factor greater than 2 can be caused by non-correction of the shape (actual size, equivalent diameter and electrical mobility diameter).
- The process parameters and the conditions governing the specific surface area of the particles emitted are different from those controlling numbers or specific mass. For the aluminium tested, statistical analysis showed that number and specific mass are governed by the material and the type of tool used. Specific surface area is dictated by the tool, the feed rate and the cutting depth. It follows that the prescription of better operating conditions becomes difficult without knowing the metric (specific surface area, number or mass concentration) the toxicologists will use to determine the exposure limits.

- NP source reduction is possible by using new machining and friction strategies. For example, the quantity of particles emitted by friction or by machining as a function of speed depends on a maximum that corresponds to a critical speed. This critical speed depends more on the workpiece material and the metric considered than on the process. Choosing the intermediate speed range between the low and high speeds must be avoided to reduce NP production at the source. For complete optimization, it is first appropriate to choose a metric for assessment of NP emissions.
- Exploitation of the simulation outcomes based on the model developed (Eq. 5) and the experimental outcomes also showed that the geometry of the tool (direction angle, rake angle, corner radius) and its coating significantly affect NP generation. More specifically, the tool coating influences the specific surface area of the particles, while the geometry influences the mass concentration of the particles emitted. The variation of the direction angle results in a change of the deformed thickness of the chip and therefore changes the dust emissions. When the width of the chip increases, the surface of the particle-emitting chip increases in turn, leading to more emissions. It was shown that a 90° direction angle results in less dust than a different angle. The farther the direction angle is from a right angle, the more significant the difference. Likewise, during an orthogonal cut, a negative angle (-7°) generates fewer microparticles and NP than a positive angle (+7°) or a zero angle. This is due to a very high degree of chip segmentation.
- NP emissions are directly related to the cutting energy and the chip formation mode. A phenomenological description was used to design a hybrid analytical model based on the activation energy and the friction during chip formation. A new formulation, describing NP emissions as a function of tool geometry, workpiece materials, chip segmentation density and cutting conditions, was proposed and validated experimentally (Eq. 5).

The analysis of the Brownian NP diffusion models allowed us to predict the losses by deposition on the wall and to conclude that the coefficients obtained from these models are highly comparable, but difficult to apply in industrial situations. The flows encountered in machining processes are turbulent, and these turbulent effects will therefore influence NP diffusion. There is a need for more in-depth studies to predict NP transport and diffusion in flows encountered in manufacturing processes.

7. APPLICABILITY OF OUTCOMES

The research published within the context of this project made it possible to obtain satisfactory scientific and industrial outcomes. The sampling technique was improved to ensure better characterization. The comparison of several measuring instruments demonstrated the limits of each, making it necessary to develop measurement correction algorithms. The sampling and characterization procedures, developed by the team for the NP emitted during the fabrication processes and during the friction tests, could be useful in many fabrication industries, especially for processes that generate a lot of dust. This procedure can also help hygienists control emissions and exposure risks in industrial environments.

The project also made it possible to quantify NP emissions and link their concentration to their size; this information can be useful to design means of protection and ventilation for such processes. It was proved that the particles emitted during machining and friction have varied sizes and shapes. This variety affects measurement, because generally the measuring instruments consider the particles to be spherical. Observation under the transmission electron microscope or the scanning electron microscope showed different perfectly heterogeneous NP shapes (spherical, cubic and flat) and highly irregular agglomerates. It would be interesting to develop measurement correction algorithms, based on image analyses and statistics.

All this work made it possible to apprehend the interactions between the cutting parameters and the NP generation modes. The revelation of the sensitivity of the emission process to cutting parameter variations demonstrates the importance of the measuring procedure (sampling, capture, particle shape analysis and correction of the concentration data in view of the shape of the particles). The present research mitigates this deficiency. We are thinking of the following discoveries, in particular:

- It was proved that the number and mass concentrations are governed by process parameters that are different from those governing the specific surface area of the NP. It is therefore recommended that information be provided on all these metrics.
- Without an adequate correction relative to the shape and density of the particles, the data provided by the metrological devices tested overvalue the particle size. The impact of a correction on this data turned out to be important from a quantitative standpoint (factor of 2).
- The particles in the 10-500 nm range were tracked during a milling process. A database was thus constituted and completed with the metrological parameters. During this operation, the number concentration essentially extended from 0.1×10^8 to 4.15×10^8 #/cm^3. A comparison with the observations reported by other studies indicates that these outcomes are obtained at high pollution levels (Khettabi et al, 2011; Kouam et al, 2011). On the other hand, it is observed that NP (10-100 nm) are dominant in the number concentration. However, larger particles (100-500 nm) visibly play a non-negligible role in terms of mass. This clearly shows that the current means of monitoring, based on mass concentration measurement, are influenced by particles larger than 100 nm.

- The experimental outcomes also showed the existence of a cutting speed and feed rate range in milling for which NP emissions are minimal. This is a remarkable breakthrough for the reduction of particulate emissions during machining.

This work can support subsequent studies in toxicology with a view to the establishment of an NP emission standard to improve air quality in machine shops.

8. RECOMMENDATIONS

This project demonstrates that measurement and control of NP constitute problems regarding which several points must be gradually resolved. The following aspects should be studied to improve knowledge in this field and increase the applicability of the outcomes:

- Conduct tests on other materials, processes and conditions used in industries and confirm NP composition by X-ray analysis. In particular, we are thinking of lubrication modes (dry, semi-dry and completely lubricated), composite materials, steels and materials that emit a large quantity of dusts, such as granites and graphite electrodes.
- Complete the analysis of NP behaviour during the process and optimize the sampling setups, according to the processes and cutting tools, in order to improve capture and measurement. In the context of metrological development and the advancement of knowledge of NP emissions, a general correction algorithm must be adapted to the data provided by the measuring instruments (such as the SMPS) to improve the particle size measurements. Image analysis and software design must also be completed. Optimization of residence time and better correction of the particle's charge and density are necessary for devices that use electrical mobility. The development of an automated image analysis procedure is also required to build reliable correction algorithms. To do this, it is necessary to use a statistical information extraction method by automatic image processing (SEM or TEM) based on the particle morphology.

Analyze NP coagulation. NP can coagulate during Brownian agitation. The mass concentration is not affected by this phenomenon. However, coagulation results in enlargement of the particles and a decrease in number concentration. Therefore, the particle size spectrum of a nanosized aerosol cannot be considered stationary if the number concentration is too high. It would also be interesting to estimate the effect of walls and NP sedimentation on coagulation. Such a study must also examine the moment when coagulation occurred: during the process or during sampling.

9. REFERENCES

Ahamed M, AlSalhi MS, Siddiqui MK (2010). Silver nanoparticle applications and human health. *Clinica Chimica Acta*, 411: 1841–1848.

Aitken RJ, Creely KS, Tran CL (2004). Nanoparticles: An occupational hygiene review. Research Report, HSE Books, Edinburgh, UNITED KINGDOM, 102 pages.

Aitken RJ, Chaudhry MQ, Boxall ABA, Hull M (2006). Manufacture and use of nanomaterials: current status in the UK and global trends. *Occupational Medicine*, 56: 300–306.

Arumugam PU, Malshe AP, Batzer SA (2006). Dry machining of aluminum-silicon alloy using polished CVD diamond-coated cutting tools inserts. *Surface and Coatings Technology*, 200(11): 3399-3403.

Balout B, Songmene V, Masounave J (2007). An experimental study of dust generation during dry drilling of pre-cooled and pre-heated workpiece materials. *Manuf. Processes*, SME, 9(1): 23-34.

Balout B, Songmene V, Masounave J (2003). Dust Formation during High Speed machining. 42th Proc. of the Int. Symposium on light metal and composite materials and their end products. Vancouver, BC, August 24-27, pp. 351-366.

Bensadoun F (2011). Développement et caractérisation d'un procédé de fabrication de composites et biocomposites à base de nanoparticules d'argile et de résine polyester insaturée destinés à l'industrie du transport. Masters Thesis, École Polytechnique de Montreal, QC, Canada.

Boczkowski J, Lanone S (2010). Nanoparticules: une prévention est-elle possible? *Revue Française d'Allergologie*, 50(3): 214-216.

Burtscher H (1992). Measurement and characterization of combustion aerosols with special consideration of photoelectric charging and charging by same ions. *Journal of Aerosol Science*, 23: 549.

Covert D, Wiedensohler A, Russell L (1997). Particle charging and transmission efficiencies of aerosol charge neutralizers. *Aerosol Science & Technology*, 27: 206–214.

Derk B (2010). Exposure to manufactured nanoparticles in different workplaces. *Journal of Toxicology*, 269: 120–127. (doi:10.1016/j.tox.2009.11.017)

Djebara A, Songmene V, Khettabi R, Kouam J (2012). An Experimental Investigation on Ultrafine Particles Emission During Milling Process Using Statistical Analysis. *International Journal of Advances in Machining and Forming Operations*, 4(1): 15-37.

Djebara A (2012). Métrologie des particules ultrafines d'usinage : optimisation de la caractérisation et de la mesure. PhD thesis under the supervision of the ETS and the IRSST, Montreal, Canada. Online:: http://espace.etsmtl.ca/1014/. [Last accessed: 16 January 2014].

Djebara A, Songmene V, Bahloul A (2013). Effects of machining conditions on specific surface of PM2.5 emitted during metal cutting. *Health*, 5(10A2): 36-43.

Djebara A, Khettabi R, Kouam J, Songmene V (2010a). Experimental investigation on ultrafine particles emission during dry machining using statistical tools. Proceedings of the International Conference on Nanotechnology: Fundamentals and Applications, Ottawa, Canada, August 4-6, Paper #490: 1-10.

Djebara A, Khettabi R, Kouam J, Songmene V (2010b). Comparison of the capability of peak function in describing real condensation particle counter profiles. Proceedings of the 2nd International Conference on Lasers & Plasma Applications in Materials Science (LAPAMS '10), Alger, Algeria, November 27-30, pp. 40-44.

EU-OSHA, (2009). Workplace exposure to nanoparticles, Edited by Joanna Kosk-Bienko, European Agency for Safety and Health at Work (EU-OSHA), Spain. Online: https://osha.europa.eu/en/publications/literature_reviews/workplace_exposure_to_nanoparticles [Last accessed: 16 January 2014].

Elder AC, Gelein R, Azadniv M, Frampton M, Finkelstein J, Oberdorster G (2004). Systemic effects of inhaled ultra fine particles in two compromised, aged rat strains. *Inhale Toxicology*, 16: 461-471.

Fuchs NA (1964). The Mechanics of Aerosols. Pergamon Press, Oxford, England and The Macmillan Company, New York, 422 pages.

Gatti A (2004). Biocompatibility of micro and nanoparticles in the colon. Part II. *Biomaterials*, 25(3): 385-92.

Görner P, Fabriès JF (1990). Techniques de mesure automatique des aérosols atmosphériques. Cahiers de notes documentaires no. 140, 3e trimestre, Institut national de recherche et de sécurité (INRS), France, pp. 595-626.

Greim, H., Gesundheitsschädliche Arbeitsstoffe : Amorphe Kieselsäuren, Toxikologischarbeitsmedizinische Begründung von MAK-Werten, WILEY-VCH, 1989.

Hallé S, Morency F, Dufresne L, Tardif R (2009). Modeling Nanoparticles Transport in an Animal Exposure Chamber: Comparison with Experimental Measurements. Compte-rendu du 2e Congrès int. sur l'ingénierie des risques industriels, Reims, France, 13-15 May.

Hands D, Sheehan MJ, Wong B, Lick HB (1996). Comparison of metalworking fluid mist exposure from machining with different levels of machine enclosure. *American industrial Hygiene Association Journal*, 57(12): 1173-1178.

Hervé-Bazin B (2007). Les nanoparticules – Une enjeu majeur pour la santé au travail? EDP Sciences, 704 pages.

Hinds WC (1999). Aerosol Technology – Properties, Behavior and Measurement of Airborne Particles. Wiley-Interscience, 483 pages.

Honnert B, Vincent R (2007). Production et utilisation industrielle des particules nanostructurées. *Hygiène et sécurité du travail*, ND 2277, 209(7): 5-21.

Hoower MD, Finch G, Mewhinney JA, Eidson AF (1990). Release of Aerosols during Sawing and Milling of Beryllium Metaland Beryllium Alloys. *Appl. Occup. Environ. Hyg.*, 5: 787-791.

Jancar J, Douglas JF, Starr FW, Kumar SK, Cassagnau P, Lesser AJ, Sternstein SS, Buehler MJ (2010). Current issues in research on structure-property relationships in polymer nanocomposites. *Polymer*, 51: 3321-3343.

Khettabi R, Songmene V, Masounave J (2007). Effect of tool lead angle and chip formation mode on dust emission in dry cutting. *J. Materials Processing Technology*, 194: 100-1009.

Khettabi R, Songmene V, Zaghbani I, Masounave J (2008). Understanding the Formation of Nano and Micro Particles During Metal Cutting. *Int. J. of Systems Signal Control and Engineering Applications*, 1(3): 203-210.

Khettabi R (2009). Modélisation des émissions de particules microniques et nanométriques en usinage. PhD Thesis. École de technologie supérieure, Montreal, 198 pages. Online: http://espace.etsmtl.ca/59/ [Last accessed: 16 January 2014].

Khettabi R, Songmene V (2009). Particle emission during orthogonal and oblique cutting. *International Journal of Advances Machining and Forming Operations*, 1(1): 1-9.

Khettabi R, Songmene V, Masounave J, Zaghbani I (2010a). Modeling of fine and ultrafine particle emission during orthogonal cutting. *Journal of Materials Engineering and Performance* (JMEPEG), ASM International, 19: 776–789.

Khettabi R, Songmene V, Masounave J (2010b). Effects of cutting speeds, materials and tool geometry on metallic particle emission during orthogonal cutting. *J. Materials Engineering and Performance* (JMEPEG), ASM International, 19: 767–775.

Khettabi R, Songmene V, Masounave J (2010c). Influence of machining processes on particles emission. 49th Annual Conf. of Metallurgists of CIM, Vancouver, 277-288.

Khettabi R, Djebara A, Kouam J, Songmene V (2010d). Characterization and Control of Micro and Nanoparticles Produced During Dry Cutting. Safety Health and Environment World Congress (SHEWC2010), July 25-28, São Paulo, Brazil, pp. 37-41.

Khettabi R, Zaghbani I, Djebara A, Kouam J, Songmene V (2011). A new sustainability model for machining processes. *Journal of Sustainability*, Risk and Environmental Challenges of the 21st Century, 2(3): 87-202.

Kouam J, Songmene V, Balazinski M, Hendrick P (2012). Dry, Semi-Dry and Wet Machining of 6061-T6 Aluminium Alloy. *Aluminium Alloys - New Trends in Fabrication and Applications*, Zaki Ahmad (Ed.), ISBN: 978-953-51-0861-0, InTech, pp. 199-222. Online: http://www.intechopen.com/books/aluminium-alloys-new-trends-in-fabrication-and-applications/dry-semi-dry-and-wet-machining-of-6061-t6-aluminium-alloy [Last accessed: 20 January 2014].

Kouam J, Songmene V, Djebara A, Khettabi R (2011). Effect of Friction Testing of Metals on Particle Emission. *J. of Materials Engineering and Performance*, 1(4): 1-8.

Kouam J, Djebara A, Khettabi R, Songmene V (2010a). Dust emission during friction: effect of friction on tribological behavior. Proceedings of the International Conference on Nanotechnology: Fundamentals and Applications, Ottawa, Ontario, Canada, 4-6 August. Paper #466: 1-8.

Kouam J, Masounave J, Songmene V, Giraudeau A (2010b). Pre-holes effect on cutting forces and particle emission during dry drilling. 49th Annual Conference of Metallurgists of CIM: Symposium on Light Metals, October 3-6, Vancouver, BC, Canada, 253-263.

Kremer A (2009). Étude du choix structurel d'outils coupants en diamant revêtu ou polycristallin massif pour l'usinage compétitif et environnemental des composites a matrice métallique et renfort céramique particulaire (CMMP AL/SiC). Thèse de doctorat, École Nationale Supérieure d'Arts et Métiers (ENSAM), Arts et Métiers ParisTech, Châlons-en-Champagne, France, 155 pages.

Kremer A, El Mansori (2009). Influence of nanostructured CVD diamond coatings on dust emission and machinability of SiC particle-reinforced metal matrix composite. *Surface and Coatings Technology* 204(6-7): 1051-1055.

Kruis FE, Fissan H (2001). Nanoparticle charging in a twin Hewitt charger. *Journal of Nanoparticles Research*, pp. 3-39.

Lademann J, Richter H, Schanzer S, Knorr F, Meinke M, Sterry W, Patzelt A (2011). Penetration and storage of particles in human skin: Perspectives and safety aspects. *European Journal of Pharmaceutics and Biopharmaceutics*, 77: 465–468.

Laoutid F, Bonnaud L, Alexandre M, Lopez-Cuesta JM, Dubois P (2009). New prospects in flame retardant polymer materials: from fundamentals to nanocomposites. *Materials Science & Engineering Reports*, 63: 100-25.

Mark D (2004). Nanomaterials: A Risk to Health at Work? 1st Int. Symp. on Occupational Health Implications of Nanomaterials, Buxton, United Kingdom, 12-14 October, 158 pages.

Malshe AP, Taher MA, et coll. (1998). A Comparative Study of Dry Machining of A390 Alloy using PCD and CVD Diamond Tools, *Trans. NAMRI/SME* Vol. XXVI: 267-272.

Mackerer CR (1989). Health Effects of Oil Mists: A Brief Review. *Toxicology & Industrial Health*, 5: 429-440.

Morency F, Hallé S, Dufresne L, Emond C (2008). Evaluation of diffusion model for airborne nanoparticules transport and diffusion. *Advanced in Fluid Mechanics VII*, Editor Rahman M, Brebbia CA, WIT Press, Southampton, England, pp. 11-120.

Morency F, Hallé S (2010). Nanoparticles Transport and Diffusion in an Animal Exposure Chamber. Advanced in Fluid Mechanics VIII, Editor Rahman M, Brebbia CA, WIT Press, Southampton, England, pp. 533-544.

Morency F, Hallé S (2013). A simplified approach for modelling airborne nanoparticles transport and diffusion. *Int. J. Comp. Meth. and Exp. Meas*., 1(1): 55–71.

Oberdörster G, Oberdörster E, Oberdörster J (2005). Nanotechnology: An emerging discipline evolving from studies of ultra fine particles. *Environmental Health Perspectives*, 113(7): 823-839.

OMS (1999). Hazard Prevention and Control in the Work Environment: Airborne Dust, Prevention and Control Exchange. WHO/SDE/OEH/99.14, Geneva, Switzerland, pp. 1-219.

Ostiguy C, Lapointe G, Ménard L, Cloutier Y, Trottier M, Boutin M, Antoun M, Normand C (2006). Les nanoparticules : État des connaissances sur les risques en santé et sécurité du travail. IRSST, Études et recherche #R-455. Online: http://www.irsst.qc.ca/files/documents/PubIRSST/R-455.pdf [Last accessed: 20 January 2014].

Palmqvist J, Gustafsson S (1999). Emission of dust in planning and milling of wood. *Holz Roh-Werkst,* 57: 164–170.

Park SH, Kruis FE, Lee KW, Fissan H (2002). Evolution of particles size distributions due to turbulent and Brownian coagulation. *Aerosol Sci. Tech*., 36: 419-432.

Prow TW, Grice JE, Lin LL, Faye R, Butler M, Becker W, Wurm EM, Yoong C, Robertson TA, Soyer HP, Roberts MS (2011). Nanoparticles and microparticles for skin drug delivery, *Advanced Drug Delivery Reviews,* 63: 470–491.

Pustkova P, Hutchinson JM, Roman F, Montserrat S (2009). Homopolymerization effects in polymer layered silicate nanocomposites based upon epoxy resin: implications for exfoliation. *Journal of Applied Polymer Science,* 114: 1040-1047.

Rautio S, Hynynen P, Welling I, Hemmila P, Usenius A, Narhi P (2007). Modelling of airborne dust emissions in CNC MDF milling. *Holz als Roh- und Werkstoff*, 65(5): 335-341.

Rudyak VY, Kharlamov GV, Belkin AA (2001). Diffusion of Nanoparticles and Macromolecules in Dense Gases and Liquids. *High Temperatures*, 39(2): 264-271.

Sadrieh N, Wokovich AM, Gopee NV, Zheng J, Haines D, Parmiter D, Siitonen PH, Cozart CR, Patri AK, McNeil SE, Howard PC, Doub WH, Buhse LF (2010). Lack of significant dermal penetration of titanium dioxide from sunscreen formulations containing nano- and submicron-size TiO2 particles. *Toxicol. Sci.,* 115: 156–166.

Songmene V, Masounave J, Khettabi R (2007). Dry Machining and its Effects on Productivity, Costs, Environment and Machine-Shop Air Quality. In: Tounsi N and Fisher C, *Proc. of the 1st International Conference on Sustainable Manufacturing*, Aerospace Manufacturing Technology Centre, Montreal, Canada, 17-18 October, pp. 51-60.

Songmene V, Balout B, Masounave J (2008a). Clean Machining: Experimental Investigation on Dust Formation - Part I: Influence of Machining Parameters and Chip Formation. *Int. J. of Environmentally Conscious Design and Manufacturing*, 14(1): 1-16.

Songmene V, Balout B, Masounave J (2008b). Clean Machining: Experimental Investigation on Dust Formation - Part II: Influence of Machining Strategies and Drill Condition. *Int. J. of Environmentally Conscious Design and Manufacturing*, 14(1): 17-33.

Songmene V, Khettabi R, Kouam J (2012). Dry high-speed machining: a cost effective and green process. *International Journal of Manufacturing Research*, 7(3): 229–256.

Sutherland JW, Kulur VN, King NC (2000). Experimental investigation of air quality in wet and dry turning. *CIRP Annals - Manufacturing Technology*, 49(1): 61-64.

SUVA (2012). Valeurs limites d'exposition aux postes de travail 2012. Form #1903, Lucerne, janvier 2012. Online: http://www.sapros.ch/images/supplier/220/pdf/01903_f.pdf [Last accessed: 21 January 2013].

SUVA (2013). Valeurs limites d'exposition aux postes de travail 2013. En ligne : http://sv-safety.epfl.ch/files/content/sites/sv-safety/files/VME-SUVA_F.pdf [Last accessed: 24 January 2013].

Subra I, Hubert G, Aubert S, Héry M, Elcabache JM (1999). Exposition professionnelle aux métaux lors de l'usinage des bois traités au cuivre, chrome, arsenic. 2nd Quarter, pp. 61-68. En ligne : http://www.hst.fr/inrs-pub/inrs01.nsf/IntranetObject-accesParReference/HST_ND%202108/$File/ND2108.pdf [Last accessed: 23 January 2014].

Tönshoff H, Karpuschewski B, Glatzel T (1997). Particle Emission and Emission in Dry Grinding. *Annals of the CIRP*, 46(2): 693-695.

Vincent JH (1989). *Aerosol Sampling – Science and Practice*. Chichester: John Wiley & Sons, 390 pages.

Witschger O, Fabriès F (2005a). Particules ultrafines et santé au travail. 1 - Caractéristiques et effets potentiels sur la santé. INRS 199: 21-35.

Witschger O, Fabriès F (2005b). Particules ultrafines et santé au travail. 2 - Sources et caractérisation de l'exposition. INRS 199: 37-54.

Witschger O, Le Bihan O, Reynier M, Durand C, Marchetto A. Zimmermann E., Charpentier D (2012). Préconisations en matière de caractérisation des potentiels d'émission et d'exposition professionnelle aux aérosols lors d'opérations mettant en oeuvre des nanomatériaux, INRS-Hygiène et sécurité du travail, 1st Quarter, ND 2355 226-12: 41-55.

Xie JQ, Bayoumi AE, Zbib HM (1996). Study on Shear Banding in Chip Formation of Orthogonal Machining. *Int. J. Mach. Tools & Manufacture,* 36(7): 835–847.

Yue Y, Gunter KL, Michalek DJ, Sutherland JW (2000). Cutting fluid mist formation in turning via atomization Part 1: Model development. *American Society of Mechanical Engineers, Manufacturing Engineering Division*, MED 11: 843-850.

Zaghbani I, Songmene V, Khettabi R (2009). Fine and Ultrafine Particle characterization and Modeling In High Speed Milling of 6061-T6 Aluminium Alloy. *Journal of Materials Engineering and Performance*, ASM International, 18(1): 38-49.

Zhang Q, Kusaka Y, Donaldson K (2000). Comparative pulmonary responses caused by exposure to standard cobalt and ultra fine cobalt. *Journal of Occupational Health*, 42: 179-184.